



Technische Universität München
Fakultät für Chemie
Professur für Molekulare Katalyse

**HIGH VALENT RHENIUM COMPOUNDS IN CATALYSIS: SYNTHESIS,
REACTIVITY AND DECOMPOSITION PATHWAYS**

Benjamin J. Hofmann

Dissertation



TECHNISCHE UNIVERSITÄT MÜNCHEN
FAKULTÄT FÜR CHEMIE
PROFESSUR FÜR MOLEKULARE KATALYSE

High Valent Rhenium Compounds in Catalysis: Synthesis, Reactivity and Decomposition Pathways

BENJAMIN JOCHEN HOFMANN

Vollständiger Abdruck der von der Fakultät für Chemie der Technischen Universität München
zur Erlangung des akademischen Grades eines

Doktors der Naturwissenschaften (Dr. rer. nat.)

genehmigten Dissertation.

Vorsitzender:

Prof. Dr. Tom Nilges

Prüfer der Dissertation:

1. Prof. Dr. Fritz E. Kühn

2. Prof. Dr. Klaus Köhler

3. Prof. Dr. João D. G. Correia

Die Dissertation wurde am 29.01.2021 bei der Technischen Universität München eingereicht und
durch die Fakultät für Chemie am 02.03.2021 angenommen.

One of the first descriptions of catalysis by the
New York Times, June 8, 1923

*“Catalysis, that strange principle of chemistry
which works in ways more mysterious and inexplicable
than almost any other of the many curious phenomena of science”*

DANKSAGUNG

Mein ganz besonderer Dank gilt meinem Doktorvater

Herrn Prof. Dr. Fritz E. Kühn

für die Aufnahme in den Arbeitskreis und die unkomplizierte Zusammenarbeit. Vielen Dank für die Möglichkeit meine vielfältigen Forschungsinteressen zu verfolgen und Ihre Unterstützung bei der Durchführung. Weiterhin bedanke ich mich für die diversen Möglichkeiten mich in Ihrem Arbeitskreis fortzubilden, das geschenkte Vertrauen und die interessanten und amüsanten Geschichten.

Ein großer Dank geht auch an **Herrn Dr. Ziche** stellvertretend für die Firma **Wacker Chemie AG** für die interessante Aufgabenstellung, die kooperative fachliche Zusammenarbeit und die Unterstützung während der Durchführung meiner Doktorarbeit. Selbstverständlich gilt dieser Dank auch den Kollegen aus dem Wacker Konsortium, die mich innerhalb des Projektes unterstützt haben.

Weiterhin möchte ich mich für die Zusammenarbeit mit **Herrn Prof. Dr. Klaus Köhler** bedanken. Von Ihnen konnte ich bereits in meinem Master Studium vieles lernen und hatte eine interessante und schöne Zeit in Ihrem Arbeitskreis. Großer Dank für die weitere Unterstützung während meiner Promotion und für die Übernahme des Postens des Zweitprüfers.

Ebenso möchte ich mich bei **Herrn Prof. Janos Mink** bedanken für die tiefen Einblicke in die Schwingungsspektroskopie und die vielen lehrreichen Stunden beim Interpretieren der Spektren. Hier natürlich ein großer Dank für die Kooperation und die vielen interessanten Gespräche

Viele Arbeiten im Arbeitskreis wären jedoch nicht möglich ohne Ihre Unterstützung, **Frau Ulla Hifinger**. Danke für die große Unterstützung bei vielerlei organisatorischen Dingen und die freundliche Zusammenarbeit.

In gleichem Maße gilt auch mein Dank den Kollegen aus dem akademischen Mittelbau. **Gabi**, danke für die schöne Zeit und konstruktive Zusammenarbeit während der Praktika – und natürlich auch für das ein oder andere Mal bei Schnitzel oder Ähnlichem, natürlich ohne Karotten. **Markus**, dir möchte ich danken für die Hilfe beim Lernen des DFT Rechnens und für die Geduld falls ich auch das ein oder andere Mal einen Cluster überlastet habe oder ein Passwort vergessen habe.

Nicht vergessen möchte ich auch **Alex Pöthig**. Durch dich habe ich über mein gesamtes Studium sehr viel gelernt und erinnere mich gerne an diverse Abende mit Bier und Wissenschaft. Es ist mir eine Freude mit dir zum Ende noch einmal publizieren zu können und danke für die Unterstützung meiner weiteren Laufbahn.

Meine Arbeit wäre aber auch nicht durchführbar gewesen ohne die Unterstützung der Techniker seitens Elementaranalyse und anderen Bereichen. Besonderer Dank gebührt hier **Jürgen Kudermann** für die ausgezeichnete Zusammenarbeit zuerst am NMR und später im Chromatographie Labor. Von dir kann man nicht nur sehr viel Fachliches lernen, sondern auch vieles über die Zusammenarbeit in einem Forschungsinstitut. Es war mir eine Freude mit dir diverse schöne Abende zu verbringen. Weiterhin geht ein großer Dank an **Maria Weindl**. Danke für die Einarbeitung und Hilfe am NMR und dir vor allem alles Gute mit deinem Kind.

Neben den ganzen bezahlten Mitarbeitern mussten auch noch ein paar Studierende unter mir Leiden. Ich hatte eine tolle Zeit mit euch, **Björn, Katharina, Jenny, Max, Yogi, Sofia** und **Steffi**. Ich danke für eure Mitarbeit, wünsche euch alles Gute im weiteren Verlauf eures Werdegangs und hoffe ihr habt noch das ein oder andere Positive aus eurer Praktikums- oder Abschlussarbeitszeit in Erinnerung.

Als nächstes möchte ich einem Kollegen danken, den ich bereits von seiner Zeit kenne als er noch von „Counter Strike“-zockenden Doktoranden geärgert wurde, der mit dem Umzug ins CRC genervt wurde und dann schlussendlich seinen wichtigen Platz bei uns im Arbeitskreis gefunden hat. Danke **Robert** für deine Hilfe in der Wissenschaft, für Korrekturen, das Pushen wenn's doch mal eher schneller als absolut korrekt gehen muss, aber auch für viele schöne Abende und gute Diskussionen. Großer Dank für deine Unterstützung (nicht nur fachlich, gerne auch persönlich) und die Hilfe für meinen weiteren Lebensweg. Wir hatten tolle Abende wie den ein oder andere Seminar Room Rave, kulturelle Fortbildung in der Nachtszene von München oder gemütlich nach der Arbeit. Deshalb freue ich mich schon auf die kommende Zeit und ich hoffe wir halten unseren Kontakt – aber was soll schon schiefgehen, wenn man einen guten Musikgeschmack hat.

Für eine schöne Zeit an der TU München hast auch du gesorgt, **Lilli**. Danke für die vielen schönen Abende, aber auch für die große Unterstützung, wenn bei mir etwas nicht rund gelaufen ist. Hat ja gerne in einem Spontanausflug nach Ingolstadt oder auch im Harry geendet. Seit Beginn des Studiums warst du eine tolle Freundin und ich wünsch dir alles Gute in deiner persönlichen und beruflichen Zukunft.

Auch dir, **Pauline**, möchte ich danken. Danke für den Spaß beim Hüpfen (Ich hab dich doch gerne mit meinen Geschichten erheitert) und die vielen guten Gespräche. Es ist zwar schwer mit deinem Redefluss mitzuhalten, aber trotz ich denke gerne zurück an die vielen schönen Abende. Gleiches gilt natürlich für **Nadine**. Es war mir immer eine Freude mit dir den Abend zu verbringen und wünsche dir einen guten Start in das Berufsleben. Ich hoffe wir können diese guten Zeiten demnächst wieder nachholen.

Im Labor mussten mich hingegen einige über sich ergehen lassen. Hier Dank für die Zusammenarbeit an **Tommy** und **Andi**, aber vor allem an **Flo**. Mit dir war die Zeit im Exillabor sehr schön. Du hast mir sehr geholfen beim Betreuen der Studierenden und bei diversen wissenschaftlichen Fragen. Ich erinnere mich gerne an viele schöne Abende bei Bier und Diskussion. Wir hatten viele faszinierend kontroverse fachliche und sachliche Diskussionen – aber abseits davon: Niemals vergessen! In heißes Wachs pustet man nicht!

Mit von der Partie waren auch gerne **Alex** und **Marco**. Für mich waren die Abende, sei es bei einer hochinteressanten Tafelpräsentation oder Kartenspiel immer schön. Weiterhin habe ich in Diskussionen mit euch viel gelernt und hoffe ich konnte euch das ein oder andere beibringen. Es war mir eine Freude mit euch zu publizieren und erzähle euch doch gerne mal wieder die ein oder andere witzige Geschichte.

Seitens der „älteren“ Garde möchte ich mich vor allem bei **Anja**, **Flo Groche**, **Sophie** und **Markus** bedanken. Als junger Doktorand habt ihr mir das „Laufen“ beigebracht und eine tolle Zeit beschert. Ich freu mich auf die nächsten Treffen der Ehemaligen, welches wir auch gerne mit dem ein oder anderen Whiskey oder Wein begießen können.

In der „mittleren“ Garde, **Dani**, **Christiane** und **Sebi**, großer Dank für die Zusammenarbeit, vor allem aber auch an **Lorenz**. Neben dem gemeinsamen Arbeiten an wissenschaftlichen Fragestellungen hatten wir öfters eine gute Zeit sei es beim Wandern, Bouldern oder abendlichen Aktivitäten. Gleichermaßen möchte ich auch bei **Jonas** und **Christian** bedanken. Danke für die schönen Gespräche, die gemeinsame Arbeit und die ein oder anderen Subs. Ich wünsche euch alles Gute in der Zukunft, vor allem aber Leberkäsemmeln. Und für **Eva** gibt's natürlich maximal ein Radler. Auch mit dir hatte ich eine schöne Zeit und wünsche dir noch eine erfolgreiche Zeit im Arbeitskreis - vor allem aber auch noch viele Besuche deiner liebenswürdigen Nachbarn.

Den „jungen Wilden“ möchte ich eine produktive und schöne Doktorandenzeit wünschen. Es war eine kurze aber schöne Zeit mit euch **Nicole, Greta** und **Michi**. Vor allem letzteren möchte ich danken für die schönen fachlichen Gespräche selbst wenn diese aufgrund etwaiger Themenstellung zur Verzweiflung geführt haben mögen.

Neben den Kollegen in unserem Arbeitskreis möchte ich mich herzlich bedanken bei **Amelie**. Danke für deine Hilfe und Diskussionen zu DFT Rechnungen und anderen fachlichen oder persönlichen Dingen. Ich habe sehr gerne mit dir „Frischlufte“ geschnappt und wünsche dir alles Gute in deiner weiteren Laufbahn.

Ein weiterer großer Dank für gilt an diverse Kollegen unterschiedlicher Arbeitsgruppen für die vielen schönen überfachlichen Abende bei denen es um alles ging, von Wissenschaft über Politik bis hin zu Gott und die Welt. Danke an die **Fischer, Köhler** und **Buchner** Arbeitsgruppe und natürlich das **KLang Lab!**

Der größte Dank geht selbstverständlich an meine **Eltern**. Danke für die Unterstützung und das Vertrauen über viele, lange Jahre des Studiums bis hin zum Ende meiner Promotion. Auch möchte ich euch für euren unermüdlichen Einsatz für meine berufliche Fortbildung danken, von Beginn der Ausbildung zum Chemielaboranten bis hin zu diesem Meilenstein. Ebenso bedanke ich mich für die schöne Zeit bei euch in Niederbayern die ich in den letzten Monaten gerne wieder genießen durfte.

KURZZUSAMMENFASSUNG

Die katalytischen Eigenschaften von hochvalente Rheniumkomplexen wurden in der Epoxidation, Metathese sowie Dehydrierung untersucht. Durch die Modifikation des organischen Liganden von Aryltrioxorhenium Verbindungen konnten eindeutige Struktur-Reaktivitäts-Beziehungen festgestellt werden. Anhand von Ethyltrioxorhenium werden exemplarisch Abbauwege dieser Substanzklasse aufgeklärt, sodass Anforderungen an die Struktur von neuen und stabileren Alkyltrioxorhenium Verbindungen bestimmt werden können. Neben organometallischen Verbindungen wird die Aktivierung von Rheniumheptoxid durch die Reaktion mit aromatischen Lösungsmitteln untersucht. Hierbei kann gezeigt werden, dass sich gemischt-valente Nanopartikel bilden, die die aktive Spezies in der Dehydrierungsreaktion darstellen wobei Rheniumheptoxid komplett inaktiv ist. Abschließend wird die Relevanz dieser Erkenntnisse dargestellt, denn Rheniumheptoxid wird in diversen katalytischen Reaktionen unter ähnlichen Bedingungen eingesetzt wird.

ABSTRACT

The catalytic performance of high valent rhenium compounds is assessed in epoxidation, metathesis and dehydration reactions. For aryltrioxorhenium compounds, the donor strength of the organic moiety is altered and direct structure-reactivity relationships are identified. Using ethyltrioxorhenium, the decomposition pathways for alkyltrioxorhenium compounds (except methyl) are assessed in order to develop new and more stable catalysts. Beside organometallic compounds, the mechanism of the activation of rhenium heptoxide by aromatic solvents is investigated showing that mixed-valence rhenium nanoparticles are formed. These nanoparticles are the active species in dehydration reactions whilst the binary oxide is completely inactive. An outlook on the relevance of this finding is given as rhenium heptoxide is applied in various other reactions using similar reaction conditions.

I. Table of Contents

I.	Table of Contents	I
II.	Abbreviations:	II
1.	Discovery of Rhenium.....	1
2.	Rhenium: From feedstock to application	2
3.	The Chemistry of Rhenium Oxides	6
3.1.	Rhenium(VII).....	6
3.2.	Rhenium(VI).....	8
3.3.	Rhenium(IV).....	10
3.4.	Rhenium(V) and (III)	11
3.5.	Rhenium Nanoparticles	11
3.6.	Summary of the Redox Chemistry of Rhenium	16
4.	Metalorganic and Coordination Chemistry of Rhenium	17
4.1.	Summary of the Metalorganic and Coordination Chemistry of Rhenium in the Oxidation States +I - +VI.....	19
5.	Rhenium(VII)trioxo complexes	19
5.1.	Synthesis of Re(VII)trioxo compounds	20
5.2.	Important Characterization Methods for Re(VII)trioxo Compounds	22
5.2.1.	Characterization of the Structure of Rhenium(VII) trioxo Compounds.....	22
5.2.2.	Characterization by ¹⁷ O-NMR spectroscopy	24
5.2.3.	Characterization by IR spectroscopy	27
5.3.	Catalytic Applications of Rhenium(VII) trioxo Compounds	29
5.3.1.	Epoxidation of Olefins by Rhenium(VII) trioxo Compounds.....	29
5.3.2.	Dehydration of Alcohols Catalyzed by Rhenium(VII) trioxo Compounds.....	34
5.3.3.	Metathesis reactions Catalyzed by High Valent Rhenium Compounds	37
5.4.	Rhenium(VII)trioxo Complexes, from Synthesis to Application	41
6.	High Valent Rhenium Compounds in Catalysis.....	42
6.1.	Synthesis, Characterization and Application of Organorhenium(VII) trioxides in Metathesis Reactions and Epoxidation Catalysis	43
6.2.	Ethyltrioxorhenium – Catalytic Application and Decomposition Pathways.....	46
6.3.	Reactivity of Re ₂ O ₇ in Aromatic Solvents – Cleavage of a β-O-4 Model Substrate by Lewis-acidic Rhenium Oxide Nanoparticles.....	48
7.	High Valent Rhenium Chemistry – An Outlook	52
8.	Conclusion	54
9.	Literature	56

II. Abbreviations:

	3			Gas-phase electron diffraction.....	23
3-MPA			H		
3-mercaptopropionic.....	13			HAD	
		C		Hexadecylamine.....	13
				HEDP	
				Hydroxyethylidene bisphosphonate	5
				HFI	
				Hexafluoroisopropanol	31
				HMPA	
				Hexamethylphosphoric triamide.....	31
			L		
				LSPR	
				Localized surface plasmon resonance.....	14
			M		
		D		mAb	
				Monoclonal antibody.....	5
				MAG ₃	
				Mercaptoacetyltryglycine	5
				MTO	
				Methyltrioxorhenium.....	20
			N		
				n.	
				Neutrons	5
				NA	
				Not available	14
				NC	
				Nanocube.....	13
				NHC	
				N-Heterocyclic carbene.....	18
				NIR	
				Near infrared.....	14
				NMR	
				Nuclear magnetic resonance.....	23
				Np	
				Suggested abbreviation for Nipponium	2
				NP	
				Nanoparticles	12
			P		
				PAH	
				Polyallylamine hydrochloride.....	12
				PBE	
				Perdew-Burke-Ernzerhof.....	7
				PCM	
				Polarizable continuum model	48
				P-ND	
				Powder neutron diffraction	23
		G			
GED					
Gas phase electron diffraction	7				
GGA					
Generalized gradient approximation.....	7				
GP-ED					

PTFE	
Polytetrafluoroethylene	12
PVP	
Polyvinyl pyrrolidone	13

R

ROMP	
Ring-Opening Metathesis Polymerization	4

S

scECP	
Small core electronic core potential	7
SC-XRD	
Single crystal X-ray diffraction	23
SERS	
Signal enhanced Raman scattering	12
SHOP	
Shell Higher Olefin Process	38
SPECT	
Single-photon emission computed tomography	5

T

tcan	
1,4,7-triazacyclononane	8

TFI	
Trifluoroethanol	31
THF	
Tetrahydrofurane	8
TOF	
Turnover frequency	32

U

USGS	
US Geological Survey	4
UV	
Ultraviolet	20

V

VOC	
Volatile organic compounds	9

X

XANES	
X-ray absorption near edge structure	12
XAS	
X-ray absorption spectroscopy	15
XPS	
X-ray photoelectron spectroscopy	15

1. Discovery of Rhenium

For centuries, chemists have tried to find a “natural order” of all known substances, in order to understand their reactivity and discover new elements. In 1869, the major breakthrough was the discovery of the periodicity of physical (e.g. atomic volume) and chemical properties (e.g. valence) of the elements independently by the Russian Dmitri Ivanovitch Mendeleev[1] and the German Lothar Meyer[2]. Both developed the predecessors of the current periodic table by ordering the elements according to their respective mass and, in contrast to their predecessors, assigning them to groups with respect to their properties. In the case of discrepancies in the periodicity of known substances, they left gaps in the periodic table predicting the existence of undiscovered elements. In contrast to Meyer, Mendeleev went even further and estimated the physical and chemical properties of some unknown elements by interpolation of the respective elements above and below the sought one (Figure 1).[3, 4] The preciseness of these predictions led to the fast discovery of eka-boron, eka-aluminum and eka-silicon, namely scandium (Nilson, 1879)[5], gallium (De Boisbaudran, 1875)[6] and germanium (Winkler, 1886)[7]. The successful application of the periodic table led to the general recognition of Mendeleev as the “inventor” of the modern periodic table, despite other scientists like Meyer or Odling (to name a few) contributed to that field significantly.[3, 8]

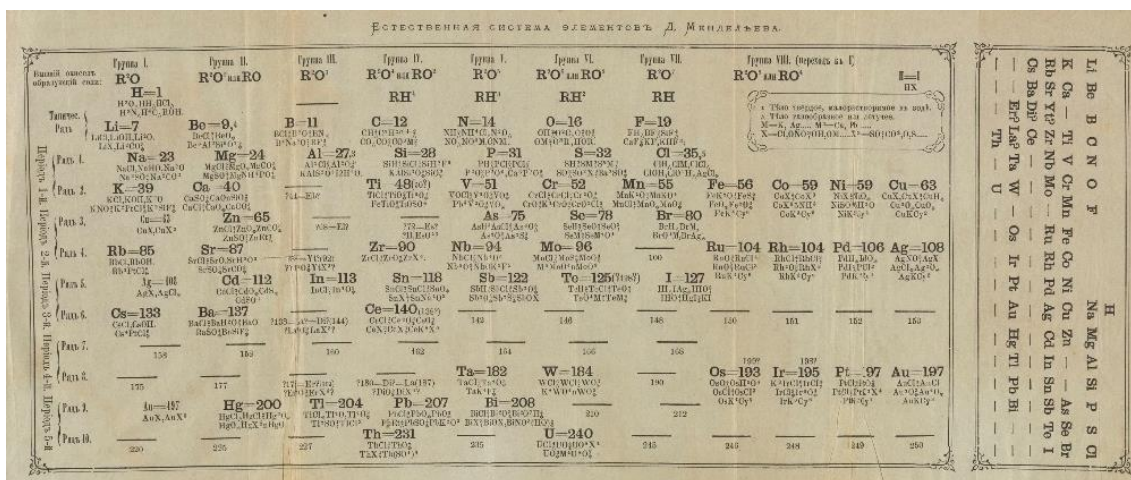


Figure 1: The revised periodic table by Dmitri I. Mendeleev published in his book *Osnovy Khimii (Principles of Chemistry)* in 1871.[9] (Creative Common License)

However, it took additional 39 years to isolate and identify the last stable element and, importantly, publish these findings in internationally recognized journals. In 1925, Ida Tacke (later Noddack) and Walter Noddack obtained a sample of approximately 20 mg containing 5 % of dwi-manganese and possibly 0.5 % of eka-manganese from 1 kg of columbite.[10] They identified the elements by means of X-ray spectroscopy and named the elements rhenium (according to the river Rhine) and masurium (according to Masuren, the homeland of W. Noddack), respectively. However, the question arises why it took that long to isolate the last unknown stable element. Retrospectively, previous attempts by several other researchers were destined to fail, as they believed in a chemical similarity of eka- and dwi-manganese with its superposed congener manganese.[11, 12] The Noddacks applied the diagonal relationship for the 2nd and 3rd row in the d-block elements and assumed a chemical similarity to chromium and molybdenum instead. That innovative application of the periodic table made it possible to predict the chemical behavior and finally concentrate the new elements from samples despite the extremely low concentration of 2×10^{-7} (rhenium in columbite) and 8×10^{-7} wt% (platinum ores) [13].

Following their publication on the discovery of rhenium, a heated debate concerning the correctness of the results flared up. Prandtl[14] and Zvjaginstsev[15] proclaimed the complete absence of the disputed elements in columbites and platinum ores. A British group (Druce and Loring)[16] and Czech scientists (Heyrowsky, Dolejek)[17] claimed the presence of rhenium in salts of manganese, which stands in contrast to the assumed diagonal relationship of the physico-chemical properties of the higher congeners of manganese. In response, the Noddacks applied the published extraction procedure of Loring and Druce on several commercial manganese salts and demonstrated the absence of detectable amounts of the dvi-manganese. They went even further and stated that the applied procedure is not suitable for isolating rhenium but to ensure the removal of even traces of the desired elements.[18] The dispute was settled as the German researchers were able to isolate 1 g of pure rhenium in 1929[19], so that it is officially included in the list of elements by the “Deutsche Atomgewichts-Kommission” in 1930.[20] Finally, Heyrowsky proved wrong the presence of significant amounts of rhenium in manganese salts. In their initial publication, he applied the new technique of polarography to identify the element. Using pure samples of potassium perrhenate, he was able to assign the observed signal to impurities. He demonstrated that even traces of > 1 ppm Re result in a characteristic signal induced by the deposition of catalytically active rhenium on the used dropping mercury cathode rendering the method “a sensitive Test for the Absence of Rhenium in Manganese salts”. [21] Despite these findings, Druce stuck to his claim to have isolated the element from manganese salts as published in his book “Rhenium” from 1948.[22] A verification of these results is not possible nowadays as the original raw materials are not available and manganese salts had a lot of fluctuating impurities by that time.[23] Therefore, there are still several publications citing both the raw materials used by the Noddacks and manganese salts as initial rhenium source, despite the negative results by Heyrowsky and the scarce abundance of rhenium in the latter feedstock.[23]

Another twist of history occurred as the element rhenium had been isolated prior to the Noddacks, by the group of Masatake Ogawa in 1908.[24] He was able to separate a sample from thorianite containing a “new element” as suggested by unidentified bands in the optical spectrum. His findings were published describing physico-chemical properties and suggesting the name “Nipponium” (Np).[25] However, a distinct assignment of the element in the periodic table failed since the characterization by X-ray spectroscopy was not invented yet.[26] Due to the low amount of sample and its low purity, he determined gravimetrically an atomic mass of 100 assigning the newly found element to the gap between molybdenum and ruthenium. Due to Ogawa’s election to the President of Tohoku Imperial University, the work was not continued until 1930 when he subjected his Nipponium samples to X-ray spectroscopy. Finally, the measurement clearly showed that he found rhenium instead of the assumed element with atomic number 43 (Tc). His sudden death in 1930 prevented the publication of the results, so that the real nature of Ogawa’s Nipponium was only revealed in the late 20th century.[24, 27]

2. Rhenium: From feedstock to application

Rhenium is one of the rarest elements with an abundance of < 1 ppb in the earth crust.[28-30] Two rhenium containing minerals are known, rheniite (ReS₂), found in hot-gas fumarols of the volcano Kudriav in Russia[31] and tarkianite discovered in the Hiture Nickel Mine in Finland.[32] Even though both minerals contain high amounts of the rare element, they are of no industrial relevance due to their extremely low abundance. The current production of rhenium is focused on its recovery from flue dust obtained from roasting molybdenite or as a by-product from the recovery of molybdenum from porphyry copper deposits.[33, 34] These feedstocks contain relatively high amounts of rhenium as it substitutes molybdenum isomorphically.[35] Very recently, a new deposit of rhenium has been identified in wolframite in Russias far east with a relatively high rhenium content of 2.9 – 3.5 %.[36]

Other sources with contents of at least 1 ppm Re like uranium deposits and gadolinite are of low relevance.[37]

Table 1: Known deposits of rhenium with a content of at least 1 ppm.[38]

Rhenium deposits	Formula	Rhenium content
Rheniite	ReS ₂	74 %
Tarkianite	(Cu,Fe)(Re,Mo) ₄ S ₈	49-56 %
Molybdenite	MoS ₂	< 10 ppm – 11.5 %
Wolframite	(Fe,Mn)(W,Nb,Re)O ₄	2.9 – 3.5 %
Castaingite	CuMo ₂ S ₅	up to 1 %
Uraninite	UO ₂	up to 0.27 %
Gadolinite	Y ₂ Fe ²⁺ Be ₂ Si ₂ O ₁₀	up to 1 ppm

As the production of rhenium is strongly linked to the copper and molybdenum production, it is a typical “by-product metal”. Consequently, its price is a good indicator for incisive political events and the development of new applications. The absolute values of the here presented prices (Figure 2) should be handled with care as most of the rhenium is traded in long-term contracts between the producer and customers.[35] In 1925, the costs for the first gram of rhenium are estimated to 15000 \$. However, the price soon dropped significantly due to the first technical preparation from molybdenite developed by W. Feit.[39]

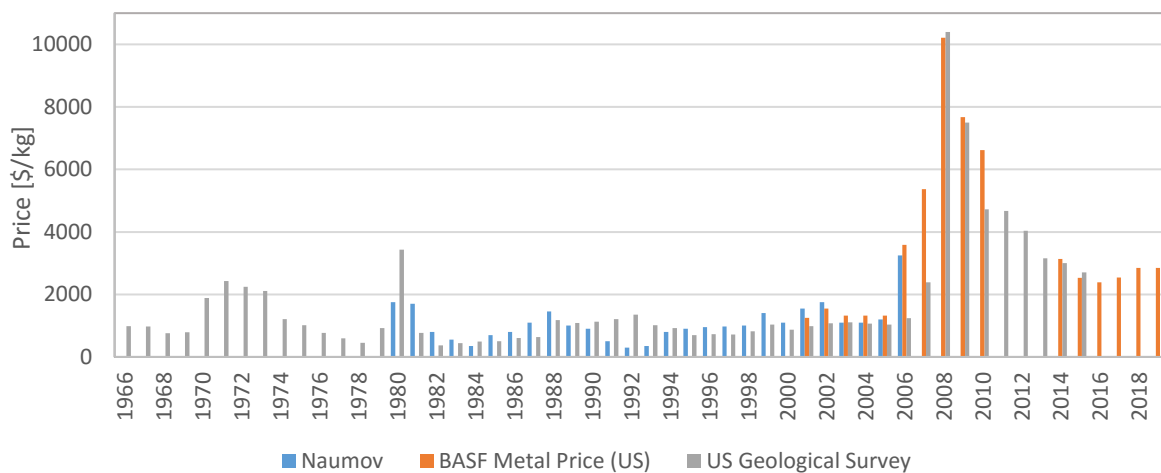


Figure 2: Price development of rhenium from 1966 to 2019 as obtained from Naumov[35], US Geological Survey (USGS) (Polyak)[40] and BASF Catalysts metal price (US)[41]. Between 2011 and 2013, the BASF metal prices are omitted, as they are kept constant during the Lehmann crisis.

After the Second World War, the price was quite constant between 1300 and 1500 \$/kg as its main application was in the relatively small market of alloys for the jackets of fuel elements in nuclear reactors.[35] The first significant increase is observed in 1970, due to the first oil crisis. Even though first experiments using rhenium as catalysts had been carried out already by Fischer and Tropsch in 1930 [42], it took additional 40 years until the first large scale application was developed. Chevron Inc. and Universal Oil Products Inc. were the first companies which apply a highly efficient platinum rhenium catalyst for the production of high-octane lead-free gasoline.[28] The price decreased to 450 \$/kg in 1978 due to the dwindling oil prices and increased production. A similar trend was observed for the Second Oil Crisis in 1979 with a peak price of 3430 \$/kg (USGS) in 1980.

After 1987, the prices rose again as rhenium alloys were found to be excellent heat-resistant alloys for turbine blades jet aircraft engines.[35] The new application would have driven the price strongly as high amounts were needed for the production of modern jets. However, the market was flooded with rhenium by the disintegration of one of the largest producer, the Soviet Union. Within the next decade, the development of new technologies in jet blades (1999, 2003 and 2006)[43] and the need for more efficient airplanes resulted in extremely high prices of over 10000 \$/kg.[28] However, the Lehmann Crisis in 2009, increasing exploitation of rhenium sources and recycling from catalysts and scrap alloys stabilized the price at approximately 2800 \$/kg.[38, 43-45]

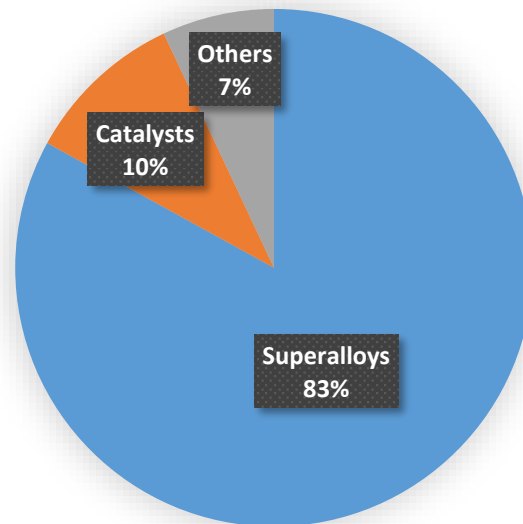


Figure 3: Industrial applications of rhenium (2017).[28] Superalloys: Ni-based alloys for high temperature purposes. Others: Mainly W-Re and Mo-Re alloys.

Currently (2017), rhenium is mainly applied in nickel based “superalloys” despite its high costs (Figure 3). They constitute 83 % of the usage worldwide due to their pronounced hardness and stability, especially at high temperatures.[46, 47] The rhenium content varies from 3 % (2nd generation) to nowadays 6.4 % (6th generation).[46] The main applications are turbine blades for aerospace and gas turbines, as well as heat shield for the reentry of spacecrafts and in nuclear reactors.

The second major field of application are catalysts for industrially relevant heterogeneous processes:

- Rheniform process: Chevron Research Ltd. developed a bimetallic platinum rhenium catalyst on a porous carrier material for the refinement of low value alkanes to high-octane aromatic compounds.[48-52] The catalyst is superior to the previously applied Pt catalyst due to a higher thermal stability, higher selectivity towards desired fractions and its resistance against sulfur poisoning.
- Olefin metathesis: High activities even at low temperatures are achieved using Re_2O_7 on a γ -alumina support for the production of both, low and high weight olefins, depending on the current demand.[53-55] Other applications include the production of polymers *via* Ring-Opening Metathesis Polymerization (ROMP) or the synthesis of fine chemicals as the fragrance Globanon[®] (cyclohexadecenone).[56] By addition of $(\text{Me})_4\text{Sn}$, the reactivity of the catalyst is enhanced so that also functionalized olefins like fatty acids are reacted.[57]
- The selective oxidation of primary alcohols is achieved using rhenium thin films or oxides on a carrier material giving the important solvent dimethoxymethane from methanol.[58-60] The major advantage to the state of the art industrially applied process, the catalytic distillation, is the circumvention of formaldehyde as raw material.[61, 62]

- Application as co-catalyst or promotor in e.g. the Fischer-Tropsch process combined with a cobalt catalyst[63, 64] and the epoxidation of ethylene combined with silver.[65]

Other applications (Figure 3, others) are tungsten and molybdenum based alloys featuring high melting points, high wear resistance, chemical stability and resistance against arc erosion. Therefore, they are applied in thermocouples (up to 2200 °C), in electrical contacts or as ignitor wires in photoflash bulbs for photography.[66] For chemists these materials are of high importance as they are applied in filaments of mass spectrometers and as targets in X-ray tubes.[66]

Beside its application in catalysts or materials, rhenium based radiopharmaceutical compounds are an emerging field. Rhenium has two isotopes of interest, Re-186 ($t_{1/2} = 3.68$ days) and Re-188 ($t_{1/2} = 16.98$ h). Both are β^- emitters with an energy of 1.07 MeV and 2.12 MeV and a γ component of 137 keV (9 % abundance) and 155 keV (15 % abundance), respectively.[67] Therefore, both isotopes are suitable for a theranostic approach, whereat the β^- emission accounts for the therapeutic effect and the γ component for monitoring by SPECT (Single-photon emission computed tomography). The application of Re-186 is limited as it is produced in nuclear reactors by neutron capture from Re-185.[68] In contrast, the isotope Re-188 is easily accessible *via* W-188 generator. Currently, the production of the mother nuclide is limited to three high flux reactors (at least 10^{15} n. $\text{cm}^{-2} \text{s}^{-1}$),[69] whereat the most powerful reactor in Germany, the FRM-II at Garching bei München (8×10^{14} n. $\text{cm}^{-2} \text{s}^{-1}$), would be also a potential source.[70, 71] Since the Re-188 generator is reasonably available only for about 20 years, the research of rhenium based radiopharmaceuticals is relatively new. However, a rapid development is observed in that research field with several compounds ready for clinical trials due to the similarity of its chemistry to its lighter homologue Tc.[67, 72, 73]

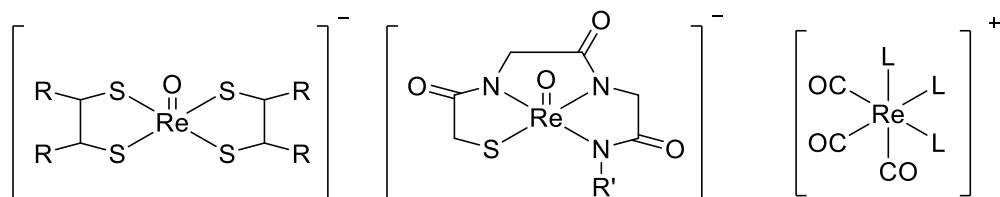


Figure 4: Most common motifs for rhenium based radiopharmaceuticals like Re(V) oxo compounds with *N*- or *S*-donors like dithioethane derivatives and the established MAG_3 (mercaptoacetyltriglycine) ligand or Re(I) tricarbonyl compounds ($L = N$ - or O -donors, or $(L)_3 = \eta^5$ -cyclopentadienyl derivatives).[74, 75]

Hot¹ perrhenate is directly obtained from the W-188 generator and applied in combination with sulfide colloids for the treatment of rheumatoid diseases.[73] However, the most common motifs are obtained by reduction of perrhenate giving low valent rhenium compounds inspired by previously developed technetium compounds.[74, 76] The first class bears a rhenium(V)oxo core which is ligated by *S*- or *N*-donors. Re-DMSA (Dimercaptosuccinic acid, Figure 4, left – $R = \text{COOH}$) is applied for medullary thyroid carcinoma[74] and Re-HEDP (hydroxyethylidene bisphosphonate) for the palliative treatment of bone metastasis[77]. Other selective treatments for cancer are developed using monoclonal antibodies (mAbs) in which the radioactive rhenium is attached either unselectively (bonding to sulfide groups in the antibody) or *via* complexation by ligands like MAG_3 (Figure 4, center) and consecutive ligation to the mAb.[74, 78] The second class bears a Re(I)(CO)₃ core (Figure 4, right) whereas the selectivity to various types of cancer is modulated by the remaining ligands (L).[79] Similar to the first class, ligands bearing a bisphosphonate are applied for the palliative treatment of bone metastasis. An attachment to mAbs is obtained *via* chelators bearing *N*- or *S*-donors or *via* functionalized Cp moieties.[75] The major advantages of the Re(I)(CO)₃ core are its high chemical stability and the facile synthesis of the compounds as they are obtained by replacement of labile aqua

¹ Radioactive perrhenate

ligands from the reactant *fac*-[Re(CO)₃(H₂O)₃]. More recently, anticancer agents using “cold” rhenium are developed.[80] These compounds are mainly based on the Re(I)(CO)₃ core and mostly exhibit photo luminescent properties facilitating the elucidation of their mode of action by *in-vivo* fluorescence spectroscopy[81] or the development of light-induced anticancer agents which are activated *in-vivo* by irradiation with visible light applicable in the photodynamic therapy.[82]

3. The Chemistry of Rhenium Oxides

As implied by its position in group 7 of the periodic table, rhenium exhibits a rich redox chemistry with oxidation states from -III to +VII.[83] In contrast to manganese, the oxidation state +II is very uncommon and high valent species are much more stable. The oxides are of high importance as they are the most common precursor for catalyst preparation or the synthesis of metalorganic compounds. The chemistry of the oxides with rhenium in the oxidation state +IV, +VI and +VII is well elaborated. In contrast, very little is known on the instable and hardly accessible analogues in the oxidation states +III and +V (Table 2).

Table 2: Coordination geometries of rhenium in the known rhenium oxides in the oxidation states III – VII. Important oxides are printed in bold.[83-85]

	Re₂O₇	ReO₃	Re ₂ O ₅	ReO₂	Re ₂ O ₃ *2 H ₂ O
Oxidation state	VII	VI	V	IV	III
Coordination number	4/6	6	6	6	
Coordination geometry	Tetrahedral/ distorted octahedral	Octahedral	Distorted tetragonal pyramidal	Octahedral	amorphous
Structure analogue	-	Perowskit	Vanadium pentoxide	Rutil	
Color	Yellow	Red	Blue	Dark blue/black	Black

3.1. Rhenium(VII)

The most prevalent oxidic rhenium compounds are in the oxidation state +VII with rhenium heptoxide as its binary compound. Re₂O₇ is a yellow powder with a melting point of 300.3 °C and can be distilled without decomposition at a boiling point of 360.3 °C (ambient pressure).[83] The compound is very stable in the presence of dry air, however, decomposes slowly upon contact to organic compounds or traces of water. It is very hygroscopic und dissolves in water yielding perrhenic acid. Its salts, the perrhenates, are very stable compounds due to their highly symmetric, tetrahedral structure (Figure 5, **e**). The volatility of the oxide and stability of the perrhenates is exploited in the commercial production of rhenium. The flue dusts from the copper or molybdenum production are roasted in a stream of oxygen. The volatile oxides of rhenium or associated platinates like osmium are distilled off and captured either on carbon filters or by wet dust trapping.[86] The separation of the platinates is achieved by the fast and irreversible solvation of Re₂O₇ even in acidic aqueous solutions. In contrast, the latter compounds have to be trapped as hydroxide complexes in so-called “osmium-traps” containing sodium or potassium hydroxide.[83] On a laboratory scale, high purity Re₂O₇ is synthesized more conveniently by oxidation of rhenium metal or lower oxides in a stream of oxygen followed by multiple sublimation steps.

In the gas phase, rhenium heptoxide resembles a molecular species with a formula of Re₂O₇. [87] Two ReO₄ tetrahedra are interconnected by one bridging oxygen (Figure 5, **b**). The Re-O-Re angle has been

a point of discussion since early results by electron diffraction (GED) studies pointed to a nearly linear conformation[88] in contrast to extensive studies on the vibrational spectra of Re_2O_7 vapor.[89, 90] In 1992, Herrmann *et al.* reinvestigated the structure by GED and determined a bent structure with an Re-O-Re angle of $143.6(9)^\circ$.[91, 92] Recently, this study was challenged by DFT calculations on a PBE-GGA//def2-TZVP/scECP level of theory resulting in a nearly linear (179.3°) ground state structure. The authors argue that the experimentally determined values (vibrational and electron diffraction) resemble the molecule in an excited state as the experiments are conducted at elevated temperatures ($\sim 300^\circ\text{C}$ for the vibrational determination and 230°C for GED).[93] Own calculations using various functionals, basis sets and methods for the treatment of relativistic effects result in various angles from 151.0° to nearly linear (see Appendix I). Even though the structure depends strongly on the selected DFT method (due to a flat potential energy surface), all sophisticated methods (B2PLYP-D3/ZORA or PBE0/ZORA) agree to a linear structure. However, the increase in symmetry results in a significant lower contributions of the rotational entropy explaining the experimentally derived bent structure.

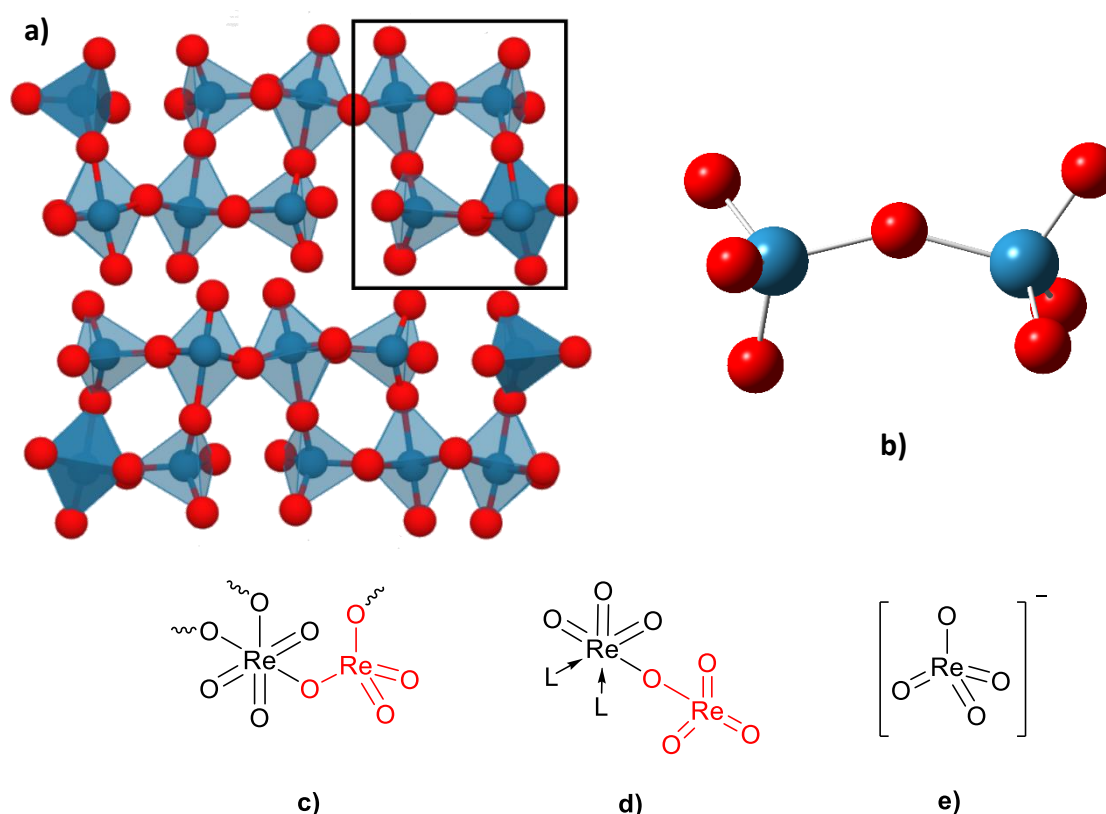
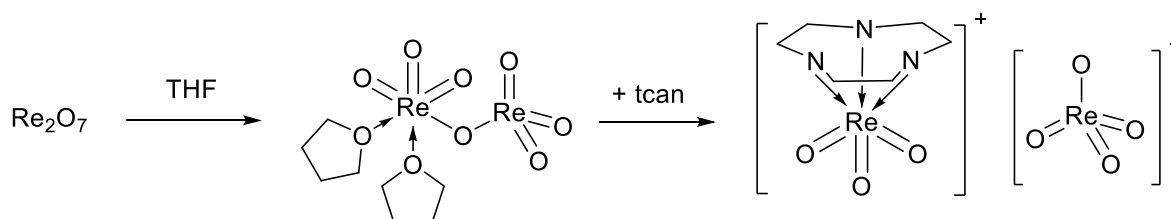


Figure 5: a) Crystal structure of rhenium heptoxide consisting of distorted octahedral ReO_6 units interconnected by distorted tetrahedral ReO_4 units. (Re: blue, O: red; CC-BY 4.0 license)[94] b) Symmetric structure of Re_2O_7 in the gas phase (B97D3/SDD//SDD (Re), def2TZVP (O)). c) Schematic representation of a Re_2O_7 unit in the crystal structure. The tetrahedral unit is marked red. d) Structure of dissolved Re_2O_7 in donor solvents ($L = \text{MeCN}, \text{THF}, \text{DMF}, \dots$). e) Structure of perrhenate formed upon dissolution of rhenium heptoxide in water.

In liquid as well as quickly condensed rhenium heptoxide (white Re_2O_7 – erroneously described as the peroxide Re_2O_8 in early literature)[95] the molecular structure is retained. In contrast, the crystalline oxide exhibits a unique polymeric crystal structure with an equal number of tetrahedral ReO_4 units and strongly distorted octahedral ReO_6 units.[96] The structure of solid Re_2O_7 differs significantly from other molecular metal oxides e.g. OsO_4 , Tc_2O_7 or Mn_2O_7 which contain isolated molecules in solid state.[83, 96] The structure of Re_2O_7 consists of rectangular subunits of four polyhedrons, which are interconnected through corners of the octahedrons (Figure 5 a)). The three-dimensional structure is

formed *via* layers with only oxygen-oxygen Van-der-Waals contacts. The Re-O bond distances range between 165.0 – 174.2 pm (terminal) and 172.5 – 216.0 pm (bridging).[97]

The oxide dissolves undecomposed exclusively in aprotic donor solvents like acetonitrile, THF or dioxane upon formation of solvent complexes best described by the formula of $L_2ReO_3(ReO_4)$ (Figure 5, **d**). The single known exception are complexes with the solvent pyridine, which incorporate an additional solvent molecule. It weakly coordinates to the ReO_4 moiety resulting in a distorted trigonal bipyramidal structure. Due to the induced steric hindrance the Re-O-Re angle is decreased to $136.2(4)^\circ$. [98] A similar compound is formed upon contact with moisture, giving solid perrhenic acid $(H_2O)_2Re_2O_7$ whose chemical and physical properties differ significantly from aqueous perrhenic acid $HReO_{4(aq)}$. The structure of solid perrhenic is described representatively. Its ReO_3 core is coordinated by two molecules of water ($Re-O(H_2O) = 221$ pm) and a nearly symmetrical ReO_4 unit ($r(Re-O)$ terminal = 173-177 pm and $r(Re-O) = 180$ pm for $L = H_2O$) with a linear Re-O-Re bond and a Re-O(ReO_4) bond length of 210 pm.[99] The asymmetric structure consisting of a positively charged ReO_3 entity coordinated by a negatively charged ReO_4 moiety is indicative for the reactivity of dissolved Re_2O_7 . Upon cleavage, one equivalent of the stable perrhenate is formed releasing a highly reactive $[ReO_3]^+$ moiety, suitable for the synthesis of metalorganic compounds (see 5.1). The intermediary formation of the perrhenyl cation upon heterolysis of Re_2O_7 has been proven by Herrmann *et al.* by trapping the fragment with appropriate tridentate N- or S-donor ligands such as 1,4,7-triazacyclononane (tcn).[100]



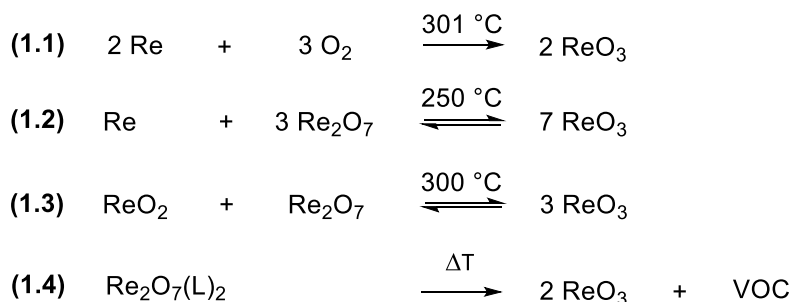
Scheme 1: Stabilization of the ReO_3^+ cation by 1,4,7-triazacyclononane in THF.

3.2. Rhenium(VI)

The most stable compound in the oxidation state +VI is the red glinting rhenium trioxide.[96] The first developed methods for its synthesis are reacting either rhenium metal or $Re(IV)$ oxide with Re_2O_7 as oxidant or the direct oxidation using oxygen (Scheme 2, **(1.1 - 1.3)**). [101, 102] The direct oxidation using oxygen is highly dependent on its stoichiometry as discrepancies result either in over-oxidation or in mixtures of rhenium metal, ReO_2 and the desired product. The solid-state reactions **(1.2 - 1.3)** have very long reaction times and yield impure products due to the limited interface between both reactants. Furthermore, the oxidation is usually incomplete as volatile Re_2O_7 escapes the reaction medium giving a product with the formal sum ReO_{3-x} with $x \approx 0 - 0.2$. [101] The problems are substantially reduced by repeated milling of the reaction mixture, stepwise addition of the oxidant Re_2O_7 or the application of closed reaction vessels like ampoules.[101, 102] Higher reaction temperatures in order to reduce the reaction time are not feasible as the oxidation states +VII, +VI and +IV are in equilibrium, so that the product would decompose significantly at $\sim 400^\circ C$ to the starting materials Re_2O_7 and ReO_2 (Scheme 2, **(1.3)** reversed).[83]

A more convenient method for its preparation is the thermal decomposition of solvent complexes of Re_2O_7 with ethers like DME, THF or dioxane **(1.4)**. [103] These precursors are stable at room temperature and therefore yield products of very high purity. Dioxane is the best choice as a suitable precursor for ReO_3 is formed despite presence of water. In dried dioxane a complex is formed with the formula $L_2Re_2O_7$ and in slightly wet dioxane solid perrhenic acid.[87, 104] The formation of ReO_3 starts already at temperatures above $105^\circ C$, whereas highest purities are achieved at $180^\circ C$. [104] In order

to obtain a product in very high purity for special purposes, ReO_3 is purified *via* a vapor transport reaction in the presence of an excess of iodine at 370 °C.[96, 105]



Scheme 2: Methods for the preparation of ReO_3 with the respective reaction temperatures given in literature. (1.4): L = ethers like THF, DME or dioxane; VOC (volatile organic compounds) summarizes the decomposition products of the respective ethers like the respective ligands, aldehydes, oxalic acid or carbon oxides.[103]

The crystal structure of ReO_3 consists of polymeric octahedral ReO_6 subunits sharing the oxygen atoms in all three directions in space (Figure 6).[106] The structure is derived from the perovskite CaTiO_3 without the central calcium cation. Rhenium is aligned in the corners forming a cubic primitive cell and the oxygen atoms are centralized on the edges. The structure is unique among the binary oxides of the type AB_3 like WO_3 , MoO_3 or CrO_3 as these compounds form either polymeric chains of MO_4 tetrahedrons (Cr) or (highly) distorted octahedrons (Mo and W).[83]

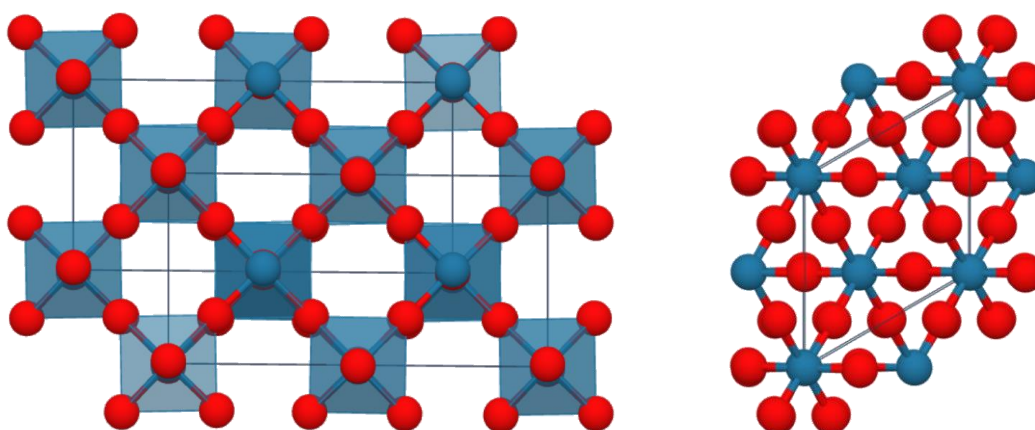


Figure 6: Crystal structure of $\alpha\text{-ReO}_3$. Re (blue) is arranged in a cubic primitive package and surrounded octahedrally by oxygen (red). Obtained from Materials Project.[107] (CC-BY 4.0)

Despite its electron configuration of $[\text{Xe}]5d^1$, the compound is diamagnetic as the valence electron is located in a conduction band.[108] The oxide behaves like a metal and its resistivity increases linearly with increasing temperature. At room temperature, its conductivity is roughly the same as for other transition metals like Ti or Cr and only ten times lower than that of copper with a value of $5.5 \times 10^4 \Omega^{-1}\text{cm}^{-1}$. [96, 109] The band structure is investigated by optical reflectance. A free-electron-like region is detected up to the sharp plasma edge at 2.3 eV (green) where interband transitions begin. This explains both the red color and the metallic luster of the oxide.[110] Since the discovery of the metallic properties of ReO_3 in 1965, its perovskite like structure became an archetype for the development of very important compounds. Examples include ferromagnetic compounds such as Cu_3N or SrRuO_3 , both used for data storage, the magneto-resistive $(\text{La}_x\text{Sr}_{1-x})\text{MnO}_3$ used in sensors or the superconducting $\text{YBa}_2\text{Cu}_3\text{O}_7$. [111]

At room temperature, ReO_3 is very stable. It is insoluble in organic solvents, acids or weak bases.[83] In strong alkalis, metastable green rhenates (ReO_4^{2-}) are formed which dismutate into perrhenate and

rhenium(IV) oxyhydrate. The equivalent in solid-state, the rhenium bronzes ($X_{1-y}Re_yO_3$ with $X = Na, K$ and $0 < y < 1$), are stable conductors with a golden metallic luster (cubic modification) in analogy to the well-known tungsten bronzes.[112] These compounds are of low importance due to the lack of reliable synthetic protocols. More importantly, ReO_3 forms hydrogen rhenium bronzes upon dissolution of hydrogen into their crystal lattice.[113, 114] They are suggested to participate in the catalytic hydrogenation using elemental hydrogen with both Re(VII) and Re(VI) as catalyst precursor.[115, 116]

3.3. Rhenium(IV)

The third stable rhenium oxide is formed in the oxidation state +IV. Its hydrate is synthesized in a colloidal form by solvolysis of rhenium(IV) halides in water or the chemical or electrochemical reduction of perrhenates.[117-119] After separation, the anhydrous blackish blue ReO_2 is obtained by heating under exclusion of oxygen as they are easily oxidized at elevated temperatures.[117] A straightforward synthesis is achieved by pyrolysis of NH_4ReO_4 or the oxidation of rhenium metal. Suitable oxidants are Re_2O_7 at 600 °C, ReO_3 at 500 °C or elemental oxygen at 300-700 °C.[83, 96, 117] Due to overoxidation, the obtained products usually have an approximate composition of $ReO_{2.2}$. [101] High purity ReO_2 and single crystals are obtained by vapor transport using iodine or more conveniently $HgCl_2$ above 900 °C.[120] Further elevated temperatures are disadvantageous as the compound decomposes at 900 °C due to disproportionation into rhenium metal and Re_2O_7 . [83, 102]

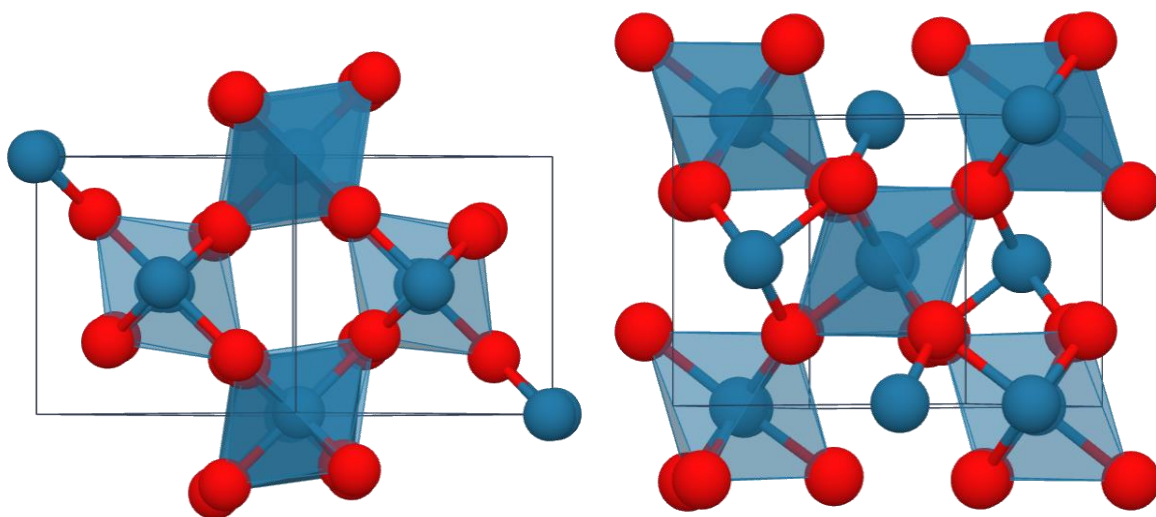


Figure 7: The monoclinic $\alpha-ReO_2$ (left) and the orthorhombic $\beta-ReO_2$ (right) modification of rhenium(IV) oxide. Obtained from Materials Project.[121] (CC-BY 4.0)

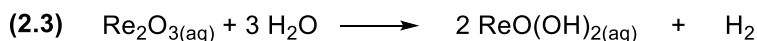
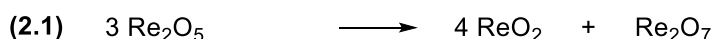
Rhenium dioxide is the single binary rhenium oxide with two known low pressure modifications. At temperatures below 300 °C, a microcrystalline powder of monoclinic $\alpha-ReO_2$ is obtained. The compound is isostructural to MoO_2 or WO_2 (distorted rutile) with corner sharing distorted ReO_6 octahedrons.[122] The ReO_6 units are tilted by 38-50° resulting in short Re-Re distances of 249 pm.[123] At elevated temperatures, the orthorhombic modification $\beta-ReO_2$ is irreversibly formed.[101, 123] The structure is very similar to its low temperature modification, however, the ReO_6 units are not tilted resulting in elongated Re-Re distances of 261 pm (Figure 7 (right)). Both Re-Re distances are akin to metal-metal bonds accounting for the conductive properties of both oxides. The highest conductivity is determined for single crystals of the orthorhombic modification $\beta-ReO_2$ with $10^4 \Omega^{-1}cm^{-1}$ which is only 5 times lower than for ReO_3 . [122]

ReO_2 is insoluble in organic solvents, which is in analogy to its congener in the oxidation state +VI. In aqueous solutions, one might suspect a higher solubility due to the facile formation of its hydrate. However, most of the hydrate forms colloids and after filtration a maximal solubility of $10^{-6} mol L^{-1}$ is

obtained.[124] Even in a supercritical 1 M KCl_{aq} solution at 510 °C, only $2 \times 10^{-4} \text{ mol L}^{-1}$ are achieved.[125] In a pH range between 2.2 to 8/9, the solubility is constant, indicating a low acidity of the hydrate. At higher pH values, an increasing rhenium concentration is determined suggesting the formation of hydroxide complexes. The dissolved rhenium(IV) oxides are relatively stable towards oxidation as the concentration is independent towards the presence of oxygen even after 14 days of exposure.[124] The corresponding anions, the rhenates (“rhenite”), are formed upon the reaction of ReO_2 in strong fused alkalis. The formed compounds are very prone to oxidation and only isolated in solid state.[96]

3.4. Rhenium(V) and (III)

The chemistry of the oxides of rhenium in the oxidation state +V and +III is less developed due to their instability and synthetic inaccessibility. In the presence of oxygen, both compounds are oxidized unselectively. In anoxic conditions, both binary oxides decompose upon dismutation (Scheme 3).



Scheme 3: Decomposition of rhenium(V) and (III) oxide upon dismutation. For Re_2O_3 , only its hydrates are known with $n = 2$ or 3. In aqueous solutions, Re_2O_3 reacts with water to Re(IV)oxide hydrate upon formation of hydrogen.

Re_2O_5 is synthesized by the electrolytic reduction of perrhenate in 72 wt%/12 M sulfuric acid. The obtained product is strongly contaminated by the electrolyte and its purification is compromised by its decomposition, giving ReO_2 and Re_2O_7 (Scheme 3 (2.1)). The chemical reduction of perrhenate is not feasible as the products are very impure.[96] A crystalline sample can be obtained by carefully oxidizing $\text{ReO}_2 \cdot \text{H}_2\text{O}$ with 1 % oxygen in nitrogen at a temperature of 80-200 °C and consecutive sublimation.[84] The compound contains decomposition products, however, microcrystals of pure Re_2O_5 are identified using an electron microscope so that its crystal structure is determined by micro X-ray diffraction. The measurement are of low quality due to constant decomposition revealing a vanadium pentoxide like structure.[84]

Oxidic species with rhenium in the oxidation state +III are more common than for +V. The black amorphous hydrate is obtained in anoxic conditions upon hydrolysis of ReCl_3 or the reduction of NH_4ReO_4 with NaBH_4 . [85, 126] The synthesis of the anhydrous oxide fails as the compound dismutates to elemental rhenium and ReO_2 (2.2). Whereat no information is available on its solubility in organic solvents, its water chemistry is well elaborated. In anoxic conditions, its solubility is more than 10 times higher than for ReO_2 with a maximal concentration of $1.2 \times 10^{-5} \text{ mol L}^{-1}$. Exposure to oxygen increases the rhenium concentration significantly, but mostly due to the formation of the very soluble perrhenate.[124] The nature of the dissolved species is unclear, as it reacts with water forming $\text{ReO}(\text{OH})_2(\text{aq})$ and H_2 (2.3). Therefore, the higher solubility of the oxide has to be also ascribed at least partially to dissolved Re(IV) species.[124]

3.5. Rhenium Nanoparticles

The chemistry of bulk rhenium oxides is well established since the discovery of the element in 1925. Since the beginning of the 21st century, the new field of (oxidic) rhenium nanoparticles (NPs) emerges with various compositions, morphologies, synthetic strategies and applications. A comparison of the published results is complicated as often the characterization of the NPs is incomplete and the articles are focused on completely different topics in chemistry. Therefore, a distinct structure-property

relationship as known for the bulk metal oxides cannot be given. In the following, all published results² of rhenium (0) and oxidic nanoparticles are summarized in order to outline the importance of these compounds.

The chemistry of supported rhenium NPs (Table 3) and isolated ones (Table 4) has to be discussed separately. Supported Re NPs are easily obtained as they are formed by impregnation of the support materials and consecutive calcination. For inorganic supports, the oxidation state of the metal is easily adjusted as harsh conditions can be applied. Re(0) NPs are obtained either by thermal decomposition of a $\text{Re}_2(\text{CO})_{10}$ (**T3.1-3**) or impregnation with NH_4ReO_4 and consecutive reduction with elemental hydrogen (**T3.4-5**). In the case of more instable supports like DNA (Deoxyribonucleic acid) or PAH (Polyallylamine hydrochloride) the mild reductant NaBH_4 is applied (**T3.6-7**). Re(0) NPs are active in catalytic reduction reactions of chromium(VI), nitro compounds, lignin derived phenols, succinic acid and water (electrocatalysis). The metallic NPs can also be applied as SERS (signal enhanced Raman scattering) probe for the detection of e.g. organic contamination in wastewater (**T3.6-8**). Beside the here discussed monometallic rhenium NPs there are numerous reports on bimetallic NPs, especially for platinum metals-Re alloy NPs in reforming catalysts[127-134] or Au-Re NPs for SERS[135, 136].

Oxidic supported NPs are obtained with Re in various oxidation states from +IV to +VII. The most common precursor is NH_4ReO_4 , which is decomposed upon calcination at temperatures above 290 °C (**T3.12-16**). These particles are active in oxidation reactions like the dehydrogenation of alcohols, deoxydehydration (DODH) of diols or in the fragmentation of lignin or lignin derived phenols.

Table 3: Published supported rhenium nanoparticles ordered by the oxidation state of the metal. * Oxidation state as given in the publication even though the synthetic method cannot yield Re(0). ** Oxidation state uncertain as the XPS narrow scan is not given. *** Only the oxidation state +VII is identified by EXAFS/XANES. PTFE (Polytetrafluoroethylene), CNT (Carbon Nanotube).

Entry	Oxidation state	Support Material	Precursor	Synthetic Strategy	Application	Citation
T3.1	Re (0)	PTFE	$\text{Re}_2(\text{CO})_{10}$	Thermal (290 °C)	-	[137]
T3.2		CNTs	$\text{Re}_2(\text{CO})_{10}$	Thermal (420 °C)	-	[138]
T3.3		Ordered mesoporous carbon	$\text{Re}_2(\text{CO})_{10}$	Microwave irradiation	Catalytic reduction of aromatic nitro compounds	[139]
T3.4		$\gamma\text{-Al}_2\text{O}_3$	NH_4ReO_4	Wet impregnation ^[140] and reduction (H_2 at 500 °C)	Model compound for reforming catalysts	[141]
T3.5		SiO_2	NH_4ReO_4	Wet impregnation and reduction (H_2 at 400 °C)	Catalytic hydrodeoxygenation of guaiacol	[142]
T3.6		PAH	NH_4ReO_4	Chemical (NaBH_4 at 0 °C)	Catalytic reduction of aromatic nitro compounds, SERS	[143]
T3.7		DNA	NH_4ReO_4	Chemical (NaBH_4 at RT)	Catalytic reduction of aromatic nitro compounds and Cr(VI) compounds, SERS	[144, 145]
T3.8		Phosphazene	KReO_4	Thermal (up to 800 °C)	SERS	[146]

² Scifinder: Search for scientific publications with: "Rhenium AND Nano", "Rhenium AND Nanoparticles", "Rhenium AND Nanocubes", "Rhenium AND Nanowires". Exception: Two Chinese papers are not included as no translation is available (12.05.2020).

T3.9	*	Si-nanowires	ReCl ₃ *HCl	Wet impregnation only	Electrocatalytic hydrogen evolution reaction	[147]
T3.10		Mesoporous Carbon	ReCl ₅	Wet impregnation and reduction (H ₂ at 450 °C)	Catalytic hydrogenation of succinic acid	[148]
T3.11	+IV	Lignin	Re(CO) ₅ Br	Mechanochemical Lignin as stabilizer and reductant	-	[149]
T3.12		PTFE	NH ₄ ReO ₄	Thermal (290 °C)	-	[137]
T3.13	+VI**	TiO ₂	Re ₂ (CO) ₁₀	Sonication at 80 °C and calcination at 480 °C	Catalytic photodegradation of toluene and acetone	[150]
T3.14	+IV, +VII	SiO ₂	NH ₄ ReO ₄	Wet impregnation, calcination at 300 °C	Catalytic hydrodeoxygenation of guaiacol	[142]
T3.15	+VII***	Al ₂ O ₃	NH ₄ ReO ₄	Wet impregnation, calcination at 300 °C	Catalytic dehydrogenation of alcohols	[151]
T3.16	0, +IV, +VI, +VII	Fe ₃ O ₄	ReCl ₅ NH ₄ ReO ₄	Wet impregnation, calcination and reduction (H ₂ at 450 °C)	Lignin fragmentation	[152]
T3.17	0, +IV, +VII	TiO ₂	NH ₄ ReO ₄	Wet impregnation	Catalytic DODH of diols	[153]

The synthesis of unsupported rhenium NPs is more challenging as most synthetic procedures lack selectivity with regards to size distribution or oxidation state. Harsh conditions as thermal treatment of Re₂(CO)₁₀ leads to agglomeration (**T4.1**), requiring either special solvents like ionic liquids or capping agents like 3-mercaptopropionic acid (3-MPA), polyvinyl pyrrolidone (PVP) or hexadecylamine (HAD) have to be applied (**T4.2-3**). In order to avoid high temperatures, isolated Re(0) NPs are conveniently synthesized by decomposition of the precursor Re₂(CO)₁₀ with pulsed laser or microwave irradiation. Their activity has been tested in the catalytic hydrogenation of cyclohexene and the isomerization of 10-undecene-1-ol. In the latter reaction the oxidation state of the NPs (or at least the reacting surface) is highly doubtful as high temperatures (200 °C) and aerobic conditions are applied.[154]

Very convenient synthetic protocols are available for NPs with rhenium in the oxidation state +VI. ReO₃ nanocubes (NCs) are obtained in the controlled thermal decomposition of Re₂O₇ dioxane or methanol complexes. The crystal structure of these NCs is similar to its bulk congener with octahedral ReO₆ units whereat rhenium is located on the corners of a cubic primitive cell. The NCs have a metallic character, as the valence electron is located in a conduction band. Therefore, they possess a strong localized plasmon resonance (LSPR) resulting in a very high extinction coefficient and a strongly enhanced Rayleigh scattering for wavelengths surpassing the NCs size. The strong absorption is exploited in the photocatalytic decomposition of VOCs in wastewater. The NCs have been shown to act as photosensitizer and catalyst in the degradation of methyl orange, aromatic compounds and acetone (**T3.13** and **T4.7**). Another application of the NCs is a theranostic approach for the treatment of cancer cells or implant related bacterial infections (**T4.8-9**). They concentrate in cells due to the EPR effect (enhanced permeability and retention effect).[155] The incubated cells are easily detected *in vivo* either by CT (computed tomography) and by photoacoustic spectroscopy facilitated by the high atomic mass of Re and the LSPR, respectively. The therapeutic effect is achieved by irradiation with a NIR laser (750 – 850 nm). Due to the LSPR, which results in a high extinction coefficient, the energy is efficiently converted into heat and the cells decompose (photothermal therapy). Furthermore, a high selectivity towards bacteria and malign tissue is induced by the pH dependent stability of the NCs towards

oxidation: The compound degrades in healthy tissue (pH \approx 7.4) by oxidation and formation of soluble perrhenate species but is stable in acidic (pH < 7) and hypoxic media like malign tissue.[156]

Table 4: Published isolated rhenium nanoparticles with and without capping agents in various oxidation states.¹ A clear distinction is not possible due to the broad signal in the XPS narrow scan. NA (not available) CVD (Chemical vapor deposition). [*] Published results obtained during this thesis.

Entry	Oxidation state	Capping Agent	Precursor	Synthetic Strategy	Application	Citation
T4.1	Re(0)		Re ₂ (CO) ₁₀	Thermal (350 – 450 °C)	-	[157]
T4.2			Re ₂ (CO) ₁₀	Microwave irradiation, in ionic liquids	Catalytic hydrogenation	[158]
T4.3		3-MPA	NH ₄ ReO ₄ Re ₂ (CO) ₁₀	Pulsed-Laser decomposition (355 nm)	Catalytic alkenol isomerization	[154]
T4.4		PVP or HDA	Re ₂ (C ₃ H ₅) ₄	Chemical (H ₂ at 120 °C)	-	[159, 160]
T4.5	+VI		ReO ₃ powder	CVD	-	[161]
T4.6			Re ₂ O ₇ -(dioxane) _x	Thermal (200 °C in toluene)	-	[162]
T4.7			Re ₂ O ₇	Thermal (250 °C in methanol)	Catalytic photodegradation of methyl orange	[163]
T4.8			Re ₂ O ₇	Thermal (250 °C in methanol)	<i>In vivo</i> imaging and treatment of implant-related infections	[156, 164]
T4.9			Re ₂ O ₇	Chemical (100 – 260 °C with ethers)	Model for the intercalation of lithium in rhenium based electrode materials	[165]
T4.10	+IV, +VII	Gum arabic	K ₂ ReCl ₆	Chemical (Hydrazine)	-	[166]
T4.11	+II - +IV ¹ , +VI, +VII		K ₂ ReCl ₆	Chemical (NaBH ₄)	-	[167]
T4.12	NA		K ₂ ReCl ₆ NH ₄ ReO ₄	Chemical (NaBH ₄ at 10 – 60 °C)	-	[168]
T4.13	0, +IV		NH ₄ ReO ₄	Thermal/ chemical (180 °C in 1-octanol)	Catalytic dehydrogenation of alcohols	[169]
T4.14	+V - +VII		NH ₄ ReO ₄	Chemical (3-octanol at 180 °C)	Catalytic DODH of polyols	[170]
T4.15	NA	Sodium bis(2-ethylhexyl) sulfosuccinate or isooctane	NH ₄ ReO ₄	Gamma irradiation or chemical (Flavonoids)	-	[171, 172]
T4.16	+III, +IV, +VI, +VII		NaReO ₄	Gamma irradiation	-	[173]
T4.17	+IV, +VI, +VII	oleic acid	Re ₂ O ₇	Chemical (1-octadecene at 200 °C)	Photoluminescence	[174]
T4.18	+IV, +VI, +VII		Re ₂ O ₇	Chemical (aromatic solvent at 135 °C)	Lignin fragmentation β -O-H model substrate	[175][*]

The last group of isolated rhenium NPs contain rhenium in various oxidation states. The publication of such NPs has two reasons: unselective synthetic procedures and/or imprecise determination of the respective oxidation states.

The chemical reduction of K_2ReCl_6 using aqueous solutions/suspensions of both hydrazine and $NaBH_4$ yields NPs in the oxidation states between "+II - +IV" - +VII (**T4.10-12**). For the low oxidation states, a range between +II and +IV is given as a discrimination was prohibited by the quality of the XPS narrow scan.[167] The low selectivity regarding the oxidation state of Re is explained by the various consecutive reactions. First, the precursor is reactive in water so that several different solvation complexes or ReO_2 are potential sources for the NPs.[176] Second, the workup of the NPs is conducted under aerobic conditions so that a consecutive oxidation is not excluded. Third, the oxidation state after the reduction is unclear. One author states that significant amounts of Re(III) might be formed during the reduction which consecutively dismutate or are reoxidized by oxygen yielding high valent Re species.[166] Similar problems are encountered during the chemical reduction of ammonium perrhenate (**T4.13-14**). The thermal decomposition of NH_4ReO_4 should yield Re(IV) oxide particles which can be reduced further by reacting with the solvent 1-octanol. Despite of their reactivity in very similar catalytic reactions (dehydrogenation of alcohols and DODH of diols), the published oxidation states differ significantly. One group[169] states the formation of NPs with an oxidation state between 0 and +IV in contrast to an oxidation state between +V and +VII by a second group[170], using the very same synthetic procedure and analytic techniques (XPS, XAS, EXAFS, XANES). One reason might be the applied analytic techniques: Within this work it could be shown that strong X-ray irradiation reduces oxidic rhenium compounds down to the oxidation state 0.

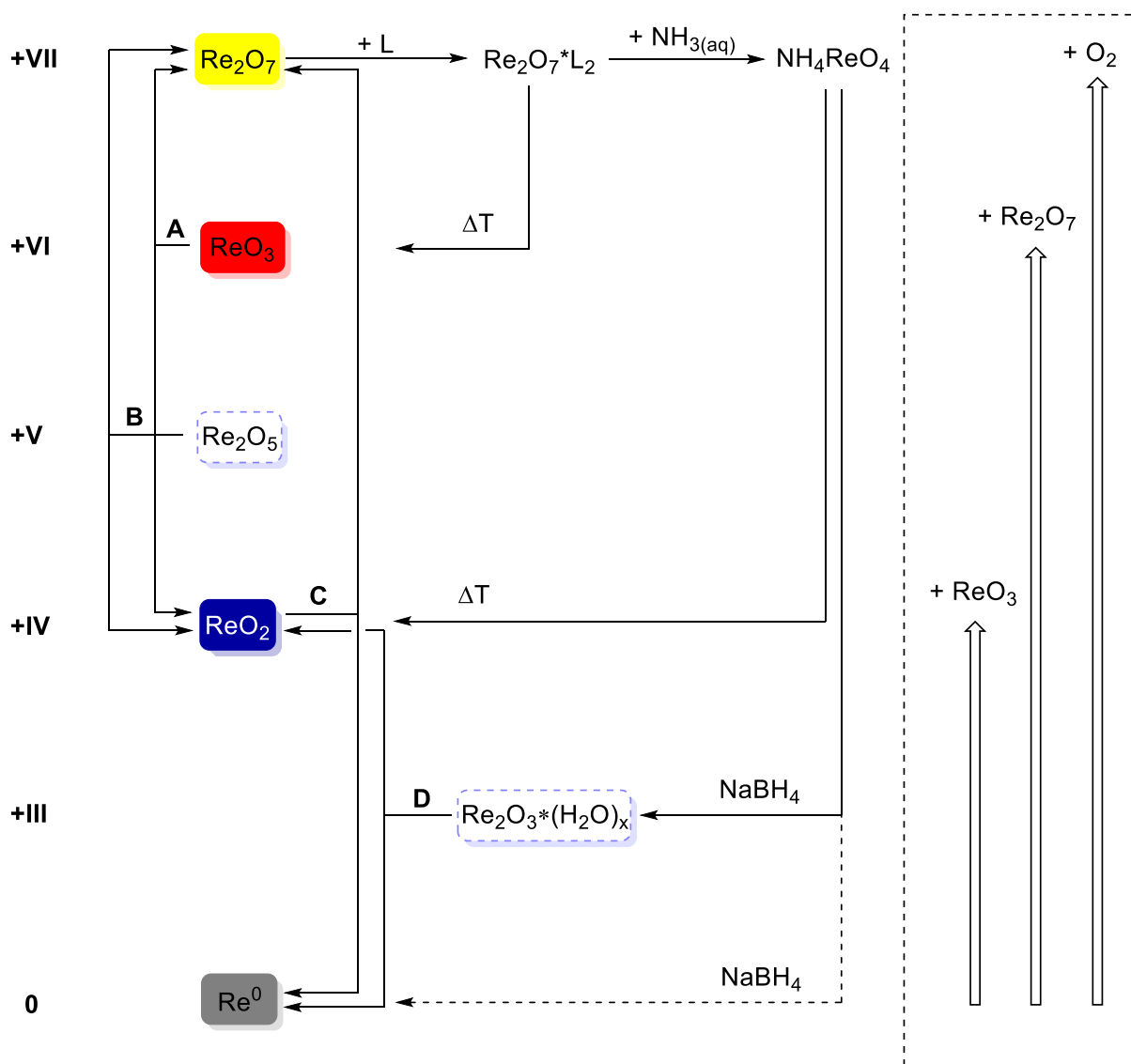
The third synthetic procedure for ReO_x NPs is the reduction of perrhenates by gamma irradiation (**T4.15-16**). Hydroxyl radicals are formed upon irradiation which consecutively reduce the Re(VII) precursor unselectively. Depending on the concentration of the precursor, radiation dose, flux and time different particle sizes and oxidation states are obtained. Therefore, the technique might be applied for the synthesis of tailored particles with the major drawback of the necessity of a Co-60 γ -radiation source. However, a detailed discussion on the oxidation states is prohibited, as its determination is conducted only by electronic spectra.

The last synthetic protocol is based on the inherent instability of Re_2O_7 . The obtained ReO_x particles are generally stable at ambient, aerobic conditions and consist of Re(IV), Re(VI) and Re(VII). In the procedure by Grzybowski *et al.*, the olefin 1-octadecene is applied as reductant and the formed NPs are capped and stabilized by oleic acid. The particles exhibit a tunable photoluminescence over the entire visible spectrum, which is remarkable as such properties have been only achieved by functionalized carbon nanodots.[174] The ReO_x particles have partially a similar structure as the ReO_3 NCs and therefore exhibit a LSPR. Extraordinary photocatalytic properties in the degradation of methyl orange are observed with a higher efficiency as the current benchmark of TiO_2 NPs. A second synthetic procedure for such NPs is developed during this dissertation and is discussed in detail in chapter 6.3. In short, the decomposition of Re_2O_7 in aromatic solvents yields ReO_x NPs, which are the active catalyst in the cleavage of a lignin model substrate, the catalytic dehydration of alcohols and the cleavage of ethers.

3.6. Summary of the Redox Chemistry of Rhenium

The chemistry of rhenium is characterized by its rich redox chemistry in line with its position in group VII of the PSE. Similar reactions are observed for bulk oxides and nanoparticles, however, the reaction conditions differ strongly. Therefore, no reaction conditions are given in Scheme 4.

The compounds are easily transformed by dismutation reactions whereat reactions **A** and **C** are reversible and the decomposition reactions of Re(V) oxide **B** and Re(III) oxide hydrate **D** are irreversible. The thermal decomposition of donor stabilized Re(VII) oxide and NH_4ReO_4 yields Re(VI) oxide and Re(IV) oxide, respectively. A further reduction is achieved with NaBH_4 yielding Re(III) oxide hydrate or elemental rhenium. The latter is only reported for the synthesis of nanoparticles. For the synthesis of high valent rhenium oxides, elemental oxygen or their congeners in higher oxidation states can be applied.



Scheme 4: Overview on the redox chemistry of oxidic rhenium compounds. The different oxides are converted into each other via dismutation reaction (A-D) or by oxidation reactions using higher valent rhenium oxides or elemental oxygen (box, right). Thermal decomposition of Re(VII) compounds or reduction by NaBH_4 yield rhenium in lower oxidation states (top). Ammonium perrhenate is given exemplarily. Stable (filled) and meta-stable (hashed) oxides are marked with their natural color.

4. Metalorganic and Coordination Chemistry of Rhenium

Despite the late discovery of rhenium, its coordination and metalorganic chemistry is well established. Whereat initial approaches in the development of molecular rhenium compounds have not been systematic, seminal works of some researchers have opened up new research fields, which have been studied in depth over the past decades.

Molecular rhenium compounds are isolated in a huge variety of oxidation states from -III to +VII.[96, 177] The synthesis of low valent rhenium compounds has been a severe challenge due to the lack of a suitable synthetic precursor. The picture changed when Walter Hieber developed the synthesis of rhenium pentacarbonyl in 1941.[178] The compound is obtained by reductive carbonylation of rhenium oxides or perrhenates at very high pressures of >360 bar giving varying yields or purities. In 1988, a more convenient method is developed by reductive carbonylation of NaReO₄ in methanol at only 220 bar.[179] Treating Re(CO)₅ with strong reducing agents like alkali metals leads to the formation of alkali pentacarbonyl rhenates(-I) or polynuclear carbonyl rhenate anions.[180] They have been the singly known rhenium compounds in the oxidation state -I until 2020, when Abram *et al.* obtained a second compound of this class bearing three carbonyls and two terphenyl isocyanide ligands.[181] Much more common are rhenium carbonyl compounds in the oxidation state +1. The firstly obtained derivatives are the rhenium pentacarbonyl halogen complexes[182] which are excellent precursors for the synthesis of a huge variety of functional rhenium(I) compounds.[183-211] Upon addition of Lewis bases like amines, pyridines, phosphines or NHCs highly stable compounds are obtained with the formula L₂Re(CO)₃X whereat the halogen can be substituted consecutively by addition of an additional Lewis base like pyridines or isonitriles.[79] Their properties are tailored by careful selection of the respective ligands. Unique photophysical properties are obtained using ligands like annulated pyridines or bipyridines[208-212] which are utilized as photosensitizer in solar cells[212], as probes in medicinal chemistry as tracing agents or for the treatment of cancer, bacterial infections and Alzheimer's disease[204-207, 213-215] or for the photocatalytic and electrocatalytic reduction of CO₂[189-201, 216]. A second class of ligands which stabilize rhenium in the oxidation state +I are η⁶ bound arenes like benzene and cyclopentadienyl and their respective derivatives. Functionalized dibenzene rhenium(I) complexes are highly stable and tailored substitutes for ferrocene as internal standard in cyclic voltammetry or as building block for dinuclear metalorganic compounds.[217, 218] The most prominent compound bearing a cyclopentadienyl ligand is CpRe(CO)₃ firstly synthesized by Green and Wilkinson in 1958.[219, 220] Its commercial availability and easy handling due to its high stability renders the compound a highly interesting (pre)catalyst for several catalytic reactions. In most reactions the active catalyst is the oxidized compound CpRe(VII)O₃ which is historically of high importance for the development of rhenium(VII) trioxo catalysts which will be discussed in chapter 5.[221] The second major application of derivatives of (Cp)Re(CO)₃ is the treatment of cancer due to their high stability and facile synthesis.[79, 203, 222].

Molecular rhenium compounds in the oxidation states +IV and +V are also very common and their application is already elaborated. In both oxidation states, classic complex chemistry dominates the literature with ligands like halogens, pseudo-halogens or N-/ O-donors. Organometallic compounds are very rare and instable with the exception of NHC complexes using ligands like a particular *bis*-NHC ligand with a functionalized methylene bridge developed in our group.[187, 223-226] Due to the d³ configuration of Re(IV), its molecular compounds reveal highly interesting magnetic properties. A giant magnetic anisotropy is observed as soon as the octahedral symmetry of homoleptic complexes is broken either by substitution of ligands, by crystallization or by application of a strong external magnetic field.[227-229] The development of such compounds is a vital field as these compounds are currently one of the best candidates for applicable single molecule magnets.[230-237] In contrast, complexes with rhenium in the oxidation state +V are diamagnetic with a low-spin d² configuration.

Beside some rare examples, these compounds comprise at least one oxo or amido moiety.[75, 225] Their facile synthesis and high stability renders them highly interesting agents for the treatment of cancer. Over the last few decades, a plethora of such compounds is synthesized and tested against multiple different cell lines with the current research focus on tailoring properties like photoluminescence and solubility.[82, 202, 224, 238-242] Beside their application in medicinal chemistry, rhenium(V) complexes are useful in organic transformations and catalytic reactions. Some are capable to activate small molecules like CO₂ and are applicable in e.g. chalcogen metathesis and oxygen transfer reactions.[243, 244] In catalytic reactions like dehydration or DODH, alkyl or cyclopentadienyl dioxo Re(V) are the active catalysts formed upon reduction of more stable Re(VII) precursors.[245-248]

Rhenium complexes in the oxidation state +II, +III and +VI are very scarce.[96] The high valent complexes are usually stabilized by +M donor ligands like alcohols, halogens and/or oxo moieties.[249-254] In the absence of such ligands, extremely reactive compounds like hexamethylrhenium(VI) are obtained.[255, 256] They are so dangerous that their developer, Prof. Wilkinson, released an "Explosion hazard" note as they explode in the absence of air even at low temperature.[257] In contrast, the low valent rhenium complexes should not be neglected as laboratory curiosity as it has been shown within the last two years that they are capable to activate small molecules.[258, 259] Compounds bearing a non-innocent pincer type ligand are of particular interest as it has been shown that they can cleave the strong bond of dinitrogen and form ammonia electrochemically using cobaltocene as cocatalyst.[260, 261] The development of such compounds is significantly facilitated since very recently, Alberto and coworkers developed a suitable and easily accessible precursor, the fully solvated $[\text{Re}(\text{MeCN})_6]^{2+}$ complex.[262]

4.1. Summary of the Metalorganic and Coordination Chemistry of Rhenium in the Oxidation States +I - +VI

The most common oxidation states for molecular rhenium compounds are +I and +V. For intermediate oxidation states (+II - +V) mainly complexes are formed. High and low valent compounds usually contain organometallic ligands. Most important applications are given in Figure 8, the respective citations in chapter 4.

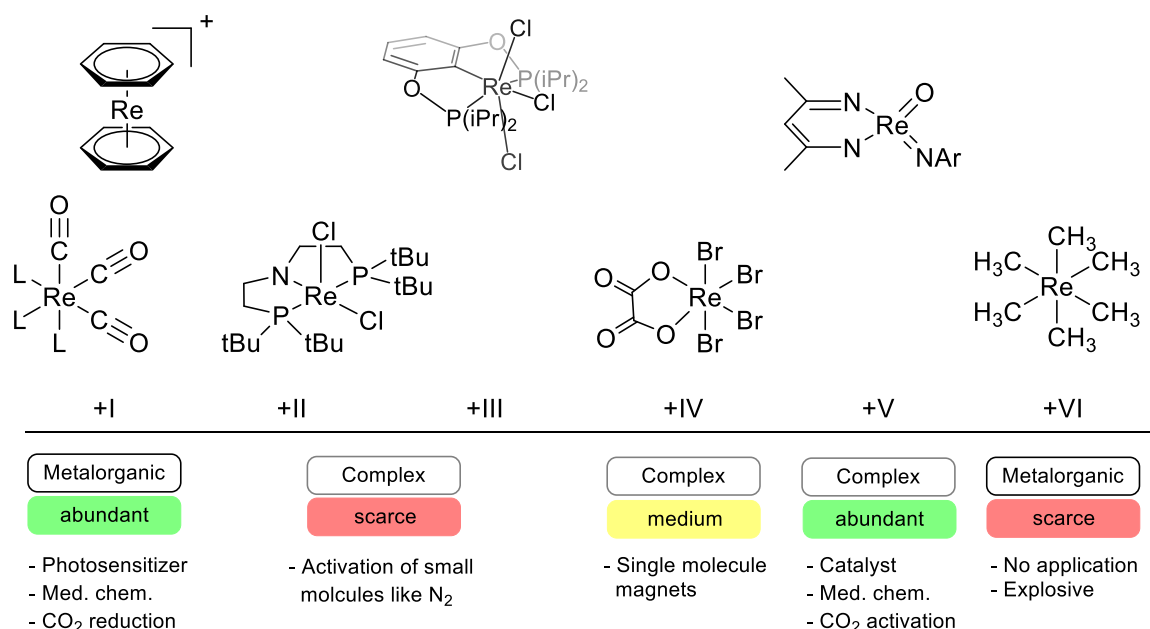


Figure 8: Some examples or structural motifs of molecular rhenium compounds for the oxidation states +I - +VI. Abundance, prevailing type of coordination compounds and application are given.

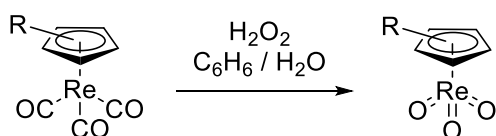
5. Rhenium(VII)trioxo complexes

The chemistry of molecular rhenium compounds in the oxidation state +VII has been dominated by the perrhenate anion or halogen complexes for a long time.[96] The first ester of perrhenic acid, trimethylsilylperrhenate, is synthesized by Schmidt and Schmidbaur in 1959.[263] Its hydride followed in 1964, when Ginsberg *et al.* unambiguously identified the compound as K₂ReH₉. [264] Starting from the enneahydride, amine and phosphine hydrido Re(VII) complexes are obtained, however, with limited success.[96] The breakthrough in the development of high valent rhenium compounds has been achieved by Herrmann *et al.* in 1984 when they have been able to synthesize Cp*ReO₃ by aerobic oxidation upon UV irradiation of the respective carbonyl precursor.[223] Although it was not the very first organometallic Re(VII) compound bearing three oxo ligands, it was the first substance which demonstrated that complex organic ligands can be stabilized at the maximally oxidized rhenium center without decomposition.[265] The first synthesis of such a compound happened by accident, when Beattie and Jones oxidized the highly sensitive ReOMe₄ to methyltrioxorhenium (MTO) in 1978.[266] The importance of that substance stayed unrecognized until Herrmann *et al.* identified it as the active catalyst in metathesis reactions of industrially important olefins as it is formed quantitatively upon mixture of rhenium heptoxide and tetramethyltin.[267] Their finding was achieved by the careful review of the literature in heterogeneous catalysis, as Re₂O₇ combined with the co-catalyst Sn(Me)₄ was known to be a highly active metathesis catalyst.[53, 268] By demonstrating both the stability of organic ligands attached to a ReO₃⁺ core and the catalytic capability of resulting compounds, the main

topic of this dissertation, the field of organyl trioxorhenium compounds and their applications is opened up.

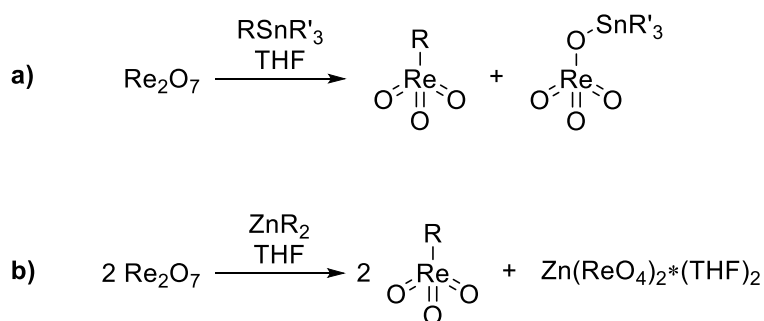
5.1. Synthesis of Re(VII)trioxo compounds

Until now, a huge variety of rhenium(VII) trioxo compounds have been synthesized and characterized. They can be assigned to three subclasses depending on the organic substituent. The first class are the 18- e^- complexes bearing a (substituted) cyclopentadienyl ligands. As long as the Cp ligand is sufficiently sterically demanding, the most convenient synthetic routes start from its $[\text{Cp}'\text{Re}(\text{I})\text{CO}_3]$ predecessor (Scheme 5).[245, 246, 269] The compound is either oxidized by aqueous hydrogen peroxide at reflux [270] or ozone at -78°C [271] in moderate yields or in a more complicated procedure using Mn_2O_7 as oxidant in high yields of $\approx 80\%$.[272]



Scheme 5: Most convenient procedure for the synthesis of substituted $\text{Cp}(\text{R}_x)\text{ReO}_3$. (R = any alkyl for $x > 4$ or bulky substituent(s) for $x < 3$)

Aryl trioxorhenium compounds are assigned to the second class and the alkyl derivatives to the third. Due to the lack of reasonable Re(I) carbonyl precursors, different synthetic strategies have been developed over the past few decades.[273] In order to synthesize such compounds a mild alkylation agent is required in order to circumvent the reduction of the ReO_3^+ core which results in the formation of low valent rhenium species which autocatalytically decompose Re(VII) species.[175, 274-276]

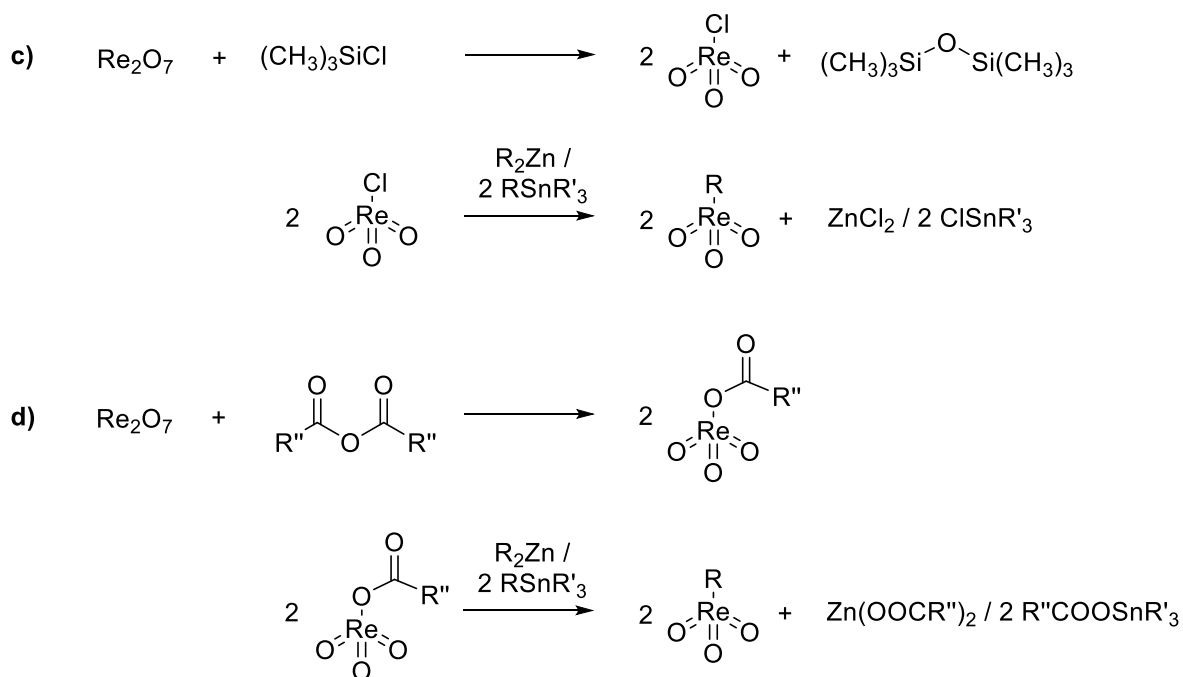


Scheme 6: The tin (a) and zinc (b) route for the synthesis of alkyl or aryl trioxorhenium compounds. (R' = usually *n*-butyl)

Two alkylation agents have proven to be effective in the synthesis of aryl and alkyl trioxorhenium compounds (Scheme 6). The firstly developed method (“tin-route”) uses tin reagents of the general formula of $\text{RSn}(\text{R}')_3$ and has proven to be very effective in the synthesis of the alkyl derivatives.[267, 273] Upon addition of the alkylation agent, one equivalent of the desired compound and one equivalent of a tin ester of perrhenate are formed. The major drawbacks are the high toxicity of the coupling agent and the limited scope of the reaction.[277] Hence, a new method has been developed using dialkyl- or diaryl zinc agents (“zinc-route”). They are generally more reactive than their tin congeners resulting in a significantly decreased toxicity³[278] and a broader synthetic scope like e.g. the synthesis of aryl trioxorhenium compounds or CpReO_3 .[279, 280] Furthermore, the synthetic procedure is facilitated as by addition of one equivalent of the respective zinc reagent to two equivalents of Re_2O_7 , two equivalents of the desired products are obtained and the byproduct, the zinc

³ The reduced toxicity compared to tin reagents originates in the quick decomposition upon exposure to water so that the intact alkylation agent cannot penetrate the tissue. For more information, visit <https://echa.europa.eu/>

perrhenate THF adduct, precipitates from the solution. However, both protocols have two major drawbacks. On the one hand, the reactivity of the alkylation agent limits the scope and yields and on the other hand, one equivalent of rhenium is lost either by formation of the unreactive stannyl perrhenate or zinc perrhenate.



Scheme 7: Modern synthetic routes for the synthesis of alkyl and aryl trioxorhenium compounds via the prior activation of the perrhenyl fragment by formation of either chlorotrioxorhenium or an active ester which are converted by tin or zinc agents to the desired products.

These problems are circumvented by two modern synthetic strategies developed in the group of W. A. Herrmann. In both reactions, the perrhenyl fragment is activated by substitution of the perrhenate leaving group by either a chloride or an active ester. In the first reaction, the oxophilicity of silicon is exploited in the clean reaction of Re_2O_7 with $(\text{CH}_3)_3\text{SiCl}$.^[281] Both rhenium centers are converted to chlorotrioxorhenium upon formation of the easily separable hexamethyldisiloxane. In the following, the intermediate can be converted by addition of the respective Zn or Sn alkylation agents. As chlorotrioxorhenium is more reactive than Re_2O_7 it is now also possible to synthesize aryl trioxorhenium compounds by tin reagents.^[273] The drawback of the reaction is the reactivity of $(\text{CH}_3)_3\text{SiCl}$ in the respective solvents leading to solvent decomposition and the formation of byproducts. The second route is even more elegant using an acid anhydride which converts Re_2O_7 to two equivalents of a ReO_3^+ active ester.^[281, 282] On the one hand, the use of the reactive chlorosilane is circumvented and on the other hand, in case of the “tin-route”, the stannyl moiety is scavenged giving an unreactive ester. Fluorinated carboxylic acids have proven best and give a significantly increased overall yield in the synthesis of the important catalyst MTO.^[282, 283]

Following these procedures, several rhenium trioxo compounds have been synthesized. Beside linear and branched alkyls and (substituted) phenyls^[275, 279, 284-286], also more sophisticated compounds are accessible resulting in derivatives bearing a cyclopropanyl^[284], allyl, alkenyls^[287], alkynyls^[288], benzyl^[287] or even a fluctuating η^1 -indenyl ligand.^[289] (Figure 9) Starting from these precursors, a rich chemistry of solvent, *O*- and *N*-adducts has been established over the past few decades summarized in several reviews.^[92, 221, 273, 290]

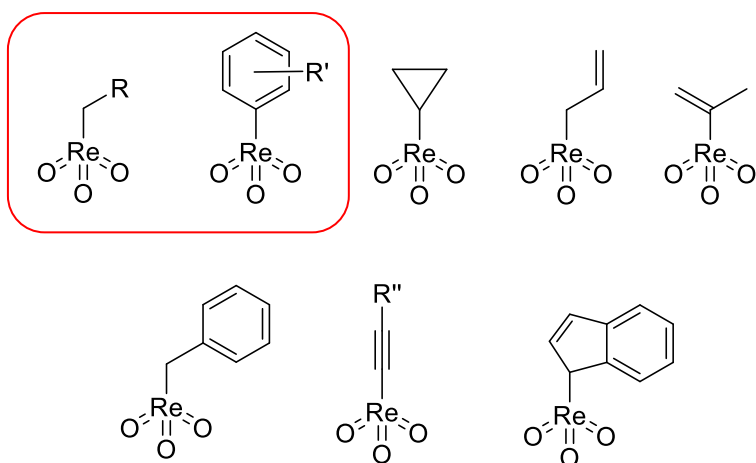


Figure 9: Selected substrate scope of organometallic rhenium(VII) trioxo compounds synthesized via the “zinc-“ or “tin-route”. The most stable and common motifs are highlighted. R = -H, n- or branched alkyls up to heptane; R' = various substitution patterns with substituents like -Me, -F, -CF₃, -OMe, -OH, -OSi(Me)₃; R'' = H, Ph, ReO₃.

5.2. Important Characterization Methods for Re(VII)trioxo Compounds

In order to correlate the reactivity of Re(VII)trioxo compounds, especially in catalytic reactions, their chemical properties have to be characterized. As the catalytic oxidation or dehydration reactions do not take place at the organic moiety, chemists working in this field should be strongly focused on the bonding situation of the ReO₃⁺ core. The most popular methods for its characterization are discussed here briefly and their strengths and weaknesses are pointed out. Important parameters are the Re=O bond strength, determined by FT-IR (Fourier-transform infrared spectroscopy), the electron density on the oxygen atoms, correlated by ¹⁷O-NMR (nuclear magnetic resonance) spectroscopy and structural features of the respective rhenium compounds, derived from SC-XRD (single crystal X-ray diffraction), GP-ED (gas-phase electron diffraction) or P-ND (powder neutron diffraction).

5.2.1. Characterization of the Structure of Rhenium(VII) trioxo Compounds

Metalorganic chemists are always highly interested in the structure of their compounds in order to identify structure-reactivity relationships. For rhenium(VII) trioxo compounds, several crystal or gas phase structures have been obtained over the past decades.[92] However, most of them have been isolated either as solvent or N-base adducts which are hardly comparable due to the influence of the additional donor ligand. In Table 5, data of all compounds is listed which have been characterized as pure substances. Fortunately, from all three substance classes at least two compounds are available so that a comparison is reasonable.

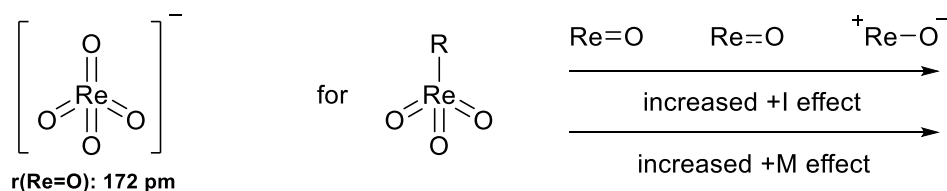


Figure 10: The tetrahedral perrhenate ion with a Re=O bond distance of 172 pm (left). Influence of the substituent depending on its electronic properties on the remaining three rhenium oxygen bonds.

In order to discuss the Re=O bond lengths, the perrhenate anion (Figure 10, left) is a perfect starting point as the compound is homoleptic and perfectly tetrahedral. The negative charge is completely delocalized resulting in a reduced bond order of formally 1.75 with a bond length of 172 pm. For

substituted rhenium trioxo compounds, the *trans* influence of R should induce either shortened bond lengths for weak ligands and *vice versa* for strong ligands with both a strong +I or +M effect (Figure 10, right).

However, the experimental data shows that the Re=O bond length is mostly invariant in comparison to the perrhenate anion with values between 170-171 pm for alkyl and Cp and slightly shortened bond lengths of 169-170 pm for aryl derivatives. The latter might be attributed to the reduced +I effect of the aryl moiety compared to the alkyls combined with a significantly decreased +M effect compared to the oxo moiety of the perrhenate. In comparison, the oxide and its aqua adduct exhibit a slightly elongated Re=O bond with 174 pm. Here, a discussion of electronic effects is not feasible due to the polymeric crystal structure of Re₂O₇ and the formation of hydrogen bonds in the crystal structure of Re₂O₇·2H₂O.[97, 99] In order to demonstrate that the invariance in the Re=O bond length towards the organic ligand is not a characteristic feature of the ReO₃⁺ core, the trimethylsilyl ester of the perrhenic acid is added to Table 5 (T5.11). The weak ligand is not able to donate sufficient electron density resulting in a short Re=O bond of 161 pm.

Therefore, all organometallic rhenium(VII) trioxo compounds reveal a reduced bond order of the Re=O bond as observed for the perrhenate anion due to the donating effect of the respective ligands, in line with theoretical calculations on these compounds.[291-293][X] However, the bond length is not indicative for any structure-reactivity relationship due to its overall very small alteration.

Table 5: Averaged Re=O bond lengths of selected rhenium(VII) trioxo compounds determined either by single crystal X-ray diffraction (SC-XRD), gas-phase electron diffraction (GP-ED) or powder neutron diffraction (P-ND). ^{a)} bond length of the Re=O bonds in the octahedral unit. ^{b)} Re-O bond length.

Entry	Compound	Technique	Re=O bond length [pm]	Re-C bond length [pm]	Average $\angle(\text{O-Re-O})$	Citation
T5.1	Re ₂ O _{7(s)}	SC-XRD	174/173 ^{a)}		109.0°	[97]
T5.2	Re ₂ O ₇ ·2H ₂ O	SC-XRD	174/175 ^{a)}		110.0°	[99]
T5.3	KReO ₄	SC-XRD	172		109.5°	[294]
T5.4	MTO-d3	P-ND	170	206	113.0°	[272, 295]
	MTO	GP-ED	171	206	113.0°	
T5.5	ETO	SC-XRD	170	210	113.6°	[293]
		GP-ED	171	210	113.9°	
T5.6	Cp	SC-XRD	170		104.2°	[296]
T5.7	CpMe ₅	SC-XRD	170		105.0°	[272]
		GP-ED	172		107.0°	
T5.8	CpMe ₄ Et	SC-XRD	170		105.7°	[269]
T5.9	Mesityl-	SC-XRD	169	203	110.8°	[279]
T5.10	4-(Me ₃ SiO)- <i>o</i> -xylyl-	SC-XRD	170	204	111.1°	[279]
T5.11	(Me ₃ Si)O-	SC-XRD	161	167 ^{b)}	110.0°	[297]

A stronger influence of the respective ligands is observed for the $\angle(\text{O-Re-O})$ angle. The inorganic compounds and the trimethylsilylester (T5.1-3,11) are (almost) perfectly tetrahedral with an angle between 109-110°. Compounds bearing Cp ligands (T5.6-8) reveal a smaller angle with 104-106° in line with the tendency for the formation of “octahedral” structures of closed-shell complexes. In contrast, alkyl substituents (T5.4-5) induce a compression of the tetrahedral subunit with angles between 113-114° due to their strong +I effect. Weaker donors like the aryl substituted compounds (T5.9-10) lead to only marginal compression with angles of approximately 111°.

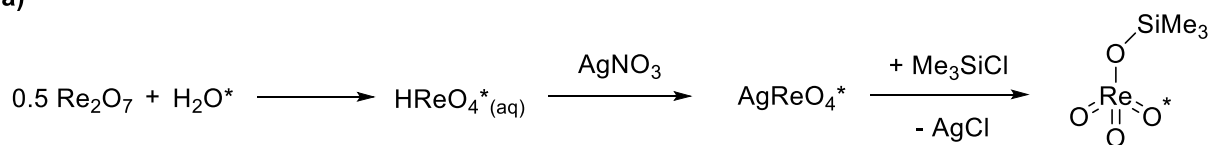
Summarized, all three ligand types alter the $\angle(\text{O-Re-O})$ to some extent, however, within the classes of rhenium(VII) trioxo compounds there are only small deviation. Therefore, the structure of the ReO_3^+ core is not indicative and a discussion of neither the Re=O bond length nor the angle is feasible. A more useful approach is the discussion of the respective Re-C bond, exemplarily shown for MTO and ETO (**T5.4-5**). For the methyl substituent, a distance of 206 pm is observed and for its homologue an elongated bond with 210 pm. As steric repulsion is not a reasonable argument, the increasing bond length is linked to a weakened Re-C bond as it will be shown within this work.

5.2.2. Characterization by ^{17}O -NMR spectroscopy

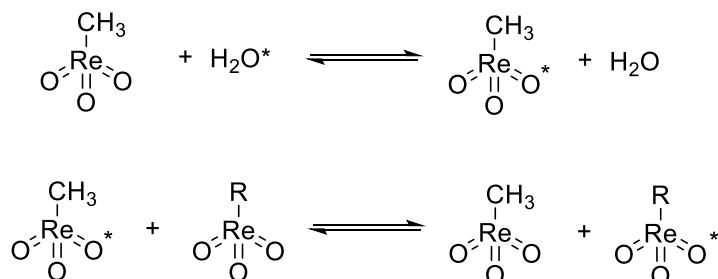
In order to investigate the electronic effects of substitution of the organic ligand, ^{17}O -NMR spectroscopy is a viable tool. Any experimenter who wants to obtain reasonably good signals or a signal at all has to be aware of its high sensitivity towards the relaxation time, temperature and symmetry of the electron density due to the quadrupole nature of the nuclide ($I = 5/2$).^[298] Therefore, an initial benchmarking of the pulse sequence might be helpful. The NMR active nuclide has a very low abundance (0.038% natural abundance) and very low receptivity compared to hydrogen (1.11×10^{-5}) or carbon (6.5×10^{-2}), so that an enriched sample is necessary in order to measure sensitive compounds.^[298] There are two major routes for the synthesis of ^{17}O enriched rhenium(VII) trioxo compounds. The first one is a stepwise reaction in order to synthesize the trimethylsilyl ester of perrhenic acid which is a viable precursor for the synthesis of labelled Re_2O_7 and alkyl or aryl substituted compounds following the previously described synthetic procedures (Scheme 8, **a**).^[299] Re_2O_7 is dissolved in ^{17}O labelled water giving perrhenic acid which is precipitated by addition of silver nitrate. The active ester is obtained by reaction with Me_3SiCl in non-polar aprotic solvents. The reaction fails in coordinating solvents as rhenium heptoxide is formed. The advantage of the reaction is the direct formation of an active ester so that standard procedures for the synthesis of rhenium(VII) trioxo compounds can be applied, however, for reactions with low yields vast amounts of highly expensive ^{17}O are lost.

The second route is more elegant for obtaining spectroscopic data of highly sensitive compounds. MTO is the established starting point due to its high stability towards water. By addition of H_2^{17}O , the rhenium compound is labeled *via* an oxygen scrambling reaction (Scheme 8, **b**). In the following, both the sensitive rhenium(VII) trioxo compound and the labelled MTO are dissolved in deuterated solvents. Due to the oxygen scrambling reaction between the rhenium compounds, both substances are easily detected by ^{17}O -NMR spectroscopy. On the one hand, the presence of MTO is advantageous as it is a reliable internal standard with a chemical shift of e.g. 829 ppm in CDCl_3 (**T6.2**). On the other hand, no pure samples of the respective rhenium(VII) trioxo compounds can be obtained. For mechanistic studies, the first route has to be applied if the reactivity of MTO interferes. Another disadvantage is that labeling of saturated 18- e^- Cp complexes fails as the scrambling reaction is inhibited.^[299]

a)



b)



Scheme 8: Procedure for the labelling of rhenium(VII) trioxo compounds with ^{17}O enriched water either by the stepwise synthesis of the labeled trimethylsilyl ester of perrhenic acid (a) or by oxygen scrambling starting (b). The asterisk marks labelled compounds. Only one oxygen is labeled in trioxo compounds and the trimethylsilyl ester for clarity.

The chemical shift of a nucleus depends primarily on its shielding by the amount and distribution of the surrounding electron density and the nature of adjacent elements. For the characterization of rhenium(VII)trioxo compounds, the influence is reduced to the amount of the electron density as the structural change of the ReO_3^+ core is marginal upon substitution of the organic moiety. The scale in ^{17}O -NMR spectroscopy is referred to H_2^{17}O ($\delta = 0$ ppm) and ranges between -50 to 1600 ppm (Figure 11). Alcohols, ethers and esters have a marginal shift from $\delta = 0$ ppm ranging from -50 to 100 ppm. Highest shifts for common organic compounds are observed for ketones and aldehydes between 500 to 620 ppm. As rhenium(VII) trioxo compounds are reported in a range between 560 – 940 ppm, the method is very useful especially for mechanistic studies as it does not interfere with signals of common organic compounds which are detected over the course of the reaction by decomposition and/or oxygen scrambling.

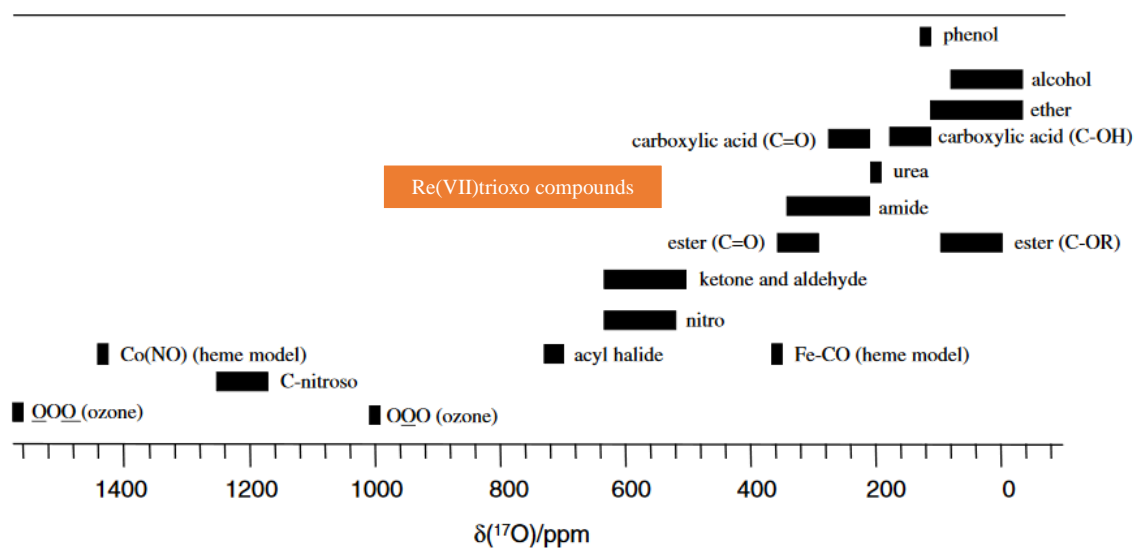


Figure 11: Typical ^{17}O shifts of common organic molecules referenced to H_2^{17}O . Adapted from Wu in *Prog. Nucl. Magn. Reson. Spectrosc.*[300]. The orange bar indicating the region of common non-coordinated Re(VII)trioxo compounds is added.

A direct comparison of all reported rhenium(VII) trioxo compounds is not trivial as they have been characterized in several different solvents. Therefore, MTO is used as benchmark substance as its chemical shift is available in all commonly used solvents (**T6.3**). For MTO, a strong shift is observed changing the solvent from nonpolar (*n*-pentane-*d*₁₂) to polar (THF-*d*₈) which is due to the coordination of the solvent to the rhenium center. As the donor complex is fluxional, a similar trend is observed for changes in temperature. These effects have been described in literature for metalorganic rhenium compounds[92, 299, 301] and depend on the substituent.

The strongest shielding of the oxygen is observed for the perrhenate anion with $\delta = 562$ ppm (**T6.1**) due to the delocalization of the negative charge. The rhenium heptoxide THF adduct is significantly shifted to high field ($\delta = 741$ ppm, **T6.2**) with only one observable signal due to its highly fluctuating behavior in solution. Among the organometallic rhenium(VII) trioxo compounds, the Cp derivatives are most shifted to high field with values between 646 – 691 ppm (**T6.15-18**). The chemical shift follows the expected trend as an increasing shielding is induced by the increasing donor strength with CpMe₄Et \approx CpMe₅ being the strongest donors. The strongest shift to low field is observed for aryl trioxorhenium compounds in a range between 821 – 939 ppm in coordinating solvents (**T6.9-14**). A similar trend is observed as for the Cp functionalized compounds with strongest shifts for aryls bearing strongly electron withdrawing groups like CF₃. An interesting feature is the strong discrepancy between aryls with and without ortho-methyl groups as the first group ranges between 912 – 939 ppm (coordinating solvents) and the latter one between 800 – 820 ppm (CDCl₃). Solvent dependency cannot account for the chemical shifts as a maximal shift of $\delta = 25$ ppm is observed for mesityl trioxorhenium (**T6.11**) changing the solvent from benzene to THF. The reason for this phenomenon is the proximity of the ortho methyl groups to the oxo moieties inducing a strong chemical shielding and should not be mistaken with the donor strength of the respective ligand.

In a similar region as the latter group, the alkyl trioxo compounds are observed (808 – 845 ppm, **T6.3-7**). The donor strength for the characterized compounds should follow the trend Me- < Me₃SiMe- < Et-. It might be assumed, that a similar trend should be observed as for all other classes of rhenium(VII) trioxo compounds. However, whereat the chemical shift for the first two complexes is in line with theory, for ETO a contrary trend is observed with a low field shift by up to $\delta = 16$ ppm compared to MTO. Comparing the shift of the MTO *N*-heterocyclic carbene adduct (**T6.19**) shows clearly that increasing electron density at the rhenium center results in a high field shift also for alkyl trioxorhenium. Therefore, the counterintuitive shift of ETO has to arise from a different phenomenon. Within this dissertation, it will be shown that the decreasing bond strength from methyl to ethyl accounts for the high field shift in line with the elongated Re-C bond of ETO (**T5.4-5**). In conclusion, additional information can be obtained by ¹⁷O-NMR spectroscopy in addition to the more commonly evaluation of the donor strength of the organic moiety. This renders this method a highly useful tool for the organometallic chemist.

Table 6: Selected compounds and their chemical shift ($\delta(^{17}\text{O})$ in ppm) in various solvents. ^{a)} Highly likely overestimated as the spectra seem to be not corrected as the MTO shift is underestimated by 7 ppm. ^{b)} Melmi = dimethyl imidazolyidene. [*] Published results obtained during this thesis.

Entry	Compound	THF- <i>d</i> ₈	DMSO- <i>d</i> ₆	CDCl ₃	C ₆ D ₆	<i>n</i> -pentane- <i>d</i> ₁₂	Citation
T6.1	KReO ₄	562					[272]
T6.2	Re ₂ O ₇ *2(THF- <i>d</i> ₆)	741					[175][*]
T6.3	MTO	872	864	829	823	835	[275, 280, 299, 301][*]
T6.4	MTO (-30 °C)			820			[276][*]
T6.5	ETO			845 ^{a)}			[301]

T6.6	ETO (-30 °C)		829			[276][*]
T6.7	Me ₃ SiMe-				808	[285]
T6.8	Allyl	894				[287]
T6.9	Phenyl-	912		856	872	[279]
T6.10	2,6-Xylyl-		820			[302]
T6.11	Mesityl-	836	811	809		[286]
T6.12	Me ₃ SiO- <i>o</i> -xylyl-	821	800	805	813	[279]
T6.13	4-(CF ₃)O-phenyl-		927			[275][*]
T6.14	4-(CF ₃)-phenyl-		939			[275][*]
T6.15	Cp-		691			[280]
T6.16	CpMe-		674			[280]
T6.17	CpMe ₅ -	653	647			[280, 299]
T6.18	CpMe ₄ Et-		646			[280]
T6.19	MTO*2MeImi ^{b)}		728			[303]

5.2.3. Characterization by IR spectroscopy

Using ¹⁷O-NMR spectroscopy, the influence of the organic ligand on the electronic structure is assessed, however, its impact on the bond strength of the rhenium oxygen bonds cannot be estimated. Therefore, infrared spectroscopy is a viable tool as the force constant of a bond can be estimated directly. For a diatomic molecule, the force constant (k) is related to the vibrational frequency (ν) and the reduced mass (μ) of the vibrating moiety (Equation 1.1-2). [304]

$$\nu = \frac{1}{2\pi} \sqrt{\frac{k}{\mu}} \quad (1.1)$$

$$\mu = \frac{m_1 m_2}{(m_1 + m_2)} \quad (1.2)$$

For larger molecules, the calculation of the reduced mass is not trivial, as it depends on the observed vibrational mode and therefore the direction and extend of the deviation of all participating atoms. However, in the case of the rhenium(VII) trioxo compounds, the vibrating moiety is structural more or less identical (see. 5.2.1) and therefore a direct comparison of the absorption bands is reasonable. For the assessment of the bond strength both stretching modes of the Re=O bond, the symmetric and the asymmetric one, are indicative, however, as the asymmetric stretching vibration is more intense (stronger induction of a dipole moment) it is most useful and discussed here.

In order to reveal trends within the three groups of rhenium(VII) trioxo compounds, one has to take care of the measurement technique. Most data are obtained in transmission mode using a variety of different matrixes. The interaction between the matrix and the highly polarized Re=O bond induces a shift of the absorption frequencies as well as an altered splitting between the asymmetric and the symmetric stretching. Therefore, the discussion is hampered by the available data and reduced to general trends.

Table 7: Frequencies of the symmetric (*s*) and asymmetric (*as*) rhenium oxo stretching vibration for selected rhenium(VII) compounds. ^{a)} degenerated modes observable in the gas-phase. For $\tilde{\nu}_s$, two modes are possible and for $\tilde{\nu}_{as}$ four. ^{b)} Shoulder; either a degenerate mode or coinciding vibration.

Entry	Compound	$\tilde{\nu}_s$ (Re=O) [cm ⁻¹]	$\tilde{\nu}_{as}$ (Re=O) [cm ⁻¹]	Technique	Citation
T7.1	KReO ₄	971	918	KBr	[272]
T7.2	ClReO ₃	1001	961	CS ₂	[272]
T7.3	Re ₂ O ₇	1062/1017 ^{a)}	955/910 ^{a)}	Gas phase	[90]
T7.4	Re ₂ O ₇ * 2(MeCN)	965	937	MeCN	[305]
T7.5	MTO	1005	958	KBr	[272]
		1003	941	Diffuse reflectance	[272]
		1001	965	CS ₂	[272]
		1000	966	CH ₂ Cl ₂	[280]
		999	966	C ₆ H ₆	[272]
T7.6	ETO		970	Gas phase	[285]
		997	970/967 ^{b)}	Ar matrix	[293]
		996	961/950 ^{b)}	CS ₂	[285]
T7.7	Isobutyl-	994	962	CS ₂	[285]
T7.8	Me ₃ SiMe-	990	965/957 ^{b)}	CS ₂	[285]
T7.9	Indenyl-	989	959	<i>n</i> -pentane	[289]
T7.10	Phenyl-	986	956	KBr	[285]
		988	960	CCl ₄	[280]
T7.11	Mesityl-	985	954	KBr	[286]
		986	953	CS ₂	[286]
T7.12	Me ₃ SiO- <i>o</i> -xylyl-	975	951	CS ₂	[279]
T7.13	4-(CF ₃)-phenyl-	987	940	ATR	[275][*]
T7.14	4-(CF ₃)O-phenyl-	991	950	ATR	[275][*]
T7.15	Cp	926	886	KBr	[296]
		929	885	Nujol	[280]
		933	907	CH ₂ Cl ₂	[280]
T7.16	CpMe	927	878	KBr	[296]
		930	898	CH ₂ Cl ₂	[280]
T7.17	CpMe ₅	921	890	KBr	[272]
		924	894	CS ₂	[272]
		918	886	CH ₂ Cl ₂	[280]
		920	890	C ₆ H ₆	[272]
T7.18	CpMe ₄ Et	920	887	KBr	[269]

The Cp derivatives are strongest shifted from MTO with a delta of ≈ 70 cm⁻¹. The Re=O bond strength is therefore weakest among all rhenium trioxo compounds. The main reason for this observation is the strength of the respective ligands and the formation of 18-e⁻ complexes. A general trend following the number of substituents having a +I effect is not observed with 886 cm⁻¹ for Cp (**T7.15**, KBr) and 887 cm⁻¹ for CpMe₄Et (**T7.18**, KBr). Among the alkyl trioxorhenium compounds, the stretching vibration of MTO is observed at highest wavenumbers (965 cm⁻¹, CS₂) indicative for the weakest bond. Therefore, the methyl substituent donates most electron density to the rhenium center compared to other compounds and weakens the Re=O bond strongest. In line with the ¹⁷O-NMR results, the observed stretching frequencies do not follow the trend in donor strength (isobutyl \approx ethyl > methyl > Me₃SiMe-) as the corresponding vibration of ethyl and isobutyl are observed at lower wavenumbers. The aryl trioxorhenium compounds are shifted to similar wavenumbers between 940 – 960 cm⁻¹. The electron

poor aryls containing CF₃- and CF₃O- substituents (**T7.13-14**) are strongest shifted in line with theory whereat the electron rich compounds are in the same region as ETO and phenyl trioxorhenium. The strength of the combination of IR with ¹⁷O-NMR spectroscopy becomes apparent in the discussion of the electronic influence of the mesityl- and Me₃SiO-*o*-xylyl moiety (**T7.11-12**). Whereat ¹⁷O-NMR spectroscopy might suggest a significantly increased donor strength of the two compounds compared to phenyl, IR spectroscopy can clearly rule out the assumption and underline the assignment of the strong ¹⁷O-NMR shift to the proximity of the methyl groups in ortho position to the oxo ligands of the respective compounds.

5.3. Catalytic Applications of Rhenium(VII) trioxo Compounds

Rhenium has been well known for its superior catalytic properties in heterogeneous catalytic reactions for a long time.[306] In contrast, their molecular counterparts have been regarded as inactive and of low relevance despite their already well established synthetic accessibility.[307] Rhenium trioxo compounds bearing polar Re-X ligands like OR, NR₂ or halogens hydrolyze rapidly decomposing to catalytically inactive compounds.[308] By shifting to the more stable, nonpolar rhenium-carbon bond, the picture changes: In 1991, Herrmann *et al.* discovered the versatile catalytic properties of MTO ranging from olefin metathesis and oxidation to aldehyde olefination, published in three articles in the same issue of "Angewandte Chemie".[309-311] Since then, several catalytic applications for MTO have been developed. It is active in the dehydration, amination and disproportionation of alcohols[312], deoxygenation of epoxides and diols[313], reduction of alkenes[313], deoxydehydration of biomass derived diols[314], oxidation of sulfur, pnictogens and halogens[315-320], Baeyer-Villiger oxidation[321], oxidation of alkynes to 1,2-diketons or carboxylic acids[322], C-H activation[323] and arene oxidation.[324] The latter reaction is suitable to selectively synthesize vitamin K₃ and precursors of vitamin E[324, 325], however, its application on an industrial scale has never been achieved as a few years later a metal free synthesis has been developed.[326]

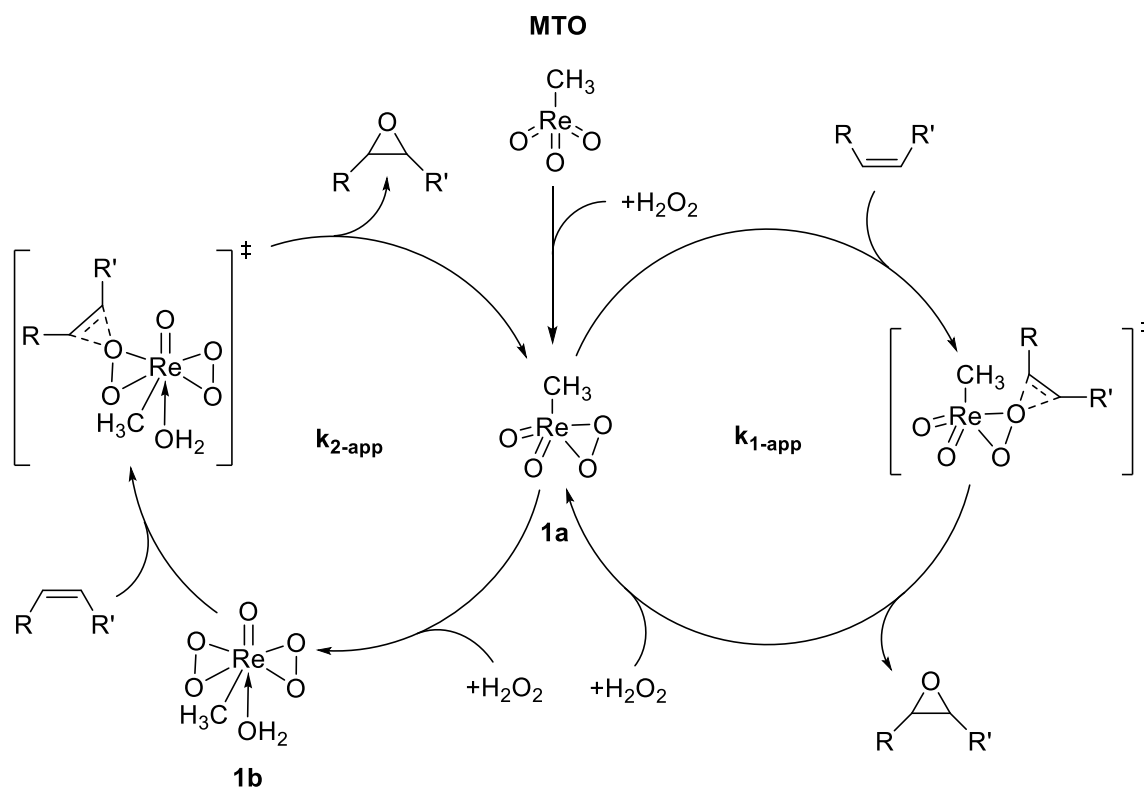
In the next three chapters, the most important reactions of rhenium compounds are discussed in detail: The epoxidation reaction catalyzed by MTO, which is probably its best examined reaction as it has been the benchmark catalyst for a very long time[327], the dehydration reaction which is of particular interest within the last decade as rhenium compounds exhibit an outstanding reactivity and selectivity in the degradation of biomass derived macromolecules[248] as well as the metathesis reaction which is generally one of the most important transition metal catalyzed reaction due to its extensive application on an industrial scale and versatility in organic synthesis.[328]

5.3.1. Epoxidation of Olefins by Rhenium(VII) trioxo Compounds

In line with the reactivity of the neighboring elements like molybdenum, tungsten and osmium, rhenium compounds are capable of oxidizing C-C double bonds.[329, 330] Whereas compounds of the Lewis acidic elements are true epoxidation catalysts, osmium tetroxide yields selectively vicinal *cis*-diols with defined osmate esters as intermediate.[331] In line with its position in the periodic table, the reactivity of rhenium compounds is intermediate and can be adjusted towards the formation of either epoxides or diols by selecting proper reaction conditions.[327]

Using MTO as catalyst precursor, the mechanism of the oxidation reaction of olefins has been well explored (Scheme 9).[332-335] MTO is oxidized by hydrogen peroxide to the monoperoxo complex **1a** and consecutively to the highly reactive bisperoxo complex **1b**. The formation of both η^2 -peroxo moieties proceed stepwise *via* energetically disfavored hydroperoxo species upon release of one equivalent of water.[336] Consecutively, the olefin coordinates to either the monoperoxo (right) or

the bisperoxo species (left) in a π -complex and the oxygen is transferred. After releasing the epoxide and reoxidation by hydrogen peroxide, the catalytic cycle is concluded.



Scheme 9: Facilitated mechanism of the epoxidation reaction of olefins using MTO as catalyst precursor. The active species is either the monoperoxo compound **1a** or the bisperoxo compound **1b**.

The catalyst **1b** has been identified unambiguously by SC-XRD after crystallization with donor ligands like HMPA (hexamethylphosphoric triamide) and application as oxidant in the epoxidation of cyclooctene.[337] Attempts to synthesize and isolate the monoperoxo compound **1a** failed yielding only MTO and **1b**. Therefore, there has been a long debate whether **1b** is also a viable catalyst for such reactions. Its reactivity is finally proven in experiments using substoichiometric amounts of the oxidant [317, 335] and ^{17}O -NMR spectroscopy[338]. However, as the apparent reaction rate constant for the catalytic cycle 1 (monoperoxo as active species) is rather low ($k_{1\text{-app}} < k_{2\text{-app}}$) its relevance in the strongly oxidizing environment of typical catalytic reactions is neglected.[339] The transition state of the oxygen transfer proceeds *via* a *spiro*-type oxygen species (tetrahedral oxygen) in order to maximize the overlap of the filled O-O π^* orbital with the empty C-C π^* orbital as demonstrated by DFT calculations.[336, 338] In line with these results, olefins in *cis*-configuration are more easily oxidized than their *trans* isomers due to the steric repulsion in such an arrangement.[339] Utilizing this effect, dienes are oxidized highly selective (diastereometric ratio > 96 %) to the respective di-epoxides with respect to the least steric repulsion within the transition state.[340]

The reactivity of MTO in oxidation reactions can be altered significantly by various donor ligands. The simplest donor ligand present in hydrogen peroxide is water. A combined experimental and DFT study demonstrated that the formation of the active species is significantly accelerated by water molecules by stabilizing critical transition states by hydrogen bond formation.[336] Even though the effect on the oxygen transfer step is rather low, switching from acetonitrile containing 2.6 M H_2O to neat H_2O results in a 100-fold increase in the reaction rate.[341] Fluorinated alcohols like HFI (hexafluoroisopropanol) or TFI (trifluoroethanol) exhibit a similar effect on the catalytic reaction. Here, the reactivity and stability are increased about 3 – 5 times compared to experiments in CH_2Cl_2 . [342, 343] However, these

techniques cannot overcome one major issue of the catalytic system MTO/H₂O₂: The consecutive formation of diols. In order to circumvent the undesired side reaction, *N*-bases are applied as additives. Whereat unsaturated amines significantly inhibit the reactivity[332, 344], the addition of pyridine even promotes the epoxidation reaction, rendering the system MTO/pyridine superior to the old widely applied *m*-CPBA procedure.[340] By the combined application of the fluorinated solvent HFI and the *N*-base additive pyrazole, the highest reported reactivity of a rhenium compound in the epoxidation of *cis*-cyclooctene was achieved with a TOF of 39 000 h⁻¹. [343]

Following the success of the simple molecule MTO, huge efforts were undertaken to develop a modified and more active rhenium(VII)trioxo compound. However, most of the synthesized compounds are either instable or inactive in the (ep)oxidation reactions. Very few reports on the activity of other rhenium(VII) trioxo derivatives are available only in combination with the stabilizing agent quinuclidine. The overall reactivities are not comparable to the benchmark TOF of MTO, however, general trends can be deduced. Whereat substituents with a stronger +I effect like ethyl or (trimethylsilyl)methylene result in lower reaction rates, cyclopropyl trioxorhenium is even more reactive than the quinuclidine adduct of MTO.[332] Phenyl substituted compounds are completely inactive using hydrogen peroxide and quinuclidine. More recently, the reactivity of the latter compound class has been reinvestigated using exemplarily *o*-xylyl trioxorhenium. The authors observed that the compound decomposes very fast in an aqueous and oxidizing environment. In contrast, anhydrous oxidants like H₂O₂ (in THF) or TBHP yield moderate results with a maximal TOF of 360 h⁻¹ which is remarkable since MTO is inactive in combination with organic peroxides.[302] Beside organometallic rheniumtrioxo compounds, perrhenates are viable catalysts in the epoxidation reaction. The anion itself is completely inactive in solid state or dissolved in common solvents like water as they are coordinatively saturated or protected by the solvent sphere. However, applied in ionic liquids moderate reactivities are achieved.[345] The activity of the catalyst is significantly altered by the respective cation with best results using a 1,2,3-substituted imidazolium cations containing a long-chain aliphatic *N*-bound substituent and two methyl groups. Whereat the former substituent tailors the polarity and micelle formation[346, 347], the latter ones are important to distribute the charge density of the imidazolium core.[348] Despite their only moderate reactivity, their application is of particular interest due to the easy handling of these stable compounds and their convenient recyclability.

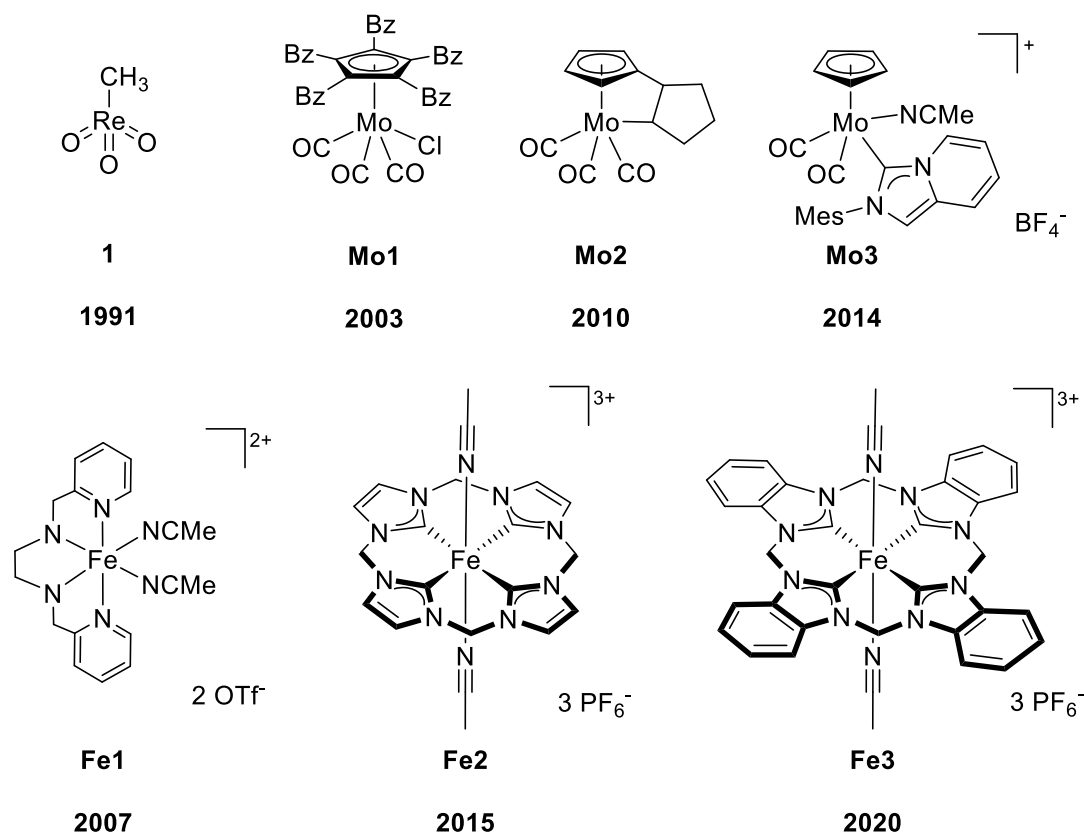


Figure 12: Structures of milestones in the development of highly active homogeneous epoxidation (pre)catalysts based on rhenium, molybdenum and iron.

The evaluated derivatives of MTO and perrhenates are no match for its outstanding reactivity, however, other catalytic systems took the lead as benchmark for the efficient catalytic epoxidation reaction, within the last two decades. The first class of compounds are based on the adjacent element molybdenum, for which the reactivity in epoxidation reactions has been already proven in the Halcon ARCO process.[349] Molybdenum based organometallic epoxidation catalysts are synthesized as stable carbonyl catalyst precursor which are consecutively activated by the oxidant to Mo(VI) dioxo or oxo peroxy species.[327]. Best activities are achieved using Cp ligands which have shown to stabilize the active species. Therefore, the first compound with at least half the reaction rate of MTO has been developed in 2001 (Figure 12, Table 8 **Mo1**) reaching a TOF of 20 000 h⁻¹ at optimized reaction conditions in the epoxidation of *cis*-cyclooctene (All TOFs are referred to this benchmark reaction). The active catalyst is a chlorido dioxo Mo(VI) compound protected by the very bulky Cp moiety.[350] In order to stabilize such high valent species, a more promising approach than steric shielding is increasing the electron density at the metal center. However, the replacement of the chloride ligand of **Mo1** by alkyl moieties is unsuccessful due to the instability of the Mo-C bond.[351] This drawback is circumvented by using *ansa*-type molybdenum catalysts like **Mo2**. Here the alkyl moiety is bound intramolecular resulting in a remarkable increase in reactivity and stability. Using the ionic liquid [BMIM]NTf₂, a higher TOF than for MTO (44 000 h⁻¹, **T8.3**) is achieved and the catalyst can be reused at least three times with only marginal reduction in yield. As increasing the electron density at the molybdenum center is verifiably beneficial for the epoxidation reaction, the consistent next step is the incorporation of an even stronger spectator ligand like a NHC. The resulting cationic compound **Mo3** exceeds the reactivity of its benchmark predecessor **Mo2** by about 20 % with a TOF of 53 000 h⁻¹ at optimized conditions. In recycling experiments applying the ionic liquid [C₈MIM]NTf₂, the catalyst is retrieved ten times without reduction of its reactivity resulting in a TON of 10 000.[352] The remarkable stability for a homogeneous molybdenum based catalyst is only surpassed by dimeric

molybdenum(VI) complex bearing two pincer-type *N*- and *O*-donor ligands with an outstanding TON of 110 000 in a single run.[353] However, despite their high reactivity and stability, MTO has still been the more prominent oxidation catalyst as the molybdenum based complexes are only applicable as epoxidation catalyst in combination with the expensive oxidant TBHP due to their intrinsic instability towards water.

Table 8: Performance of important epoxidation catalysts in the epoxidation of *cis*-cyclooctene. [*] Published results obtained during this thesis.

Entry	Compound	TOF [h ⁻¹]	Oxidant	Additional notes	Citation
T8.1	1	39000	H ₂ O ₂	Solvent: HFI Additive: Pyrazole	[343]
T8.2	Mo1	20000	TBHP	-	[350]
T8.3	Mo2	44000	TBHP	Solvent: [BMIM]NTf ₂	[354]
T8.4	Mo3	53000	TBHP	-	[352]
T8.5	Fe1	25000	H ₂ O ₂	Oxidant is added gradually Additive: Acetic acid	[355]
T8.6	Fe2	184000	H ₂ O ₂	-	[356][*]
T8.7	Fe2	415000	H ₂ O ₂	Additive: Sc(OTf) ₃	[357]
T8.8	Fe3	95000	H ₂ O ₂	Additive: Sc(OTf) ₃	[358][*]

One class of compounds which circumvents the main disadvantage of molybdenum based epoxidation catalysts are iron complexes stabilized by chelating ligands. This currently emerging research field is driven by the high abundance of the metal, its usually assumed low toxicity and its ability to stabilize a huge variety of oxidation states.[359] Already in 2007, the first highly active iron based epoxidation catalyst **Fe1** has been developed by Que and coworkers with a TOF of 25 000 h⁻¹ using hydrogen peroxide as oxidant.[355] Its application is strongly limited as it suffers from fast deactivation and low selectivity due to its Fenton-type reactivity. This reactivity renders common iron compounds inapplicable for selective oxidation reactions.[360] Therefore, the benchmark TOF of **Fe1** is only achieved by the careful adjustment of reaction conditions: The oxidant is added very slowly in order to slow down the decomposition reaction. Furthermore, an additive, acetic acid, is applied to decrease the Fenton-type reactivity by promoting the formation of the active species in the epoxidation reaction.[361] However, addition of acids is counterproductive due to their inherited reactivity towards the desired products. The formation and nature of the active species in non-heme iron epoxidation catalysts are decisive for their selectivity.[356] Upon oxidation of an intermediate Fe(III) species, either an Fe(IV) or Fe(V) oxo species is formed.[362-365] Whereat catalytic reactions proceeding *via* the latter species are mostly selective, the formation of Fe(IV) oxo species is accompanied by the simultaneous formation of hydroxyl radicals which reduce the selectivity significantly. Possible methods to circumvent this Fenton-type reactivity are the application of water or acids to assist the clean formation of Fe(V) oxo species or stabilization of the high valent species by either increasing the denticity of the ligands or their donor strength. Until now, the latter pathway has demonstrated to be more successful in line with the enhancement of the reactivity of the previously discussed molybdenum catalysts. The first active non-heme iron oxidation catalyst which is also stable in strongly oxidizing environments bears a tetradentate methylene bridged bis-(dipyridyl)NHC ligand.[366] Despite of its significantly increased stability, the compound performs quite poorly in the catalytic reaction with a TOF of only 2600 h⁻¹. The catalyst precursor also decomposes the oxidant due to an initial single electron oxidation step from Fe(II) to Fe(III) to form the active catalyst. These drawbacks are overcome in the Fe(III) catalyst **Fe2** which outperforms all so far known homogeneous epoxidation catalysts with a remarkable TOF of 184000 h⁻¹. Excellent selectivities are achieved (>99 %)

in line with the absence of a Fenton-type reactivity. The reactivity can be further increased by addition of a Lewis acid resulting in a TOF of 415000 h⁻¹ without consecutive diol formation.[357] The overall high reactivity of **Fe2** might be ascribed to the strong donor strength of the four NHC ligands stabilizing the central metal in high oxidation states. However, experimental and theoretical data demonstrate that the cyclic and strained geometry of the ligand is responsible for the high stability and reactivity in the catalytic reaction.[358, 367-369] The very good performance of **Fe2** is also its major drawback. As the active species is extremely reactive the reaction can be performed properly only at low temperatures using activated olefins as substrates. The latest development in iron epoxidation catalysts, **Fe3**, overcomes this by replacing the strongly donating imidazole moieties by benzimidazoles. Even though the compound is less reactive with a TOF of 95000 h⁻¹ using Sc(OTf)₃ as additive, it is more applicable than its predecessor as it covers a broader substrate scope even at elevated temperatures of up to 80 °C.

5.3.2. Dehydration of Alcohols Catalyzed by Rhenium(VII) trioxo Compounds

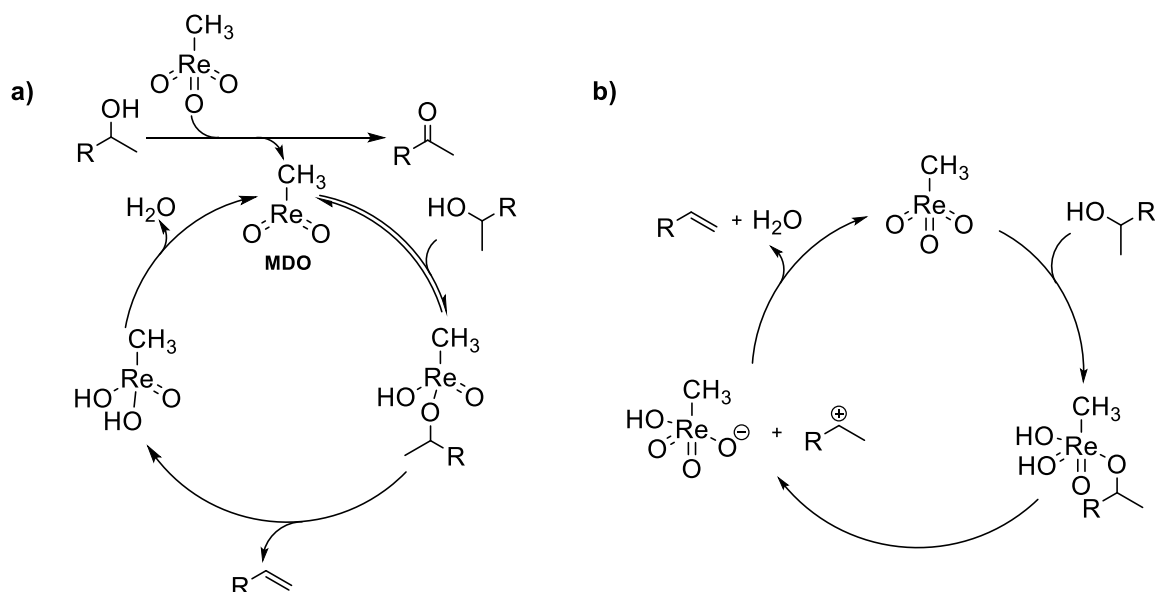
The field of dehydration catalysts is dominated by cheap and durable catalysts like solid acids (alumina, zirconia, zeolites, transition metal halides and fluorinated sulfonic acid polymers) [370-376], inorganic acids[377-379] or organic acids like triflic or *p*-toluenesulfonic acid [380, 381]. Over the last decade interest has increased in the application of rhenium(VII) compounds due to their high selectivity, good reactivity and tolerance towards functional groups.[248] MTO is unsurprisingly the best examined compound active in both, the classical dehydration and deoxydehydration (DODH) reaction.[314] The latter reaction is a reductive dehydration of vicinal diols catalyzed also by perrhenates and derivatives of Cp'ReO₃ which will not be discussed here in detail.[245, 246, 382]

The dehydration reaction is of high importance for the “green” production of chemicals and fuels from biomass by increasing the carbon to oxygen ratio. [382, 383] Increasing the carbon to oxygen ratio is advantageous for increasing the energy density of a molecule and the formation of reactive compounds like olefins or aldehydes from (poly)ols. One of the most prevalent feedstock is lignocellulosic biomass consisting mainly of cellulose (40-50 %), hemicellulose (20-30 %) and lignin. The sugar polymers are already widely exploited by the pulping industry, for the production of fuels or the production of polymers.[382, 384] In contrast, lignin is widely discarded as waste product despite its valuable aromatic content.[385, 386] Within the change from traditional oil based chemistry to a sustainable future, the need arises for “green” base chemicals. Especially in this context, the (deoxy)dehydration reaction is of high importance. Important examples for the current development are:

- Ethanol, derived from the fermentation of sugars, is dehydrated to ethylene by solid acids.[387-389]
- Various sugars are dehydrated to e.g. sorbitol, succinic acid, 5-HMF, adipic acid and levulinic acid[390-394]
- Lactic acid or 3-hydroxypropionic acid derived from glucose fermentation are dehydrated to acrylic acid[395]
- Coniferyl, coumaryl and sinapyl alcohols are obtained by depolymerization of lignin[385]
- Further dehydration of fragments of lignin yields phenols, catechols and vanillin[375]

The processing of these chemicals yields a huge variety of aromatic and (unsaturated) aliphatic base chemicals ready for their application in already established processes. A recent review by Barta and coworkers summarizes very well the current state of the art in the valorization of lignocellulosic biomass.[396] The authors underline the need for selective catalysts in order to suppress the decomposition of valuable products. As rhenium-based compounds have already proven their high

selectivity and tolerance to functional groups, the development of more active and stable such compounds is of particular interest.



Scheme 10: Facilitated mechanisms for the dehydration reaction of alcohols catalyzed by MTO. a) The suggested active catalyst MDO is formed by the in-situ reduction of MTO by one equivalent of alcohol, b) Proposed ionic mechanism with MTO as active catalyst.

The reactivity of rhenium oxo compounds towards alcohols is mainly ascribed to its Lewis acidity indicated by the reliable formation of stable Lewis base adducts. However, the nature of the active species in dehydration reactions is still debated. The mechanism using MTO has been examined by Klein Gebbink *et al.* and our group (Scheme 10). The former applied MTO in the dehydration reaction of simple organic molecules like benzylic, aliphatic or terpene alcohols.[397-399] Using these substrates, an involvement of reduced rhenium species like MDO is ruled out as in stoichiometric control experiments only small amounts of ketone are observed. The alcohol coordinates to the Lewis acidic rhenium center giving a penta-coordinated rhenium species. Consequently, the olefin can be released *via* two pathways: concerted (E₂) or ionic (E₁). In order to discriminate between both possibilities, the authors conducted a substrate screening revealing following trend for the reaction rates:



and within one class of compounds



Therefore, the reactivity corresponds to the stability of the respective carbenium ion. Furthermore, when applying isoborneol as substrate the product camphene is formed quantitatively. The reaction is well known as the Wagner-Meerwein rearrangement and proceeds *via* a 1,2-sigmatropic shift with a carbenium ion as intermediate (Figure 13, **a**). Consequently, the experimental data points clearly to a E₁ mechanism which is also supported by DFT calculations.[399] These calculations also suggest the participation of a second equivalent of alcohol and two molecules of water assisting the abstraction of the hydroxyl moiety. Evidence is given by the inhibition of the reaction when applying non-coordinating *N*-bases like DIPEA.

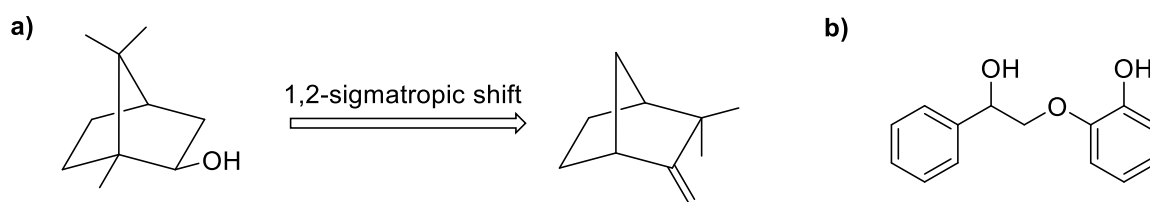


Figure 13: **a)** Camphene is obtained in the Wagner-Meerwein rearrangement from isoborneol. **b)** Mechanism (Scheme 10 a)) is postulated for the dehydration of this β -O-4 model substrate.

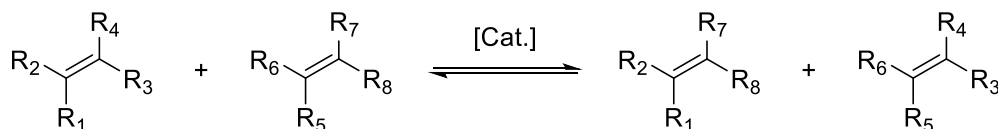
The second mechanism is based on the reactivity of MTO towards the cleavage of a β -O-4 model substrate (Figure 13, **b**). The catalyst MDO is formed by reduction by one equivalent of the alcohol. The substrate coordinates to the active species forming a tetra coordinated rhenium oxo hydroxo species. Upon release of the olefin an intermediate dihydroxo species is formed which returns the catalyst by releasing one equivalent of water. In contrast to the mechanism postulated by Klein Gebbink *et al.*, the activity of MTO is ruled out as a significant induction period is observed even at high temperatures of 135 °C. The active species MDO is characterized as a metastable 3-hexyne adduct by NMR spectroscopy using a ^{17}O -enriched sample of the catalyst precursor. When applying the synthesized MDO-3-hexyne adduct in the cleavage reaction of the model substrate, the induction period is eliminated clearly supporting the suggested mechanism. DFT calculations indicate a significantly higher barrier with 33.6 kcal/mol compared to the MTO based mechanism (11.8 kcal/mol). In accordance with these results, the β -O-4 model substrate is much more reluctant in the dehydration reaction compared to styrene which has been used by Klein Gebbink and coworkers. For the cleavage of the former substrate, 5 mol% of MTO are required to obtain full conversion after 10 h at 155 °C and for the latter one only 1 mol% giving full conversion after 24 h at only 100 °C reaction temperature. The reason for the occurrence of two completely different mechanisms in the dehydration of benzylic alcohols is still unclear. A reasonable explanation might be the presence of the α -ether moiety in the β -O-4 model substrate. The lone pairs of the oxygen atom are repelled by the oxo groups of MTO, so that a reduction is necessary in order to access the Lewis acidic rhenium center. The assumption is supported by the catalytic results of MTO/ H_2 or $\text{Cp}'\text{ReO}_3/\text{PR}_3$ in the DODH of vicinal diols. Following the first mechanism, also the mono dehydration products like ketones or aldehydes have to occur, however, the selectivity for the olefin is throughout >99%. [245, 246, 248]

Beside the organometallic rhenium(VII) compounds, the binary oxide Re_2O_7 has also been applied in the dehydration reaction of various alcohols. Its reactivity is superior to the molecular catalysts exemplarily shown by the TOF of 430 h^{-1} for 1-phenylethanol compared to merely 37 h^{-1} when catalyzed by MTO. [397] Furthermore, the selectivity towards the olefin is increased as the competing acid catalyzed ether formation is almost prevented. However, the mechanism using Re_2O_7 has been widely unknown. It is apparent that the oxide does not fully dissolve in the applied solvent (toluene) pointing to a heterogeneous mechanism and supported by a low reaction order of only 0.15. Experiments using three different sieve fractions also point to a mass-transfer limitation as the initial rates increase upon decreasing particle size. In contrast, reuse experiments fail with diminishing initial reaction rates already after the first recycling step. Another assumption has been the participation of perrhenic acid formed upon hydrolysis of Re_2O_7 . However, the performance of the Brønsted acid differs strongly in terms of reactivity and selectivity. The authors suggest that the overall reactivity of Re_2O_7 might be explained by both, the heterogeneous oxide and dissolved perrhenium species. [399] This is not the case and will be demonstrated in the summary of the third publication within this thesis.

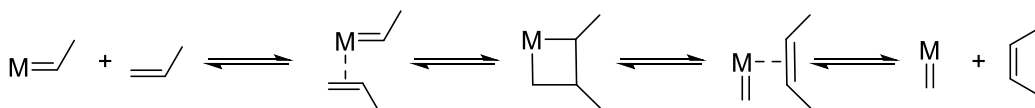
5.3.3. Metathesis reactions Catalyzed by High Valent Rhenium Compounds

One of the most important transition metal catalyzed reactions is the metathesis reaction. Since its serendipitous discovery by Banks and Bailey in 1964[400], several large scale applications have emerged from oil refinery (e.g production of propene from ethylene and butane), organic synthesis to the valorization of biomass.[56, 328, 401] The reaction is best described by the title of the original publication as an “olefin disproportionation” scrambling vicinal substituents of two olefins in an equilibrium reaction (Scheme 11, a)).

a)



b)



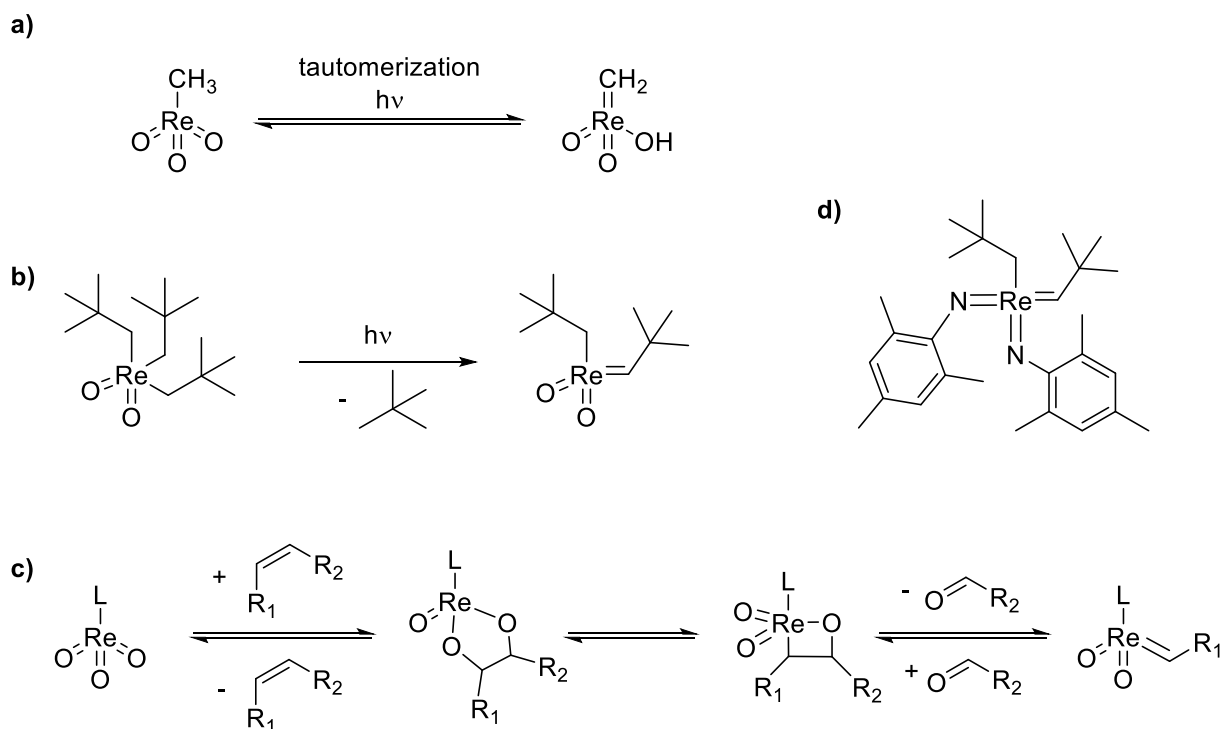
Scheme 11: a) General equation of the metathesis reaction. b) Mechanism according to Chauvin of one step in the self-metathesis of propene.

The currently accepted mechanism has been proposed by Chauvin and Hérisson in 1971 (Scheme 11, b)).[402] The olefin coordinates to a metal alkylidene and forms a metallacyclobutane. The consecutive cleavage of this species can either occur perpendicular to the initially coordinated olefin yielding the product (but-2-ene in the depicted example) or in the same plane, representing the back reaction. Therefore, the reaction is fully reversible and the respective reaction rates depend on the ligand sphere of the metal and the substituents of the olefins.

W, Mo or Re oxides or carbonyls on supports like Al_2O_3 , SiO_2 and Nb_2O_5 are applied on an industrial scale.[403] Tungsten and molybdenum based catalysts require high reaction temperatures of 400 °C and 200 °C, respectively. In contrast, rhenium catalysts are already active at room temperature.[53] Therefore, the catalysts are applied in different industrially relevant processes:

- Tungsten: Lummus OCT process for the production of propene *via* ethenolysis of 2-butene and the reverse reaction in the Philipps triolefin process[56]
- Molybdenum: The highly relevant Shell Higher Olefin Process (SHOP) for the production of α -olefins[404]
- Rhenium: Disproportionation of short and long chain olefins developed by British Petroleum[405]

The reactivity of the latter catalytic system can be significantly enhanced by the addition of SnMe_4 as the highly active catalyst MTO is formed (see 5.3).[92] The reactivity is assigned mainly to chemisorbed MTO as on the one hand, similar activities are achieved by treating Re_2O_7 with SnMe_4 and impregnation of the carrier with MTO and on the other hand, similar active sites are identified for both catalysts.[406] Beside its application as heterogeneous catalyst, MTO performs very well in metathesis reactions in solution.[309] In order to develop new rhenium based metathesis catalysts it is of high importance to understand how the active species is formed. According to the Chauvin mechanism, such a species has to be coordinatively unsaturated and must contain an alkylidene moiety.



Scheme 12: Formation mechanisms for alkylidene species active in the metathesis reaction. a) Photolytic tautomerization reaction observed for MTO. b) Intramolecular elimination reaction of an alkyl ligand. Such alkylidines are effectively stabilized by exchanging the oxo with amido ligands d). c) Currently accepted Pseudo-Wittig mechanism for the activation of alkyl-, aryl- and cyclopentadienyltrioxorhenium compounds.

For MTO, a first activation mechanism is identified by photolysis using UV-light on isolated samples in an argon matrix. The methyldiene is formed in a tautomerization reaction by exchanging a proton from the methyl carbon to an oxo moiety.[407, 408] For higher alkylrhenium(VII) complexes such a mechanism has not been observed yet. Hoffman *et al.* observed a second pathway for the formation of rhenium alkylidene species.[409] A trialkyldioxo rhenium compound eliminates one alkyl moiety photochemically upon formation of a rhenium(V)dioxo alkylidene complex. A few years later, Schrock *et al.* proved the activity of such species in the metathesis reaction.[410] In order to circumvent the photolytic activation, stable alkylidines are synthesized (Scheme 12, d)) over the last few decades. However, these catalysts have to be activated by either a solid support like Al_2O_3 or *N*-bases in order to react in the metathesis reaction.[92]

All these mechanisms cannot account for the activity of aryl- and cyclopentadienyltrioxorhenium⁴ compounds.[92, 411] These problems are circumvented by the Pseudo-Wittig mechanism (Scheme 12, c)). The formation of diolate complexes by reacting trioxorhenium complexes with olefins in a [3+2] addition has been known for decades.[412] However, the consecutive formation of the metallaoxetane, the formal [2+2] addition of the olefin, has been firstly examined in the beginning of the 21st century. Chen and coworkers identified the intermediates and product distribution in collision-induced dissociation (CID) experiments analyzed by tandem ESI-MS.[413, 414] Computational studies support the postulated mechanism and identify requirements for such a [2+2] addition:[415, 416]

- The rhenium species has to be four-coordinate
- At least one ligand has to be a σ -donor
- The σ -donor should be electron deficient

⁴ It should be noted that only CpReO_3 is active in the metathesis reaction. Fully substituted Cp derivatives are inactive.

These predictions have been proven experimentally using phenyltrioxorhenium and perfluorinated phenyltrioxorhenium as catalysts in the ring-opening polymerization (ROMP) of norbornene.[411] Whereat the electron rich PhReO_3 gives only moderate yields at elevated temperatures of 100 °C, full conversion is achieved by the perfluorinated derivative at room temperature. However, a systematic screening of trioxorhenium compounds has not been performed yet.

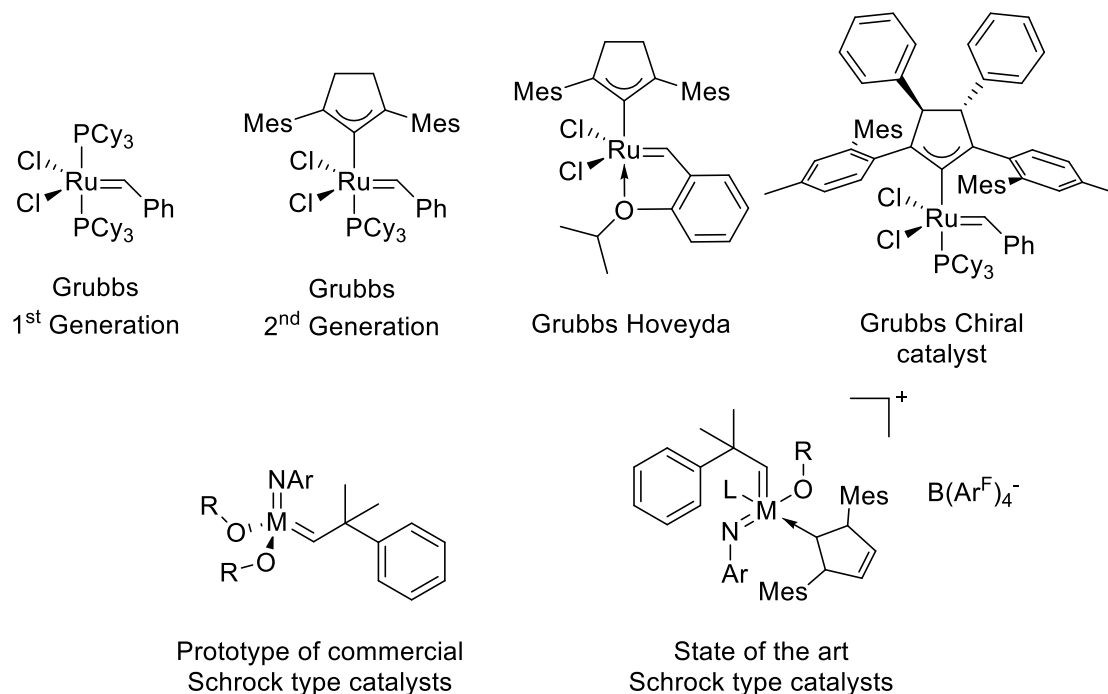


Figure 14: (top) Development of Grubbs type ruthenium based metathesis catalysts ranging from the 1st generation to the chiral catalyst. (bottom) Typical motif of Schrock type metathesis catalysts with M = Mo and W. (bottom, right) Newest development of Schrock type catalysts containing NHCs with significantly increased stability without decrease in reactivity.

The major issues responsible for the underdevelopment of homogeneous rhenium based catalysts are the difficult synthesis of such compounds and the great success of other catalytic systems like the previously discussed heterogeneous catalysts and molecular catalysts based on Ru, Mo and W. The most common ruthenium based catalysts are known as Grubbs catalysts which are widely applied in organic synthesis due to their high tolerance towards functional groups and stability towards ambient conditions.[401] These compounds exhibit a trigonal-bipyramidal structure containing in plane two chlorido ligands and a benzylidene moiety and at least one strong sigma donor. The development of this type of catalyst is very advanced, starting from the initial compound containing two phosphine ligands in apical position (Figure 14, top left). Its reactivity is significantly increased by replacing one of these phosphines with a NHC ligand, developed simultaneously by Grubbs, Nolan, Herrmann and Fürstner.[401] The Hoveyda catalysts exhibit a significantly increased reactivity and are very efficient in asymmetric metathesis reactions by replacing one strong donor ligand with an intramolecular bound oxygen donor. Finally, high selectivities are achieved by Grubbs' chiral catalyst. The chirality is induced by asymmetric wing-tips and backbone modifications of a saturated NHC. Beside the Grubbs-type catalysts, there are manifold highly active compounds based on molybdenum and tungsten, generally known as Schrock-type catalysts. The classical Schrock-type complexes exhibit a distorted tetrahedral structure with one alkylidene, two alkoxides and one imino ligand with bulky substituents. These compounds are also tolerant to functional groups and considerably more active than Grubbs-type catalysts, however their application is less advantageous due to their instability at ambient conditions.[417] Several approaches have been tried to overcome this intrinsic problem, however, most approaches led to less active catalysts.[418] Very recently, this major drawback is finally

overcome by the group of Buchmeiser.[419] By incorporation of one NHC ligand (Figure 14, bottom right), even more active metathesis catalysts are obtained which can be handled at aerobic conditions as no decomposition is observed upon storing these compounds for six days at ambient conditions. The catalytic activity is tailored by the respective NHC ligand with best results obtained using “weak” donors like backbone chlorinated unsaturated NHCs.[420] Therefore, also in this context, NHCs demonstrate superior properties compared to other strong donor ligands underlining the importance of these compounds.

5.4. Rhenium(VII)trioxo Complexes, from Synthesis to Application

Within Chapter 5, the design and application of rhenium(VII)trioxo compounds is presented. The compounds are synthesized starting from Re_2O_7 or more conveniently from chlorotrioxorhenium or acyltrioxorhenium either by the zinc- or tin-route. The former route should be generally applied due to the easy accessibility and low toxicity of the zinc reagents. Tin reagents are important for the synthesis of very sensitive compounds due to the low Lewis acidity of the metal. The synthesized compounds should be analyzed by IR spectroscopy, ^{17}O -NMR spectroscopy and SC-XRD in order to assess the electronic influence of the organic moiety. Finally, the compounds are tested in various catalytic reactions. The most important reactions to date are the epoxidation, the metathesis and the dehydration reaction. However, as highlighted in chapter 5.3, several other applications are conceivable.

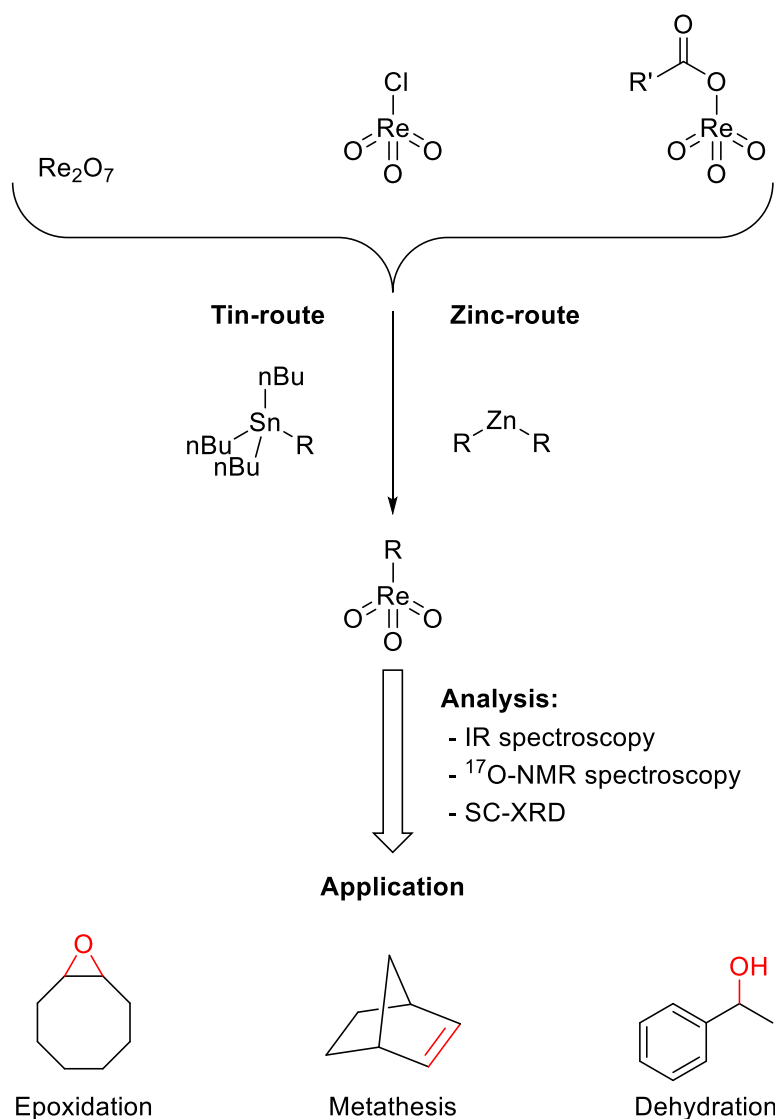


Figure 15: From synthesis to application: A guideline for the successful development of $\text{Re}(\text{VII})$ trioxo compounds. R = aryl, alkyl or cyclopentadienyl.

6. High Valent Rhenium Compounds in Catalysis

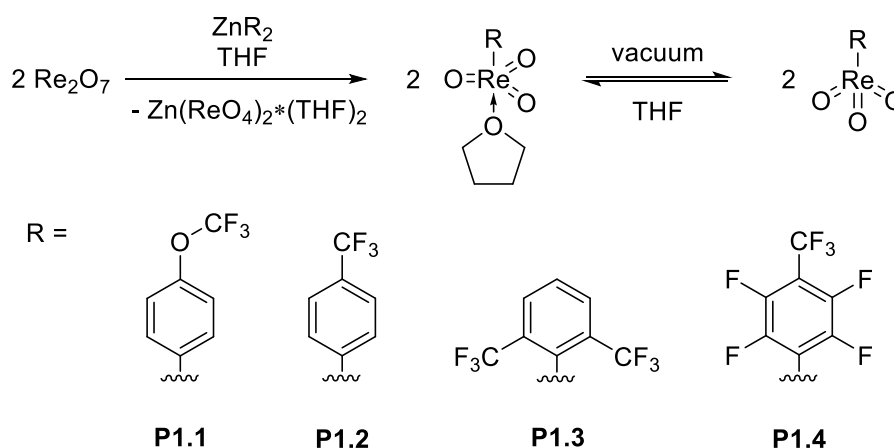
After giving a brief introduction on the redox chemistry of rhenium and the chemistry of organometallic rhenium(VII) trioxo compounds, the next chapters will provide an overview of the main research articles of this dissertation. Within the first publication, the synthesis and application of fluorinated aryltrioxo rhenium compounds is demonstrated. The compounds are thoroughly characterized by ^1H , ^{13}C , ^{17}O and ^{19}F NMR, IR and MS spectroscopy, elemental analysis and partially by SC-XRD. They are applied in the epoxidation reaction of *cis*-cyclooctene using different oxidants. It will be shown, that decreasing the electron density at the rhenium center by incorporation of electron withdrawing groups is beneficial for the catalytic reaction as implied in the chapter 5.3.1. Furthermore, their activity in metathesis reactions is proven. The compounds are active in the self-metathesis of 1-hexene and the ring-opening metathesis of norbornene. In the second publication, the reactivity of an already known alkyl trioxorhenium compound, namely ethyltrioxorhenium, is investigated. In contrast to the results obtained by Herrmann *et al.* a few decades ago (5.3.1), ETO is an applicable catalyst in the epoxidation reaction of *cis*-cyclooctene using a fluorinated solvent and the anhydrous oxidant TBHP (in decane). NMR studies are conducted using ^{17}O labelled compounds revealing that the active catalyst is highly likely a monoperoxo compound. Furthermore, the decomposition pathway of ETO is investigated experimentally and theoretically. Upon thermal treatment, ethane, ethylene and partially methane are observed indicating that both, the radical and the β -hydride elimination pathway, are feasible in line with DFT calculations. The application of rhenium heptoxide in the dehydration reaction of a β -O-4 model substrate is the main topic of the third publication. The compound performs very well in the catalytic reaction with a high turnover frequency and outstanding selectivity towards the sensitive products. However, the kinetic profiles of the reaction and the advantageous product distribution raise questions about the true nature of the catalytic active species. By carefully investigating the reaction products, mechanisms as suggested for MTO (see 5.3.2) are excluded. Analyzing the decomposition products reveal the formation of mixed valence nanoparticles characterized by TEM, DLS, Raman and XPS. A feasible mechanism for their formation is given in line with the well-known redox behavior of rhenium oxides (see 3.1-3.6). Finally, the NPs are unambiguously identified as the active catalyst by filtration experiments and alteration of the reaction conditions so that their formation is inhibited.

6.1. Synthesis, Characterization and Application of Organorhenium(VII) trioxides in Metathesis Reactions and Epoxidation Catalysis

Florian Dyckhoff, Su Li, Robert M. Reich, Benjamin J. Hofmann, Eberhardt Herdtweck and Fritz E. Kühn

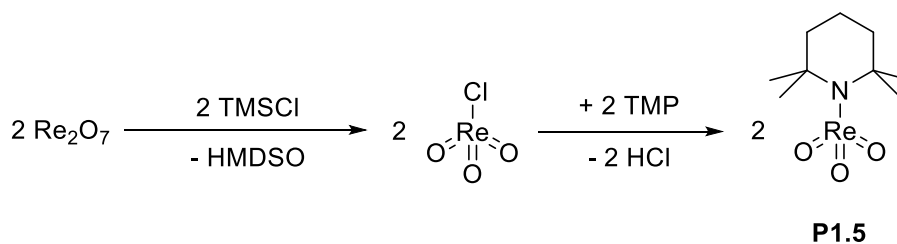
Dalton Trans., **2018**, 47, 9755.

In 2013, the first aryl trioxorhenium compound has been successfully applied in a catalytic epoxidation reaction by using the anhydrous oxidant TBHP.[302] However, only xylyl trioxorhenium is tested so that no insights are obtained on the influence of the substitution pattern of the aryl substituent. Until then it is only assumed that decreasing the electron density at the rhenium center is beneficial for the catalyst's performance. To fill this gap, a series of four fluorinated aryl trioxorhenium compounds are synthesized and tested in catalytic reactions. In addition, an amino trioxorhenium complex is synthesized to prove whether this class of compound is also capable to perform in such reactions.



Scheme 13: Synthesis of four new fluorinated aryl trioxorhenium compounds via the zinc route.

The fluorinated compounds are synthesized *via* the zinc-route. The zinc reagents are obtained by lithiation of the respective bromides and reacted with Re_2O_7 to obtain the desired compounds. Whereat in solution, stable THF complexes are obtained in good yields, the isolation of solvent free products is problematic. The compounds are autocatalytically decomposed by low valent rhenium species, so that the decomposition reactions have to be inhibited. Therefore, two strategies are of high importance: The used rhenium heptoxide has to be of high purity (bright yellow; greenish, partially decomposed Re_2O_7 is not applicable) and the solvent removal has to be performed at low temperature and complete (best results are obtained using *n*-hexane as entrainer).



Scheme 14: Synthesis of the Re(VII)amino complex via chlorotrioxorhenium(VII). TMSCl: Trimethylsilylchloride, HMDSO: hexamethyldisiloxane, TMP: 2,2,4,4-tetramethylpiperidine.

Tetramethylpiperidienyl rheniumtrioxo (**P1.5**) is synthesized starting from Re_2O_7 via the Re(VII)trioxo chloride in a one-pot reaction. Although the isolated yields are mediocre with only 15 %, the crystalline compound is remarkable stable and can be handled at ambient conditions. In contrast, compounds **P1.1-4** are highly sensitive to moisture and decompose to the respective aryl derivative and HReO_4 . Compound **P1.3** is only obtained as THF adduct highly likely due to the strong electron withdrawing effect of the aryl moiety and the isolation of **P1.4** fails.

Table 9: Key properties of compounds **P1.1-3** and **P1.5**, derived from IR spectroscopy (ATR), ^{17}O -NMR spectroscopy (oxygen exchange using labelled MTO, measured in DMSO-d_6) and SC-XRD. ^{a)} Compound characterized as THF adduct.

Analysis	P1.1	P1.2	P1.3 ^{a)}	P1.5
IR: ν_{as} [cm^{-1}]	950	940	931	920
^{17}O -NMR: δ [ppm]	927	939		723
SC-XRD: $r(\text{Re}=\text{O})$ [pm]	170 ^{a)}	171 ^{a)}		171
SC-XRD: $\alpha(\text{O}-\text{Re}-\text{O})$ [°]	118.1 ^{a)}	118.2 ^{a)}		108.9

The electronic properties of the respective aryl moieties are characterized by the previously discussed standard methods. The asymmetric stretching vibration of the $\text{Re}=\text{O}$ bond follows the expected trend from 950 cm^{-1} for the weakest donor in **P1.1** to 920 cm^{-1} for the strongly donating amino ligand in **P1.5**. The results for **P1.3** should be handled with care due to the different coordination geometry. The ^{17}O -NMR results are less straightforward. The amino moiety in **P1.5** is clearly the strongest donor with a remarkable shift of 723 ppm close to the MTO NHC adduct (see 5.2.2). However, **P1.2** has a higher shift than **P1.1** in contrast to the results obtained by IR spectroscopy. This is assigned to the +M-effect induced by the attached oxygen in the latter compound. The structural features of the crystallized complexes are as previously discussed very similar to reference compounds. The $\text{Re}=\text{O}$ bond length varies from 170 – 171 pm and the O-Re-O angle of **P1.5** points out an almost perfect tetrahedral structure. The angles in **P1.1-2** are close to 120° in line with the trigonal bipyramidal geometry.

Table 10: Catalytic epoxidation of *cis*-cyclooctene using complexes **P1.1-3** and **P1.5**. ^{a)} initial TOF determined after 5 min.

Catalyst	Oxidant	Solvent	T [°C]	Y [%]	TOF ^{a)} [h^{-1}]
2	H_2O_2	CH_2Cl_2	r.t.	3	<1
1	TBHP	CHCl_3	55	81	1400
2	TBHP	CHCl_3	55	85	1420
3	TBHP	CHCl_3	55	85	1310
5	TBHP	CH_2Cl_2	r.t.	-	-

In the epoxidation reaction, the compounds behave similar to xyllyltrioxorhenium as almost no product is obtained with the oxidant H_2O_2 . In contrast, good conversions are achieved using TBHP in chlorinated solvents. Only the amino compound **P1.5** is completely inactive in the oxidation reaction. The trend in the TOFs (**P1.1** \approx **P1.2** > **P1.3** > xyllyltrioxorhenium) correlates with the electron withdrawing character of the aryl moiety supporting the assumption that electron withdrawing groups increase the reactivity of Re(VII) trioxo compounds. However, overall the compounds are no match for its congener MTO. One reason for the low performance is the reversible inhibition of the catalyst by the formed *tert*-butanol.

In addition, it is demonstrated that compound **P1.2** and **P1.5** are capable to convert olefins in metathesis reactions using alkyl aluminum chlorides as cocatalysts. The performance in the self-metathesis of 1-hexene is very low with a yield of >60 % only after 24 h compared to MTO after 5 min. However, good results are obtained for both catalysts in the ROMP of norbornene with a molecular weight of $1.3 - 1.6 \times 10^6 \text{ gmol}^{-1}$ and a high *cis*-/*trans*-ratio of >90 % at optimized conditions. Compound

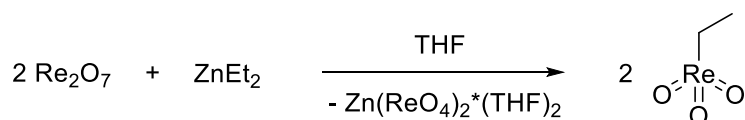
P1.5 is therefore the first amino trioxorhenium compound applicable in metathesis reactions which is remarkable since the predictions for the development of highly active Re(VII)trioxo catalysts suggest, that electron deficient ligands should result in high activities. In contrast, the amino ligand is a good donor as indicated by IR and ^{17}O -NMR spectroscopy.

6.2. Ethyltrioxorhenium – Catalytic Application and Decomposition Pathways

Benjamin J. Hofmann, Stefan Huber, Robert M. Reich, Markus Drees and Fritz E. Kühn

J. Organomet. Chem., **2019**, *885*, 32-38.

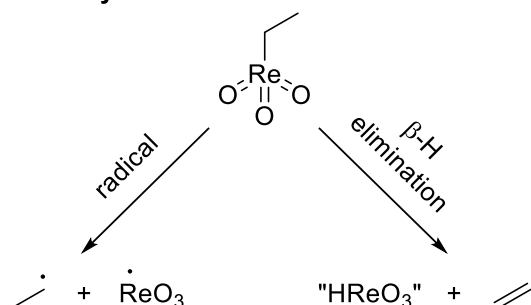
As the performance of the aryl substituted trioxorhenium compounds is not satisfying, the reactivity of the next class of compounds is examined. ETO is probably the best available complex among the alkyltrioxorheniums beside MTO. It is synthesized *via* the zinc-route by reacting Re_2O_7 with diethylzinc. Good yields are only obtained using a diluted solution of 0.05 mol/L of pure yellow Re_2O_7 and low temperatures between $-78\text{ }^\circ\text{C}$ to $-10\text{ }^\circ\text{C}$ during the removal of the solvent THF.



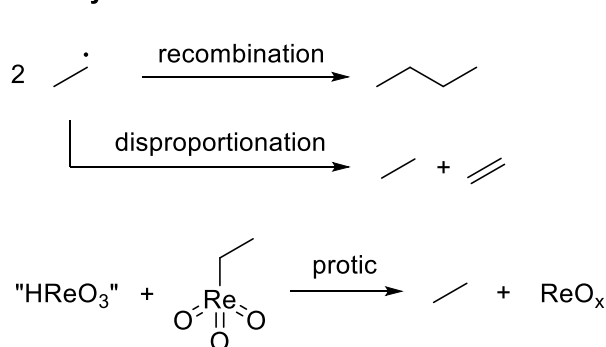
Scheme 15: Synthesis of ETO via the zinc-route.

The activity of the compound is tested in the epoxidation reaction of *cis*-cyclooctene. Using an aqueous solution of H_2O_2 (50 %) only 10 % yield are obtained. Its performance is therefore poor albeit slightly better than for the aryltrioxorhenium compounds. By changing the oxidant to TBHP, yields up to 75 % are achieved using 1 eq. of the catalyst. The limiting decomposition of ETO is less temperature dependent than the epoxidation reaction, so that best results are obtained at $50\text{ }^\circ\text{C}$. In order to increase the reactivity, the previously described methods are tested. Using the fluorinated solvent HFI, the reaction is significantly accelerated so that 60 % conversion is achieved within three minutes giving a TOF of 1200 h^{-1} . Consequently, the compound is more reactive than XTO and only marginally inferior to the presented fluorinated aryltrioxorhenium compounds. The second technique, the addition of a pyridine, did not result in an improved reaction rate but an almost complete inhibition. Using 10 eq. of 4-*tert*-butylpyridine a conversion of 1 % is observed after 24 h reaction time. The reason for the inhibition is the formation of a stable ETO-pyridine complex as detected by ^1H and ^{13}C -NMR spectroscopy which inhibits the formation of the active species. In contrast to the MTO/ H_2O_2 system, the active species is identified as a monoperoxo complex of ETO and one eq. of *tert*-butanol or TBHP ($\text{EtReO}_2(\text{O}_2)\cdot\text{L}$) as shown by ^{17}O -NMR experiments. The peroxo complex is more instable than for XTO in line with its higher reactivity in the epoxidation reaction.

Primary:



Secondary:



Scheme 16: Reaction pathways of ETO in the thermal decomposition in THF. The primary pathways (left) yield highly reactive products which might react in a secondary (right) reaction to yield typical gaseous decomposition products.

As the stability of ETO is limiting, it is of high importance to elucidate the decomposition pathways of the compound. Therefore, ETO is dissolved in THF and heated to $60\text{ }^\circ\text{C}$. The solution turns dark due to

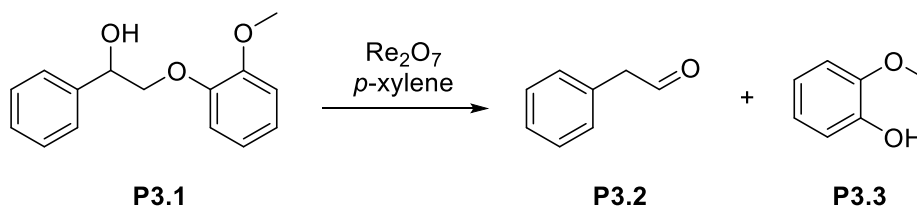
the formation of oxidic rhenium species. The formed gaseous products are quantified by GC-FID. A significant induction period is observed with only 4 % rel. yield of gaseous products after 5 d and almost 50 % after 11 d. Such a behavior is typical for the trioxorhenium compounds due to the well-known autocatalytical decomposition. Ethane and ethylene are formed almost equimolar throughout the whole reaction time. Such a product distribution might be explained by a purely radical mechanism and consecutive disproportionation (Scheme 16). However, as no butane is detected, the solution has to be too diluted for such a follow-up reaction. The second possibility might be a purely β -H-elimination giving 1 eq. of ethylene and formally rhenic acid. Such a Brønsted acid might react with a second molecule of ETO giving 1 eq. of ethane and rhenium oxides. In order to discriminate between these pathways, a DFT calculation is performed. The transition state for a proton induced decomposition is not reasonable with a Gibbs free energy barrier of 103 kcal/mol. Therefore, the product distribution is only explainable by a simultaneous decomposition by the radical mechanism and β -H-elimination. In line with this assumption are the calculated Gibbs free energy barriers for both reactions with 51.9 and 54.0 kcal/mol, respectively, using a PCM solvent model with THF as solvent. The barrier is overestimated due to the applied DFT method, however, the results are feasible as the decomposition reaction takes 11 days to obtain approximately 50 % rel. yield. Therefore, both, protons in β -position and substituents which favor a radical decomposition are weak spots for trioxorhenium compounds with longer alkyl chains than methyl.

6.3. Reactivity of Re_2O_7 in Aromatic Solvents – Cleavage of a β -O-4 Model Substrate by Lewis-acidic Rhenium Oxide Nanoparticles

Benjamin J. Hofmann, Reentje G. Harms, Sebastian P. Schwaminger, Robert M. Reich and Fritz E. Kühn

J. Catal., **2019**, 373, 190-200.

Beside the molecular rhenium compounds, the binary oxide Re_2O_7 is of particular interest in catalytic reactions. Although it has been applied in various different types of reactions, very little is known about its mechanism. To fill this gap, a systematic study on the reactivity of Re_2O_7 in the dehydration reaction of a lignin model substrate is conducted. Lignin is a condensed polymer of sinapyl, coniferyl and *p*-coumaryl alcohols. A variety of different bonding types are identified between these monomers very well summarized in several reviews.[375, 383, 395, 396, 421, 422] Among these, the β -O-4 bond is the most abundant one rendering the model substrate **P3.1** an ideal substrate to assess the ability of Re_2O_7 to degrade the biomass derived polymer. The cleavage of **P3.1** is typically catalyzed by acids yielding the products guaiacol **P3.3** and phenylacetaldehyde **P3.2** *via* an enol-ether. A major disadvantage is the consecutive repolymerization of the latter compound under such conditions. Therefore, the applied acid has to be strong enough to cleave the β -O-4 bond but too weak to repolymerized the sensitive aldehyde **P3.2**. Until then, no such acid has been identified and scavengers are commonly used to inhibit the undesired side-reaction.[380, 423]



Scheme 17: Cleavage of a lignin model substrate by rhenium heptoxide to the products phenylacetaldehyde and guaiacol.

The catalytic results using Re_2O_7 are promising with a high TOF of 240 h^{-1} under optimized conditions and full conversion even at low catalyst loadings of 0.1 mol%. Very high selectivities are achieved especially to the sensitive product **P3.2**. The comparison to other Lewis acids indicate that only $\text{Sc}(\text{OTf})_3$ and SnCl_4 are capable to compete with Re_2O_7 , however, with significantly reduced selectivity. In order to elucidate, whether the oxidic nature is the reason for the catalyst performance, other related metal oxides are tested. However, no conversion is detected throughout all tested compounds.

Table 11: Excerpt of selected tested Lewis acids and related metal oxides in comparison to Re_2O_7 . Reaction conditions: 5 wt% catalyst, *p*-xylene, 140°C , $t = 4 \text{ h}$.

Catalyst	Conversion P3.1 [%]	Yield P3.2 [%]	Yield P3.3 [%]
Re_2O_7	>99	71	75
AlCl_3	16	0	4
FeCl_3	72	2	46
$\text{Sc}(\text{OTf})_3$	>99	7	71
SnCl_4	>99	0	36
MoO_3	0	0	0
WO_3	0	0	0

Unlike in oxidation reactions, the reactivity of Re_2O_7 is not most reactive in coordinating solvents but in unpolar, aromatic solvents like *p*-xylene. Using THF, the yield is reduced to only 26 %. In aliphatic solvents a very low conversion of only 8 % after 4 h using 0.1 mol% of Re_2O_7 is obtained. In aromatic solvents, the compound should behave as a heterogeneous catalyst, as it is generally assumed to be insoluble. However, recycling experiments fail as almost 87 % of the reactivity is lost within the first filtration step and the performance gradually decreases within the following steps.

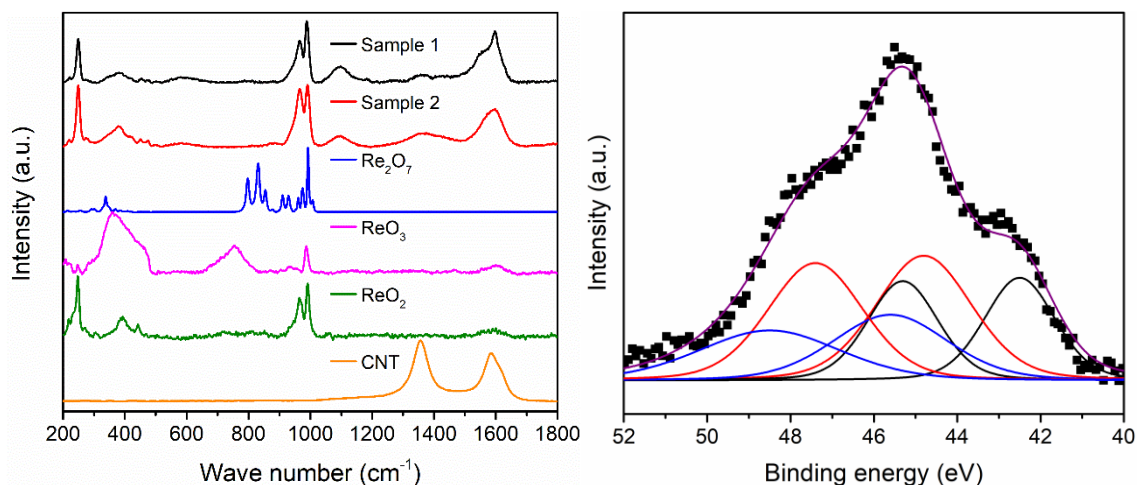
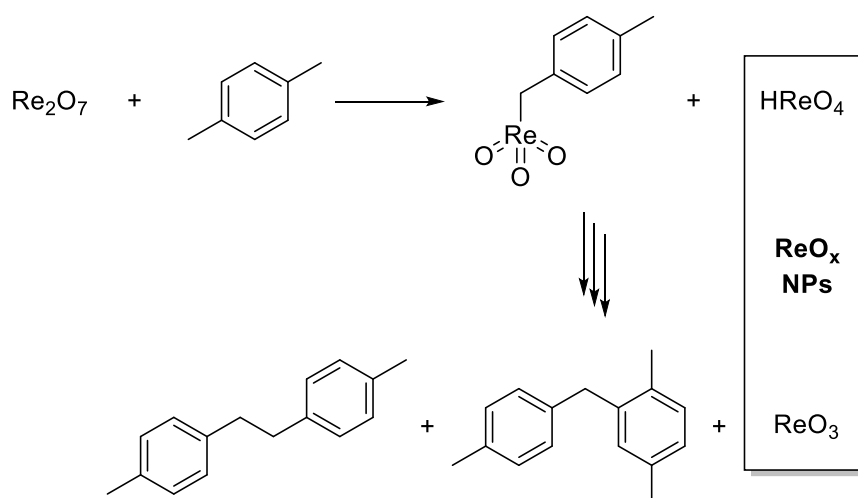


Figure 16: Analysis of the black precipitate formed after the cleavage reaction of **P3.1** by Raman (left) and XPS (right). (left) references of authentic samples are given. (right) Deconvolution of the $\text{Re}4f$ region narrow scan.

Therefore, the real nature of the active catalyst is questionable. Within the reaction, a black precipitate is formed which is analyzed by Raman and XPS in order to get insights into active species. The XPS narrow scan of the $\text{Re}4f$ region reveals, that the oxide is partially reduced to Re(VI) and Re(IV) (Figure 16, left) with variable content depending on the reaction and workup conditions. The Raman spectra support the assumption that Re_2O_7 is completely converted to a mixed valence oxide supported on char. The full conversion of Re_2O_7 is identified by the absence of the bridging Re-O-Re vibrations in the region of $\approx 800 \text{ cm}^{-1}$. The formation of char is identified by the strong signal in the region of 1590 cm^{-1} assigned to sp^2 -hybridized carbon. Similar spectra are obtained for reactions without the substrate **P1.1** identifying the solvent as exclusive reaction partner.



Scheme 18: Activation of Re_2O_7 by *p*-xylene and the consecutive decomposition of the formed 4-methylbenzyltrioxorhenium to organic recombination products and rhenium oxides

After a careful analysis of the reaction (products) of Re_2O_7 with *p*-xylene using GC-MS, UV/Vis, *in-situ* IR and ^{17}O -NMR spectroscopy a highly likely mechanism is postulated. Re_2O_7 reacts with *p*-xylene giving the extremely instable 4-methylbenzyltrioxorhenium. The compound decomposes following a radical mechanism. The released radicals react with a second solvent molecule and forms bisxylyls (Scheme 18) in the recombination reaction. The formation of char is attributed to the radical polymerization of *p*-xylene. The composition of the formed rhenium oxide is attributed to the manifold disproportionation reactions known for rhenium oxides as discussed in chapter 3.6. The discussed activation reaction is crucial for the formation of an active catalyst shown in a solvent screening experiment. The reactivity of the catalyst is not sensitive to the substitution pattern ranging from electron rich aromatics like mesitylene to electron deficient ones like 1,4-difluorobenzene. However, when using a solvent which cannot be deprotonated such as C_6F_6 , the reaction is fully inhibited.

Table 12: Test reactions in the dehydration of **P3.1** catalyzed by identified decomposition products of Re_2O_7 in *p*-xylene.

Compound	Conversion	Yield	Yield
	P3.1 [%]	P3.2 [%]	P3.3 [%]
ReO_2	0	0	0
ReO_3	0	0	0
KReO_4	5	0	0
$\text{HReO}_4(\text{aq})$	34	19	26
$\text{Re}_2\text{O}_7 \cdot 2(\text{H}_2\text{O})$	86	45	58
Mesityltrioxorhenium	0	0	0
Re_2O_7	87	57	63

The question arises, which of the formed compounds is responsible for the good performance of the precatalyst Re_2O_7 . Control experiments are performed with authentic samples of the identified compounds (Table 12). All rhenium oxides, potassium perrhenate and an aryltrioxorhenium compound are inactive in the dehydration reaction. Perrhenic acid is capable to convert **P3.1**, however, with an overall lower performance. Only solid perrhenic acid gives similar conversions but with reduced selectivity towards **P3.2** in line with the reactivity of Brønsted acids. Therefore, none of the applied substances can constitute to the overall good performance.

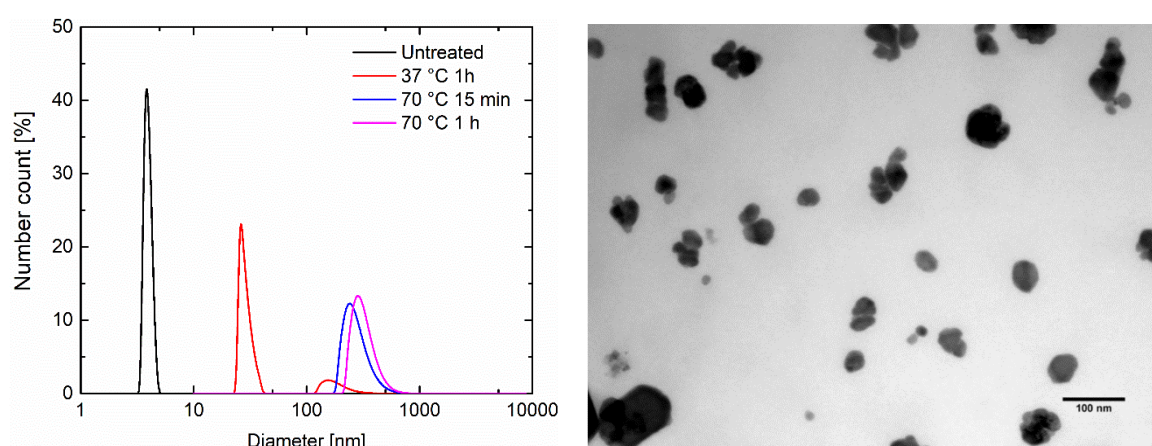


Figure 17: Analysis of the mixed valence rhenium nanoparticles by DLS (left) and TEM (right). The TEM image is obtained from a sample treated at 70 °C.

As spectroscopic methods did not succeed in the identification of the active catalyst, the analysis of the morphology of the rhenium oxides is conducted. Therefore, the formation of char is suppressed by addition of a radical scavenger. The analysis of the supernatant solution of a reaction of Re_2O_7 reveals the formation of small NPs (4 nm) which agglomerate with increasing reaction temperature (Figure

17). These NPs are unambiguously identified as the active catalyst performing a splitting experiment. The cleavage reaction of **P3.1** is stopped after 20 min and one part is filtrated over celite. Whereat the unfiltrated solution gives normal yields, the reaction stops completely after filtration. Furthermore, pre-synthesized nanoparticles are capable to convert **P3.1** even in the inert solvent C₆F₆. Therefore, Re₂O₇ reacts with the aromatic solvent yielding Lewis acidic mixed-valence rhenium particles which are highly active in dehydration reactions and tolerant towards the sensitive products.

7. High Valent Rhenium Chemistry – An Outlook

The presented work displays the manifold reactivity of high valent rhenium trioxo compounds and improves our understanding by getting deeper insights into the structure-reactivity relationship in some catalytic reactions. Within the first publication, the accessibility of electron deficient aryltrioxorhenium compounds is proven. The good performance of these type of compounds is in line with the predictions of Chen and coworkers, however, these compounds are no match to the well elaborated Grubbs and Schrock-type catalysts (see 5.3.3). More interestingly, the aminotrioxorhenium compound **P1.5** is also highly active in the ROMP of norbornene. This finding is in stark contrast to the DFT derived suggestions for the synthesis of highly active Re(VII)trioxo catalysts. One possibility might be the formation of an imino moiety within the catalytic reaction significantly reducing the σ -donor properties of the ligand. Such a compound is closely related to Schrock-type catalysts and might account for the high reactivity. Tuning the electronic and steric properties of the amino ligand might result in higher reactivities and selectivities. The amino moiety is a perfect template to synthesize enantio- or regioselective catalysts by using asymmetric substituted cyclic amines. Therefore, the development of such catalysts might be an interesting new field in high valent rhenium chemistry even though they have to compete against the previously described well-established Ru, Mo and W based compounds.

Concerning the epoxidation reaction, the reactivity of the differently substituted compounds follows very well the predictions. With decreasing donor properties of the ligand, the reactivity decreases although only marginally. This finding important as it underlines that the reactivity of rhenium(VII)trioxo compounds in the epoxidation reaction is well understood, however, tuning the electronic properties of aryl ligands is not particularly suitable for the more active catalysts than MTO. Increasing reactivities by using weaker donors clearly underlines that the properties of the active species is different when compared to Mo and Fe based catalysts. For the latter catalytic systems, it is of high importance to stabilize the active species by strong donors whereat for Re compounds higher activities are achieved by destabilizing the formed peroxo species. Turning to alkyltrioxorhenium compounds, the development of new compounds is significantly hampered by their intrinsic instability. As shown within this work, both, the radical and β -H-elimination pathway contribute to the decomposition of such compounds rendering the development of new catalysts challenging. Increasing the chain-length facilitates the β -H-elimination whilst branched alkyls or benzylic compounds are prone to eliminate radically in line with the generally known trends in stability. Using β -fluorinated alkyls might result in a better performance although it such a modification might also result in even weaker Re-C bonds as observed for highly electron deficient aryltrioxorhenium compounds. Another approach might be the application of strained, cyclic alkyls like substituted cyclopropyl derivatives. As discussed in chapter 5.3.1, the unsubstituted derivative has already proven to be more effective in the epoxidation reaction than MTO using a stabilizing *N*-donor as additive. Applying such additives is highly effective to increase the reactivity and stability of such compounds, however, only when combined with H_2O_2 as oxidant. The TBHP route is generally less successful as significantly reduces TOFs are observed. From a scientific perspective, it is highly interesting as it gives insights into the formation of active species, however, from a user's point of view, using this oxidant is not beneficial. The bulky *tert*-butyl moiety prevents the formation of a bisperoxo species as demonstrated by ^{17}O -NMR experiments which highly likely accounts for the moderate reaction rates. Therefore, it is more interesting to combine derivatives of MTO with stabilizing *N*-donors and fluorinated solvents. Within the literature, there is a general and successful trend in using NHCs as stabilizing donors. Replacing the weak *N*-donors with these elaborated spectator ligands might also result in new, highly active catalytic systems. However, all in all, these compounds have to compete with the recent developments in iron

epoxidation catalysts. It is doubtful whether rhenium-based catalysts can step up to these compounds with regard to reactivity, synthetic accessibility and especially its price.

The most important finding within this dissertation is the identification of the active species in the dehydration reaction using Re_2O_7 as precatalyst and the elucidation of its activation mechanism. Despite the very good performance of the here presented catalytic system, its application is doubtful as the depolymerization of lignin is a challenge on a very large industrial scale and, as shown here, catalyst leaching is expectable due to both, loss of NPs and formation of dissolved rhenium complexes. However, from a scientific perspective there are some very important insights to highlight:

1. The misleading and inconclusive debate on the properties of Re_2O_7 in apolar solvents is settled

Rhenium heptoxide is indeed insoluble in non-coordinating and apolar solvents. However, it reacts with the solvent forming the nanoparticles. Therefore, the particle size of Re_2O_7 is important for its reactivity as described by Klein Gebbink and coworkers, however only in the activation step not in catalysis. The catalytic reaction is homogeneous and follows the kinetic laws of this reaction type.

2. The NPs represent an easy to handle catalyst highly likely active in various different catalytic reactions

The stability of the NPs towards ambient conditions is proven within this work. NPs purified in ambient conditions exhibit similar reaction rates and yields when compared to NPs worked up under inert conditions. They are easily synthesized by exposing Re_2O_7 to an aromatic solvent and are obtained either supported on char or pure by using a radical scavenger. Their size can be adjusted by choosing the proper temperature reaction time within the synthesis. However, its relevance is not yet tested and such experiments will be challenging without the application of stabilizing additives. Gaining better insights into the size-oxidation state-reactivity relationship will be highly interesting as the synthesis of (mixed-valence) rhenium NPs is currently a vital field as shown in chapter 3.5. Beside catalytic reactions, these particles are applied from medicinal and analytical chemistry to wastewater treatment and such the here presented simple synthetic protocol might facilitate their development. Most important are the applications in which their participation is not identified (yet). Rhenium heptoxide is applied under similar reaction conditions in various catalytic transformations like the oxidation of alcohols[424], DODH[425, 426], Friedel-Craft benzylation[427], benzylation of amines[428], substitution of alcohols by amines[429], modification of hemi-acetals and aldehydes[430], formation of *spiro*-alkanes[431], the arene homologation[432] and cycloetherification reactions[433]. Very recently, Re_2O_7 has shown to be active in the demethoxylation and alkylation of guaiacol. The XPS analysis suggests a similar oxidation state of rhenium as presented here, however, the nature of the active catalyst is not analyzed yet.[434] Therefore, the participation of these nanoparticles is highly likely in at least some of these reaction and should be tested systematically. The scope of application of these NPs should be also extended to heterogeneous catalysis. As previously described, such catalysts are applied in several important reactions. Using Re_2O_7 , most catalysts have to be pretreated in order to obtain well defined nanostructures.[169] In contrast, the application of the here presented NPs will facilitate this process and might result in better defined and more active catalysts.

3. Organometallic Re(VII)trioxo compounds are suitable precursor for the synthesis of mixed-valence NPs

Within the activation mechanism of Re_2O_7 in *p*-xylene it is shown that benzyltrioxorhenium is an intermediate species. Within the decomposition of that compound, char and the NPs are formed. Therefore, other defined metalorganic Re(VII)trioxo compounds are also suitable precursor for synthesis. A first hint on this reactivity is given by the kinetic profiles of such compounds in various

reactions. There are several examples exhibiting an initial “burst” phase with high reaction rates followed by a moderate but steady second phase. Catalyst deactivation might contribute to such a reaction profile, however, in most cases, the steady phase is too pronounced so that a consecutive active species is more likely. For the synthesis of defined Re NPs, the decomposition pathway of the respective precursor should be taken in account. A long-chain aliphatic compound will decompose mainly in a β -H elimination reaction and a branched or benzylic one radically. Whereat the first reaction formally yields Re(V), the latter one results in Re(VI). Therefore, by choosing the right precursor, the oxidation state of these particles might be adjusted. The influence on their composition is, of course, not predictable due to the complex redox chemistry of rhenium (see chapter 3.6). However, it might be a reasonable approach to obtain defined and novel NPs. Furthermore, it is unclear whether the surface is covered at least partially with the respective organic moiety. If this is the case, the modification of the precursor should finally result in varied physico-chemical properties.

8. Conclusion

The chemistry of high valent rhenium compounds is dominated by the versatility and performance of MTO. However, since the discovery of its superior catalytic properties no other molecular rhenium compound has been developed with at least similar properties and the question arises, what is the next step in the development of such compounds.

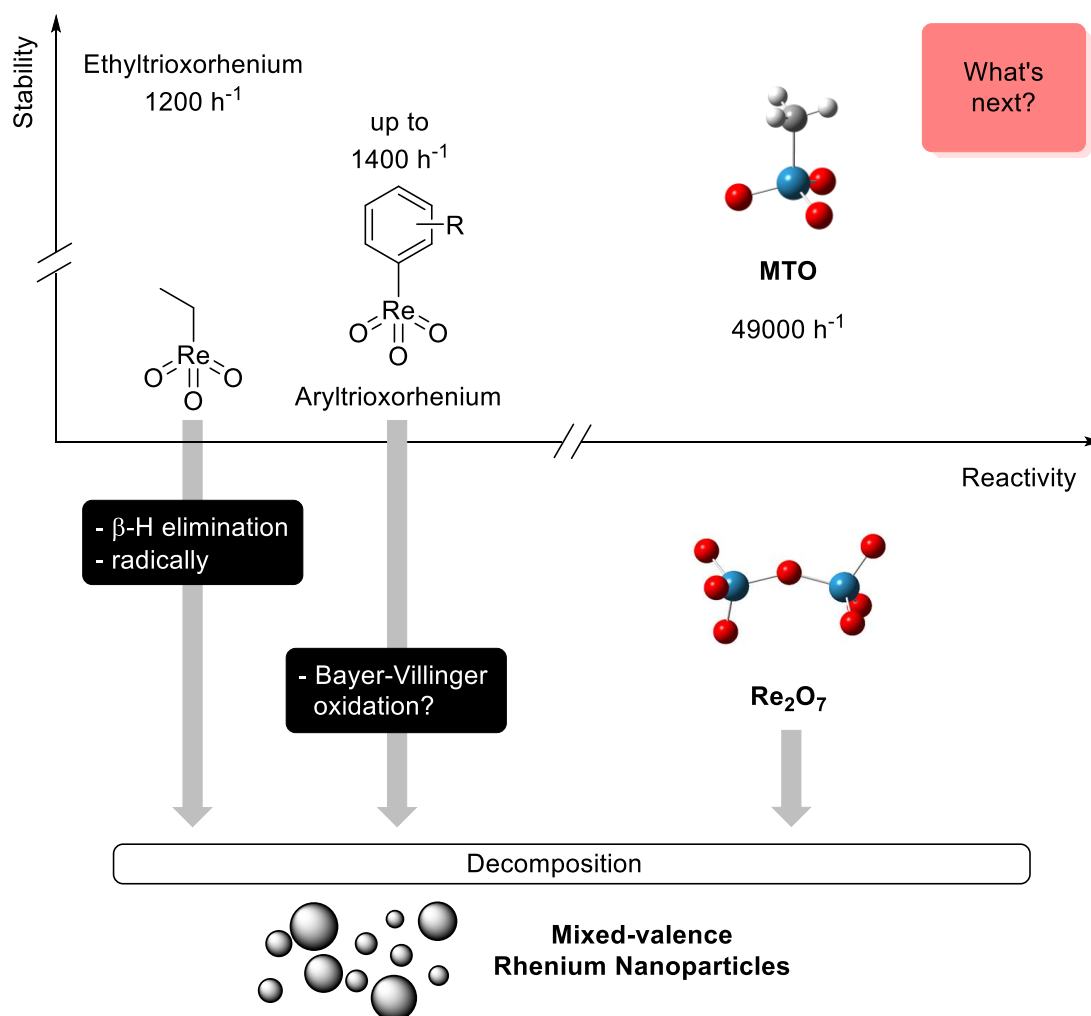


Figure 18: Summary of the results obtained within the dissertation.

Within this work, fundamental key properties of two classes of compounds are assessed by spectroscopy and catalytic examinations (mainly epoxidation reaction). The reactivity in the epoxidation reaction is indeed tunable by altering the electronic properties as shown by the incorporation of electron withdrawing groups in aryltrioxorhenium compounds. However, overall, the observed impact is less convincing as expected. Aryl- and the tested alkyltrioxorhenium compounds are much less reactive than its congener MTO, however, the real activity is hard to assess due to the concurrent decomposition reaction. With regard to aryltrioxorhenium, the decomposition reaction is not analyzed yet and might follow a similar Baeyer-Villiger-type mechanism as MTO. The stability of alkyltrioxorhenium compounds is dependent mainly on two properties: The stability of the respective radical species and the presence of protons in β -position. A more stable compound has to fulfill both criteria as otherwise one of the existing decomposition pathways cannot be avoided. Despite their limited success as catalyst in several reactions, these compounds are suggested to be of high relevance in the synthesis of tailored mixed-valence rhenium nanoparticles. Within the dehydration reaction of a lignin model substrate by Re_2O_7 , the formation of such nanoparticles is observed. These particles are identified as the true active species and the binary oxide is completely inactive. The activation mechanism is elucidated showing that an intermediate benzyltrioxorhenium species decomposes to these NPs. Therefore, all instable trioxorhenium might be reasonable precursors for the defined synthesis of such compounds. Depending on the respective decomposition pathway, the oxidation states within the particles might be altered and possibly the surface differently modified. The high importance of such NPs is highlighted as they are known to be excellent catalysts, applied in the treatment of cancer or as sensitizers in SERS. Furthermore, as rhenium heptoxide is applied as “catalyst” in several other reactions using similar conditions, there might be various other, not yet explored applications which just wait for their discovery.

9. Literature

- [1] D.I. Mendeleev, Zh. Russ. Fiz.-Khim. Obsch., (1869) 60.
- [2] L. Meyer, Die Natur der chemischen Elemente als Function ihrer Atomgewichte, in: F. Wöhler, J. Liebig, H. Kopp (Eds.) Annalen der Chemie und Pharmacie: Supplementband, C. F. Winter'sche Verlagshandlung, 1869, pp. 354-364.
- [3] J.W. van Spronsen, J. Chem. Educ., 46 (1969) 136.
- [4] E.C. Constable, Dalton Trans., 48 (2019) 9408-9421.
- [5] F.L. Nilson, Chem. Berichte, 12 (1879) 554-557.
- [6] M.L. de Boisbaudran, Acad. Sci., Paris, 81 (1875) 493.
- [7] C. Winkler, Chem. Berichte, 19 (1886) 210-211.
- [8] H. Cassebaum, G.B. Kauffman, Isis, 62 (1971) 314-327.
- [9] D.I. Mendeleev, Periodic table of the elements, in: Osnovy Khimii (Principles of Chemistry), Volume II, Saint Petersburg, Russia (Federation), 1871.
- [10] W.T. Noddack, Ida, Die Naturwissenschaften, 13 (1925) 567-574.
- [11] B.V. Tiggelen, The Discovery of New Elements and the Boundary Between Physics and Chemistry in the 1920s and 1930s. The Case of Elements 43 and 75, in: Chemical Sciences in the 20th Century, 2001, pp. 131-145.
- [12] V. Karpenko, Ambix, 27 (1980) 77-102.
- [13] I. Noddack, W. Noddack, in: Zeitschrift für Physikalische Chemie, 1931, pp. 207.
- [14] W. Prandtl, Angew. Chem., 39 (1926) 1049-1051.
- [15] O. Zvjaginstsev, Nature, 118 (1926) 262-263.
- [16] J.G.F. Druce, F.H. Loring, Chem. News, 131 (1925) 273-277.
- [17] V. Dolejek, J. Heyrovský, Nature, 116 (1925) 782-783.
- [18] W. Noddack, I. Noddack, Angew. Chem., 40 (1927) 250-254.
- [19] J. Noddack, W. Noddack, Z. Anorg. Allg. Chem., 183 (1929) 353-375.
- [20] M. Bodenstein, O. Hahn, O. Höning Schmid, R.J. Meyer, Berichte der deutschen chemischen Gesellschaft (A and B Series), 63 (1930) 1-24.
- [21] J. Heyrovský, Nature, 135 (1935) 870-871.
- [22] J.G.F. Druce, Rhenium, Cambridge University Press, Cambridge 1948.
- [23] N.N. Greenwood, A. Earnshaw, 24 - Manganese, Technetium and Rhenium, in: Chemistry of the Elements (Second Edition), Butterworth-Heinemann, Oxford, 1997, pp. 1040-1069.
- [24] H.K. Yoshihara, Proceedings of the Japan Academy, Series B, 84 (2008) 232-245.
- [25] M. Ogawa, Chem. News, 98 (1908) 249-251.
- [26] H. Moseley, Nature, 92 (1914) 554-554.
- [27] H. Onishi, Kagaku to Kogyo, 43 (1990) 1717.
- [28] D.A. John, R.R. Seal II, D.E. Polyak, in: K.J. Schulz, J.J.H. DeYoung, R.R. Seal II, D.C. Bradley (Eds.) Professional Paper, Reston, VA, 2017, pp. 62.
- [29] P. Voudouris, V. Melfos, P. Spry, L. Bindi, R. Moritz, M. Ortelli, T. Kartal, Minerals, 3 (2013) 165-191.
- [30] T.A. Millensifer, Rhenium and Rhenium Compounds, in: Kirk-Othmer Encyclopedia of Chemical Technology, 2010, pp. 1-22.
- [31] M.A. Korzhinsky, S.I. Tkachenko, K.I. Shmulovich, Y.A. Taran, G.S. Steinberg, Nature, 369 (1994) 51-52.
- [32] K.K. Kojonen, A.C. Roberts, O.-P. Isomäki, V.V. Knauf, B. Johanson, L. Pakkanen, Can. Mineral, 42 (2004) 539-544.
- [33] I.E. Campbell, D.M. Rosenbaum, B.W. Gonser, Journal of the Less Common Metals, 1 (1959) 185-191.
- [34] I.F. Barton, C.A. Rathkopf, M.D. Barton, Mining, Metallurgy & Exploration, 37 (2020) 21-37.
- [35] A.V. Naumov, Russian Journal of Non-Ferrous Metals, 48 (2007) 418-423.
- [36] V.I. Alekseev, Y.B. Marin, Doklady Earth Sciences, 478 (2018) 250-252.
- [37] M. Min, J. Chen, J. Wang, G. Wei, M. Fayek, Ore Geology Reviews, 26 (2005) 51-69.
- [38] U. Kesime, A. Chrysanthou, M. Catulli, Int. J. Refract. Met. Hard Mater., 82 (2019) 150-158.

- [39] W. Feit, *Angew. Chem.*, 43 (1930) 459-462.
- [40] in <https://s3-us-west-2.amazonaws.com/prd-wret/assets/palladium/production/mineral-pubs/historical-statistics/ds140-rheni.xlsx>, accessed at 23.04.2020
- [41] in <https://apps.catalysts.basf.com/apps/eibprices/mp/DownloadFile.aspx?ChartType=Yearly&Category=&MetalName=Rhenium&FromDate=01/01/2001&ToDate=04/23/2020&Market=EIB>, accessed at 23.04.2020
- [42] H. Tropsch, R. Kassler, *Berichte der deutschen chemischen Gesellschaft (A and B Series)*, 63 (1930) 2149-2151.
- [43] C.D. Anderson, P.R. Taylor, C.G. Anderson, *Mining, Metallurgy & Exploration*, 30 (2013) 59-73.
- [44] L.G. Kasikov, A.M. Petrova, *Theor. Found. Chem. Eng.*, 43 (2009) 544-552.
- [45] Z.S. Abisheva, A.N. Zagorodnyaya, N.S. Bekturganov, *Hydrometallurgy*, 109 (2011) 1-8.
- [46] W. Xia, X. Zhao, L. Yue, Z. Zhang, *J. Mater. Sci.*, 44 (2020) 76-95.
- [47] B.H. Ge, Y.S. Luo, J.R. Li, J. Zhu, *Scripta Mater.*, 63 (2010) 969-972.
- [48] H.E. Klusdahl, (1967), US3415737A. United States of America
- [49] M.J. Dees, M.H.B. Bol, V. Ponec, *Appl. Catal.*, 64 (1990) 279-295.
- [50] V.K. Shum, J.B. Butt, W.M.H. Sachtler, *J. Catal.*, 96 (1985) 371-380.
- [51] L.W. Jossens, E.E. Petersen, *J. Catal.*, 76 (1982) 265-273.
- [52] J. Xiao, R.J. Puddephatt, *Coord. Chem. Rev.*, 143 (1995) 457-500.
- [53] J.C. Mol, *Catal. Today*, 51 (1999) 289-299.
- [54] V.G. Kessler, G.A. Seisenbaeva, *Minerals*, 2 (2012) 244-257.
- [55] R.F. Morrison, N. Lipscomb, R.B. Eldridge, P. Ginn, *Ind. Eng. Chem. Res.*, 53 (2014) 19136-19144.
- [56] J.C. Mol, *J. Mol. Catal. A: Chem.*, 213 (2004) 39-45.
- [57] J.C. Mol, *Top. Catal.*, 27 (2004) 97-104.
- [58] S. Krompiec, M. Penkala, K. Szczubiałka, E. Kowalska, *Coord. Chem. Rev.*, 256 (2012) 2057-2095.
- [59] T. Tsoncheva, S. Vankova, O. Bozhkov, D. Mehandjiev, *Can. J. Chem.*, 85 (2007) 118-123.
- [60] A.S.Y. Chan, W. Chen, H. Wang, J.E. Rowe, T.E. Madey, *J. Phys. Chem. B*, 108 (2004) 14643-14651.
- [61] X. Zhang, S. Zhang, C. Jian, *Chem. Eng. Res. Des.*, 89 (2011) 573-580.
- [62] S. Satoh, Y. Tanigawa, (1999), US6379507B1
- [63] A.K. Dalai, B.H. Davis, *Appl. Catal. Gen*, 348 (2008) 1-15.
- [64] N.E. Tsakoumis, M. Rønning, Ø. Borg, E. Rytter, A. Holmen, *Catal. Today*, 154 (2010) 162-182.
- [65] Y. Jun, D. Jingfa, Y. Xiaohong, Z. Shi, *Appl. Catal. Gen*, 92 (1992) 73-80.
- [66] N. Eliaz, E. Gileadi, *Induced Codeposition of Alloys of Tungsten, Molybdenum and Rhenium with Transition Metals*, in: C.G. Vayenas, R.E. White, M.E. Gamboa-Aldeco (Eds.) *Modern Aspects of Electrochemistry*, Springer New York, New York, NY, 2008, pp. 191-301.
- [67] G.L. Griffiths, D.M. Goldenberg, A.L. Jones, H.J. Hansen, *Bioconjugate Chem.*, 3 (1992) 91-99.
- [68] J. Vucina, R. Han, *Med Pregl*, 56 (2003) 362-365.
- [69] M. R.A. Pillai, A. Dash, F. F. Knapp, *Curr. Radiopharm.*, 5 (2012) 228-243.
- [70] in <https://www.mlz-garching.de/englisch/neutron-research/neutron-source.html>, accessed at 25.04.2020
- [71] B. Ponsard, J. Hiltunen, P. Penttilla, H. Vera Ruiz, A.L. Beets, S. Mirzadeh, F.F. Knapp, *J. Radioanal. Nucl. Chem.*, 257 (2003) 169-174.
- [72] H.J. Biersack, F. Stelzner, F.F. Knapp, *Nuklearmedizin*, 54 (2015) N50-N54.
- [73] R. Klett, U. Lange, H. Haas, M. Voth, J. Pinkert, *Rheumatology (Oxford)*, 46 (2007) 1531-1537.
- [74] J. R. Dilworth, S. J. Parrott, *Chem. Soc. Rev.*, 27 (1998) 43-55.
- [75] P.S. Donnelly, *Dalton Trans.*, 40 (2011) 999-1010.
- [76] A. Badar, J. Williams, R.T.M. de Rosales, R. Tavaré, F. Kampmeier, P.J. Blower, G.E.D. Mullen, *EJNMMI Research*, 4 (2014) 14.
- [77] E. Savio, J. Gaudiano, A.M. Robles, H. Balter, A. Paolino, A. López, J.C. Hermida, E. De Marco, G. Martinez, E. Osinaga, F.F. Knapp, *BMC Nuc. Med.*, 1 (2001) 2.
- [78] N. Iznaga-Escobar, *Appl. Radiat. Isot.*, 54 (2001) 399-406.
- [79] A. Leonidova, G. Gasser, *ACS Chem. Biol.*, 9 (2014) 2180-2193.

- [80] A.A. Haase, E.B. Bauer, F.E. Kühn, D.C. Crans, *Coord. Chem. Rev.*, 394 (2019) 135-161.
- [81] C.C. Konkankit, S.C. Marker, K.M. Knopf, J.J. Wilson, *Dalton Trans.*, 47 (2018) 9934-9974.
- [82] A. Kastl, S. Dieckmann, K. Wähler, T. Völker, L. Kastl, A.L. Merkel, A. Vultur, B. Shannan, K. Harms, M. Ocker, W.J. Parak, M. Herlyn, E. Meggers, *ChemMedChem*, 8 (2013) 924-927.
- [83] N. Wiberg, A.F. Holleman, N. Wiberg, E. Wiberg, G. Fischer, *Lehrbuch der Anorganischen Chemie*, De Gruyter, 2008.
- [84] D. Colaitis, D. Lebas, C. Lécaille, *Mater. Res. Bull.*, 8 (1973) 627-634.
- [85] W. Geilmann, F.W. Wrigge, *Z. Anorg. Allg. Chem.*, 214 (1933) 239-243.
- [86] A.G. Vodop'yanov, G.N. Kozhevnikov, *Russ. J. Appl. Chem.*, 85 (2012) 1567-1569.
- [87] B. Krebs, A. Müller, *Z. Naturforsch., B*, 23 (1968) 415.
- [88] V.S. Vinogradov, V.V. Ugarov, N.G. Rambidi, *J. Struct. Chem.*, 13 (1972) 661-662.
- [89] I.R. Beattie, T.R. Gilson, P.J. Jones, *Inorg. Chem.*, 35 (1996) 1301-1304.
- [90] I.R. Beattie, G.A. Ozin, *J. Chem. Soc. A*, (1969) 2615-2619.
- [91] W.A. Herrmann, W. Scherer, M. Kleine, M. Elison, P. Kiprof, K. Rypdal, H.V. Volden, S. Gundersen, A. Haaland, F.E. Kuehn, *Bull. Soc. Chim. Fr.*, 129 (1992) 655-662.
- [92] C.C. Romão, F.E. Kühn, W.A. Herrmann, *Chem. Rev.*, 97 (1997) 3197-3246.
- [93] K.V. Lawler, B.C. Childs, D.S. Mast, K.R. Czerwinski, A.P. Sattelberger, F. Poineau, P.M. Forster, *Inorg. Chem.*, 56 (2017) 2448-2458.
- [94] K. Persson, in, *The Materials Project*, 2017.
- [95] J. Noddack, W. Noddack, *Z. Anorg. Allg. Chem.*, 181 (1929) 1-37.
- [96] G. Rouschias, *Chem. Rev.*, 74 (1974) 531-566.
- [97] B. Krebs, A. Mueller, H.H. Beyer, *Inorg. Chem.*, 8 (1969) 436-443.
- [98] J.W. Johnson, J.F. Brody, G.B. Ansell, S. Zentz, *Acta Crystallogr. Sect. C*, 40 (1984) 2024-2026.
- [99] H. Beyer, O. Glemser, B. Krebs, *Angew. Chem.*, 80 (1968) 286-287.
- [100] W.A. Herrmann, P.W. Roesky, F.E. Kühn, W. Scherer, M. Kleine, *Angew. Chem. Int. Ed.*, 32 (1993) 1714-1716.
- [101] P.A. Shcheglov, D.V. Drobot, *Russ. J. Phys. Chem.*, 80 (2006) 1819-1825.
- [102] W. Biltz, *Z. Anorg. Allg. Chem.*, 214 (1933) 225-238.
- [103] H. Nechamkin, A.N. Kurtz, C.F. Hiskey, *J. Am. Chem. Soc.*, 73 (1951) 2828-2831.
- [104] B. Krebs, D. Fischer, G. Paul, *Z. Anorg. Allg. Chem.*, 622 (1996) 448-454.
- [105] R.K. Quinn, P.G. Neiswander, *Mater. Res. Bull.*, 5 (1970) 329-334.
- [106] K. Meisel, *Z. Anorg. Allg. Chem.*, 207 (1932) 121-128.
- [107] K. Persson, in, *The Materials Project*, 2016.
- [108] J.H.E. Griffiths, J. Owen, I.M. Ward, B. Bleaney, *Proc. R. Soc. London, Ser. B*, 219 (1953) 526-542.
- [109] A. Ferretti, D.B. Rogers, J.B. Goodenough, *J. Phys. Chem. Solids*, 26 (1965) 2007-2011.
- [110] J. Feinleib, W.J. Scouler, A. Ferretti, *Phys. Rev.*, 165 (1968) 765-774.
- [111] H.A. Evans, Y. Wu, R. Seshadri, A.K. Cheetham, *Nat. Rev. Mater.*, 5 (2020) 196-213.
- [112] D.J.M. Bevan, P. Hagenmuller, *Non-Stoichiometric Compounds: Tungsten Bronzes, Vanadium Bronzes and Related Compounds*, Elsevier Science, 2013.
- [113] M.T. Weller, P.G. Dickens, *Solid State Ionics*, 9-10 (1983) 1081-1085.
- [114] S. Horiuchi, N. Kimizuka, A. Yamamoto, *Nature*, 279 (1979) 226-227.
- [115] W.H. Davenport, V. Kollonitsch, C.H. Klein, *Ind. Eng. Chem.*, 60 (1968) 10-19.
- [116] M.A. Ryashentseva, K.M. Minachev, V.N. Khandozhko, P.E. Kolobova, *Bull. Acad. Sci. USSR, Chem. Sci.*, 39 (1990) 2596-2598.
- [117] I. Noddack, W. Noddack, *Z. Anorg. Allg. Chem.*, 215 (1933) 129-184.
- [118] H.V.A. Briscoe, P.L. Robinson, E.M. Stoddart, *J. Chem. Soc. (Resumed)*, (1931) 666-669.
- [119] H. Hölemann, *Z. Anorg. Allg. Chem.*, 202 (1931) 277-291.
- [120] J. Feller, H. Oppermann, M. Binnewies, E. Milke, *Z. Naturforsch., B*, 53 (1998) 184.
- [121] K. Persson, in, *The Materials Project*, 2016.
- [122] D.B. Rogers, R.D. Shannon, A.W. Sleight, J.L. Gillson, *Inorg. Chem.*, 8 (1969) 841-849.
- [123] A. Magnéli, *Acta Chem. Scand.*, 11 (1957) 28-33.

- [124] E. Kim, J. Boulègue, *Radiochim. Acta*, 91 (2003) 211.
- [125] Y. Xiong, S.A. Wood, *Chem. Geol.*, 158 (1999) 245-256.
- [126] R.A. Pacer, *J. Inorg. Nucl. Chem.*, 35 (1973) 1375-1377.
- [127] T. Gjervan, M. Rønning, R. Prestvik, B. Tøtdal, C.E. Lyman, A. Holmen, Bimetallic nano-particle formation in the Pt-Re reforming catalysts revealed by STEM/EDX, XANES/EXAFS and chemical characterization techniques. Effects of water and chlorine, in: A. Corma, F.V. Melo, S. Mendioroz, J.L.G. Fierro (Eds.) *Studies in Surface Science and Catalysis*, Elsevier, 2000, pp. 3189-3194.
- [128] Z. Liu, S. Kang, M. Shamsuzzoha, D.E. Nikles, *J. Nanosci. Nanotechnol.*, 10 (2010) 4266-4272.
- [129] H.I. Karan, K. Sasaki, K. Kuttiyiel, C.A. Farberow, M. Mavrikakis, R.R. Adzic, *ACS Catal.*, 2 (2012) 817-824.
- [130] K. Baranowska, J. Okal, W. Tylus, *Appl. Catal. Gen*, 511 (2016) 117-130.
- [131] D. Raciti, J. Kubal, C. Ma, M. Barclay, M. Gonzalez, M. Chi, J. Greeley, K.L. More, C. Wang, *Nano Energy*, 20 (2016) 202-211.
- [132] T. Ayvalı, P.-F. Fazzini, P. Lecante, A. Mayoral, K. Philippot, B. Chaudret, *Dalton Trans.*, 46 (2017) 15070-15079.
- [133] P. Veerakumar, A. Sangili, S.-M. Chen, A. Pandikumar, K.-C. Lin, *ACS Sustain. Chem. Eng.*, 8 (2020) 3591-3605.
- [134] H. Xia, L. Zhang, H. Hu, S. Zuo, L. Yang, *Nanomaterials* 10 (2020) 73.
- [135] S. Ghosh, K. Biswas, C.N.R. Rao, *J. Mater. Chem.*, 17 (2007) 2412-2417.
- [136] A. Liang, J. Li, C. Jiang, Z. Jiang, *Bioprocess Biosyst. Eng.*, 33 (2010) 1087-1094.
- [137] N.A. Taratanov, G.Y. Yurkov, Y.A. Koksharov, V.M. Bouznic, *Inorg. Mater. Appl. Res.*, 2 (2011) 118-124.
- [138] K.V. Kremlev, A.M. Obiedkov, S.Y. Ketkov, B.S. Kaverin, N.M. Semenov, G.A. Domrachev, S.A. Gusev, D.A. Tatarskiy, P.A. Yunin, *J. Surf. Invest-X-ray+*, 9 (2015) 694-698.
- [139] P. Veerakumar, P. Thanasekaran, K.-C. Lin, S.-B. Liu, *J. Colloid Interface Sci.*, 506 (2017) 271-282.
- [140] S.R. Bare, S.D. Kelly, F. D.Vila, E. Boldingh, E. Karapetrova, J. Kas, G.E. Mickelson, F.S. Modica, N. Yang, J.J. Rehr, *J. Phys. Chem. C*, 115 (2011) 5740-5755.
- [141] N. Yang, G.E. Mickelson, N. Greenlay, S.D. Kelly, F.D. Vila, J. Kas, J.J. Rehr, S.R. Bare, *AIP Conference Proceedings*, 882 (2007) 591-593.
- [142] K. Leiva, N. Martinez, C. Sepulveda, R. García, C.A. Jiménez, D. Laurenti, M. Vrinat, C. Geantet, J.L.G. Fierro, I.T. Ghampson, N. Escalona, *Appl. Catal. Gen*, 490 (2015) 71-79.
- [143] S. Kundu, L. Ma, W. Dai, Y. Chen, A.M. Sinyukov, H. Liang, *ACS Sustain. Chem. Eng.*, 5 (2017) 10186-10198.
- [144] S. Anantharaj, K. Sakthikumar, A. Elangovan, G. Ravi, T. Karthik, S. Kundu, *J. Colloid Interface Sci.*, 483 (2016) 360-373.
- [145] K. Sakthikumar, S. Anantharaj, S.R. Ede, K. Karthick, S. Kundu, *J. Mater. Chem. C*, 4 (2016) 6309-6320.
- [146] C.D. Valenzuela, M.L. Valenzuela, S. Caceres, C. O'Dwyer, *J. Mater. Chem. A*, 1 (2013) 1566-1572.
- [147] L. Yang, S. Lu, H. Wang, Q. Shao, F. Liao, M. Shao, *Electrochim. Acta*, 228 (2017) 268-273.
- [148] U.G. Hong, H.W. Park, J. Lee, S. Hwang, J. Yi, I.K. Song, *Appl. Catal. Gen*, 415-416 (2012) 141-148.
- [149] M.J. Rak, T. Friščić, A. Moores, *Faraday Discuss.*, 170 (2014) 155-167.
- [150] M. Stucchi, C.L. Bianchi, C. Pirola, S. Vitali, G. Cerrato, S. Morandi, C. Argirusis, G. Sourkouni, P.M. Sakkas, V. Capucci, *Appl. Catal.*, B, 178 (2015) 124-132.
- [151] K. Kon, W. Onodera, T. Toyao, K.-i. Shimizu, *Catal. Sci. Technol.*, 6 (2016) 5864-5870.
- [152] C. Opris, B. Cojocar, N. Gheorghe, M. Tudorache, S.M. Coman, V.I. Parvulescu, B. Duraki, F. Krumeich, J.A. van Bokhoven, *ACS Catal.*, 7 (2017) 3257-3267.
- [153] L. Sandbrink, E. Klindtworth, H.-U. Islam, A.M. Beale, R. Palkovits, *ACS Catal.*, 6 (2016) 677-680.
- [154] Y.Y. Chong, W.Y. Chow, W.Y. Fan, *J. Colloid Interface Sci.*, 369 (2012) 164-169.
- [155] J.W. Nichols, Y.H. Bae, *J. Controlled Release*, 190 (2014) 451-464.

- [156] W. Zhang, G. Deng, B. Li, X. Zhao, T. Ji, G. Song, Z. Xiao, Q. Cao, J. Xiao, X. Huang, G. Guan, R. Zou, X. Lu, J. Hu, *Biomaterials*, 159 (2018) 68-81.
- [157] G.H. Lee, S.H. Huh, S.H. Kim, B.J. Choi, B.S. Kim, J.H. Park, *J. Korean Phys. Soc.*, 42 (2003) 835-837.
- [158] C. Vollmer, E. Redel, K. Abu-Shandi, R. Thomann, H. Manyar, C. Hardacre, C. Janiak, *Chem. Eur. J.*, 16 (2010) 3849-3858.
- [159] T. Ayvalı, P. Lecante, P.-F. Fazzini, A. Gillet, K. Philippot, B. Chaudret, *Chem. Commun.*, 50 (2014) 10809-10811.
- [160] T. Ayvalı, P. Lecante, P.-F. Fazzini, A. Gillet, K. Philippot, B. Chaudret, *MRS Proceedings*, 1675 (2014) 157-162.
- [161] D. Myung, Y. Lee, J. Lee, H.K. Yu, J.-L. Lee, J.M. Baik, W. Kim, M.H. Kim, *physica status solidi (RRL) – Rapid Research Letters*, 4 (2010) 365-367.
- [162] K. Biswas, C.N.R. Rao, *J. Phys. Chem. B*, 110 (2006) 842-845.
- [163] Y.Y. Chong, W.Y. Fan, *J. Colloid Interface Sci.*, 397 (2013) 18-23.
- [164] W. Zhang, C. Yang, Z. Lei, G. Guan, S.-a. He, Z. Zhang, R. Zou, H. Shen, J. Hu, *ACS Appl. Mater. Interfaces*, 11 (2019) 25691-25701.
- [165] S. Ghosh, H.-C. Lu, S.H. Cho, T. Maruvada, M.C. Price, D.J. Milliron, *J. Am. Chem. Soc.*, 141 (2019) 16331-16343.
- [166] M.R. Mucalo, C.R. Bullen, *J. Colloid Interface Sci.*, 239 (2001) 71-77.
- [167] K.M. Babu, M.R. Mucalo, *J. Mater. Sci. Lett.*, 22 (2003) 1755-1757.
- [168] J. Bedia, L. Calvo, J. Lemus, A. Quintanilla, J.A. Casas, A.F. Mohedano, J.A. Zazo, J.J. Rodriguez, M.A. Gilarranz, *Colloids Surf., B*, 469 (2015) 202-210.
- [169] J. Yi, J.T. Miller, D.Y. Zemlyanov, R. Zhang, P.J. Dietrich, F.H. Ribeiro, S. Suslov, M.M. Abu-Omar, *Angew. Chem. Int. Ed.*, 53 (2014) 833-836.
- [170] J.H. Jang, H. Sohn, J. Camacho-Bunquin, D. Yang, C.Y. Park, M. Delferro, M.M. Abu-Omar, *ACS Sustain. Chem. Eng.*, 7 (2019) 11438-11447.
- [171] A.A. Revina, M.A. Kuznetsov, A.M. Chekmarev, *Doklady Chemistry*, 450 (2013) 119-121.
- [172] A.A. Revina, M.A. Kuznetsov, A.M. Chekmarev, E.E. Boyakov, V.I. Zolotarevskii, *Prot. Met. Phys. Chem*, 54 (2018) 43-50.
- [173] J.V. Rojas, C.H. Castano, *Radiat. Phys. Chem.*, 99 (2014) 1-5.
- [174] Y.-K. Jeong, Y.M. Lee, J. Yun, T. Mazur, M. Kim, Y.J. Kim, M. Dygas, S.H. Choi, K.S. Kim, O.-H. Kwon, S.M. Yoon, B.A. Grzybowski, *J. Am. Chem. Soc.*, 139 (2017) 15088-15093.
- [175] B.J. Hofmann, R.G. Harms, S.P. Schwaminger, R.M. Reich, F.E. Kühn, *J. Catal.*, 373 (2019) 190-200.
- [176] E.A. Shusharina, A.V. Zadesenets, S.A. Gromilov, *J. Struct. Chem.*, 52 (2011) 439-442.
- [177] F.E. Kühn, C.C. Romão, W.A. Herrmann, in: T. Imamoto (Ed.) *Category 1, Organometallics*, Georg Thieme Verlag, Stuttgart, 2003.
- [178] W. Hieber, H. Fuchs, *Z. Anorg. Allg. Chem.*, 248 (1941) 256-268.
- [179] L.S. Crocker, G.L. Gould, D.M. Heinekey, *J. Organomet. Chem.*, 342 (1988) 243-244.
- [180] W. Hieber, G. Braun, *Z. Naturforsch., B. Chem. Sci.*, 14 (1959) 132-133.
- [181] F. Salsi, M. Neville, M. Drance, A. Hagenbach, C. Chan, J.S. Figueroa, U. Abram, *Chem. Commun.*, 56 (2020) 7009-7012.
- [182] W. Hieber, R. Schuh, H. Fuchs, *Z. Anorg. Allg. Chem.*, 248 (1941) 243-255.
- [183] M. Waki, K.-i. Yamanaka, S. Shirai, Y. Maegawa, Y. Goto, Y. Yamada, S. Inagaki, *Chem. Eur. J.*, 24 (2018) 3846-3853.
- [184] C.P. Casey, M.A. Andrews, D.R. McAlister, J.E. Rinz, *J. Am. Chem. Soc.*, 102 (1980) 1927-1933.
- [185] M.U. Pilotti, F.G.A. Stone, I. Topaloğlu, *J. Chem. Soc., Dalton Trans.*, (1991) 1621-1626.
- [186] S. Sato, O. Ishitani, *Coord. Chem. Rev.*, 282-283 (2015) 50-59.
- [187] C. Hille, F.E. Kühn, *Dalton Trans.*, 45 (2016) 15-31.
- [188] R. Fraser, C.G.C.E. van Sittert, P.H. van Rooyen, M. Landman, *J. Organomet. Chem.*, 835 (2017) 60-69.
- [189] L.A. Paul, S. Rajabi, C. Jooss, F. Meyer, F. Ebrahimi, I. Siewert, *Dalton Trans.*, (2020).

- [190] K.-H. Chen, N. Wang, Z.-W. Yang, S.-M. Xia, L.-N. He, *ChemSusChem*, n/a (2020).
- [191] S.-Y. Li, S. Meng, X. Zou, M. El-Roz, I. Telegeev, O. Thili, T.X. Liu, G. Zhu, *Microporous Mesoporous Mater.*, 285 (2019) 195-201.
- [192] C.J. Stanton, C.W. Machan, J.E. Vandezande, T. Jin, G.F. Majetich, H.F. Schaefer, C.P. Kubiak, G. Li, J. Agarwal, *Inorg. Chem.*, 55 (2016) 3136-3144.
- [193] H.-P. Liang, A. Acharjya, D.A. Anito, S. Vogl, T.-X. Wang, A. Thomas, B.-H. Han, *ACS Catal.*, 9 (2019) 3959-3968.
- [194] Z. Fu, X. Wang, A.M. Gardner, X. Wang, S.Y. Chong, G. Neri, A.J. Cowan, L. Liu, X. Li, A. Vogel, R. Clowes, M. Bilton, L. Chen, R.S. Sprick, A.I. Cooper, *Chem. Sci.*, 11 (2020) 543-550.
- [195] Y. Kuramochi, Y. Fujisawa, A. Satake, *J. Am. Chem. Soc.*, 142 (2020) 705-709.
- [196] H. Kumagai, G. Sahara, K. Maeda, M. Higashi, R. Abe, O. Ishitani, *Chem. Sci.*, 8 (2017) 4242-4249.
- [197] D. Saito, Y. Yamazaki, Y. Tamaki, O. Ishitani, *J. Am. Chem. Soc.*, (2020).
- [198] J.D. Shipp, H. Carson, S.J.P. Spall, S.C. Parker, D. Chekulaev, N. Jones, M.Y. Mel'nikov, C.C. Robertson, A.J.H.M. Meijer, J.A. Weinstein, *Dalton Trans.*, 49 (2020) 4230-4243.
- [199] L. Suntrup, F. Stein, J. Klein, A. Wilting, F.G.L. Parlane, C.M. Brown, J. Fiedler, C.P. Berlinguette, I. Siewert, B. Sarkar, *Inorg. Chem.*, 59 (2020) 4215-4227.
- [200] C.-X. Tian, S.-C. Cui, X.-Y. Liu, J.-G. Liu, *Res. Chem. Intermed.*, 46 (2020) 1-13.
- [201] A. Zhanaidarova, S.C. Jones, E. Despagnet-Ayoub, B.R. Pimentel, C.P. Kubiak, *J. Am. Chem. Soc.*, 141 (2019) 17270-17277.
- [202] X. van Niekerk, T.I.A. Gerber, E.C. Hosten, *Polyhedron*, 175 (2020) 114195.
- [203] A. Frei, E. Fischer, B.C. Childs, J.P. Holland, R. Alberto, *Dalton Trans.*, 48 (2019) 14600-14605.
- [204] N. Wiratpruk, A. Noor, C.A. McLean, P.S. Donnelly, P.J. Barnard, *Dalton Trans.*, 49 (2020) 4559-4569.
- [205] A. Frei, M. Amado, M.A. Cooper, M.A.T. Blaskovich, *Chem. Eur. J.*, 26 (2020) 2852-2858.
- [206] S. Cauteruccio, M. Panigati, L. Veronese, N. Zaffaroni, M. Folini, E. Licandro, *J. Organomet. Chem.*, 887 (2019) 32-39.
- [207] L.C.-C. Lee, K.-K. Leung, K.K.-W. Lo, *Dalton Trans.*, 46 (2017) 16357-16380.
- [208] M.Y. Petyuk, A.S. Berezin, I.Y. Bagryanskaya, O.I. Artyushin, V.K. Brel, A.V. Artem'ev, *Inorg. Chem. Commun.*, 119 (2020) 108058.
- [209] A. Bonfiglio, K. Magra, C. Cebrián, F. Polo, P.C. Gros, P. Mercandelli, M. Mauro, *Dalton Trans.*, 49 (2020) 3102-3111.
- [210] J.M. Favale, E.O. Danilov, J.E. Yarnell, F.N. Castellano, *Inorg. Chem.*, 58 (2019) 8750-8762.
- [211] D. Sinha, S.P. Parua, K.K. Rajak, *NISCAIR Online Periodicals Repository*, 58A (2019) 621-628.
- [212] L. Veronese, E. Quartapelle Procopio, T. Moehl, M. Panigati, K. Nonomura, A. Hagfeldt, *Physical Chemistry Chemical Physics*, 21 (2019) 7534-7543.
- [213] M.A. Klenner, G. Pascali, B. Zhang, G. Ciancaleoni, M. Massi, B.H. Fraser, *Aust. J. Chem.*, 72 (2019) 288-294.
- [214] A.P. King, S.C. Marker, R.V. Swanda, J.J. Woods, S.-B. Qian, J.J. Wilson, *Chem. Eur. J.*, 25 (2019) 9206-9210.
- [215] J. Borràs, V. Mesa, J. Suades, R. Barnadas-Rodríguez, *Langmuir*, 36 (2020) 1993-2002.
- [216] J. Hu, Q.J. Bruch, A.J.M. Miller, *J. Am. Chem. Soc.*, (2020).
- [217] D. Hernández-Valdés, L. Wettstein, R. Fernández-Terán, B. Probst, T. Fox, B. Spingler, Q. Nadeem, R. Alberto, *Chem. Commun.*, (2020).
- [218] D. Hernández-Valdés, F. Avignon, P. Müller, G. Meola, B. Probst, T. Fox, B. Spingler, R. Alberto, *Dalton Trans.*, 49 (2020) 5250-5256.
- [219] M.L.H. Green, L. Pratt, G. Wilkinson, *J. Chem. Soc. (Resumed)*, (1958) 3916-3922.
- [220] M.L.H. Green, G. Wilkinson, *J. Chem. Soc. (Resumed)*, (1958) 4314-4317.
- [221] W.A. Herrmann, *J. Organomet. Chem.*, 500 (1995) 149-173.
- [222] T.W. Spradau, J.A. Katzenellenbogen, *Bioconjugate Chem.*, 9 (1998) 765-772.
- [223] W.A. Herrmann, R. Serrano, A. Schäfer, U. Küsthardt, M.L. Ziegler, E. Guggolz, *J. Organomet. Chem.*, 272 (1984) 55-71.

- [224] D. Bornemann, L. Schlemper, N. Trapp, A. Togni, *Eur. J. Inorg. Chem.*, 2020 (2020) 1004-1010.
- [225] H. Braband, T.I. Kückmann, U. Abram, *J. Organomet. Chem.*, 690 (2005) 5421-5429.
- [226] R. Zhong, A. Pöthig, S. Haslinger, B. Hofmann, G. Raudaschl-Sieber, E. Herdtweck, W.A. Herrmann, F.E. Kühn, *ChemPlusChem*, 79 (2014) 1294-1303.
- [227] S.K. Singh, G. Rajaraman, *Nat. Commun.*, 7 (2016) 10669.
- [228] C.H. Woodall, G.A. Craig, A. Prescimone, M. Misek, J. Cano, J. Faus, M.R. Probert, S. Parsons, S. Moggach, J. Martínez-Lillo, M. Murrie, K.V. Kamenev, E.K. Brechin, *Nat. Commun.*, 7 (2016) 13870.
- [229] C. Rojas-Dotti, A. Sanchis-Perucho, M. Orts-Arroyo, N. Moliner, R. González, F. Lloret, J. Martínez-Lillo, *Magnetochemistry*, 6 (2020) 20.
- [230] X. Feng, J.-L. Liu, K.S. Pedersen, J. Nehr Korn, A. Schnegg, K. Holldack, J. Bendix, M. Sigrist, H. Mutka, D. Samohvalov, D. Aguilà, M.-L. Tong, J.R. Long, R. Clérac, *Chem. Commun.*, 52 (2016) 12905-12908.
- [231] A.H. Pedersen, M. Julve, E.K. Brechin, J. Martínez-Lillo, *CrystEngComm*, 19 (2017) 503-510.
- [232] D. Armentano, M.A. Barquero, C. Rojas-Dotti, N. Moliner, G. De Munno, E.K. Brechin, J. Martínez-Lillo, *Cryst. Growth Des.*, 17 (2017) 5342-5348.
- [233] P. A. Reynolds, B. Moubaraki, K. S. Murray, J. W. Cable, L. M. Engelhardt, B. N. Figgis, *J. Chem. Soc., Dalton Trans.*, (1997) 263-268.
- [234] K.S. Pedersen, M. Sigrist, M.A. Sørensen, A.-L. Barra, T. Weyhermüller, S. Piligkos, C.A. Thuesen, M.G. Vinum, H. Mutka, H. Weihe, R. Clérac, J. Bendix, *Angew. Chem. Int. Ed.*, 53 (2014) 1351-1354.
- [235] J. Martínez-Lillo, T.F. Mastropietro, E. Lhotel, C. Paulsen, J. Cano, G. De Munno, J. Faus, F. Lloret, M. Julve, S. Nellutla, J. Krzystek, *J. Am. Chem. Soc.*, 135 (2013) 13737-13748.
- [236] D. Armentano, J. Martínez-Lillo, *RSC Adv.*, 5 (2015) 54936-54940.
- [237] C. Rojas-Dotti, A. Sanchis-Perucho, M. Orts-Arroyo, F. Lloret, J. Martínez-Lillo, *C. R. Chim.*, 22 (2019) 490-497.
- [238] K. Suntharalingam, S.G. Awuah, P.M. Bruno, T.C. Johnstone, F. Wang, W. Lin, Y.-R. Zheng, J.E. Page, M.T. Hemann, S.J. Lippard, *J. Am. Chem. Soc.*, 137 (2015) 2967-2974.
- [239] J. Mukiza, O. Blacque, G. Habarurema, E. Kampire, *New J. Chem.*, 44 (2020) 7080-7090.
- [240] R.F. Einrem, A.B. Alemayehu, S.M. Borisov, A. Ghosh, O.A. Gederaas, *ACS Omega*, 5 (2020) 10596-10601.
- [241] C. Scholtysik, C. Njiki Noufele, A. Hagenbach, U. Abram, *Inorg. Chem.*, 58 (2019) 5241-5252.
- [242] N. Chrysochos, M. Ahmadi, S. Wahlefeld, Y. Rippers, I. Zebger, M.A. Mroginski, C. Schulzke, *Dalton Trans.*, 48 (2019) 2701-2714.
- [243] T.D. Lohrey, E.A. Cortes, R.G. Bergman, J. Arnold, *Inorg. Chem.*, 59 (2020) 7216-7226.
- [244] T.D. Lohrey, E.A. Cortes, J.I. Fostvedt, A.K. Oanta, A. Jain, R.G. Bergman, J. Arnold, *Inorg. Chem.*, 59 (2020) 11096-11107.
- [245] S. Raju, J.T.B.H. Jastrzebski, M. Lutz, R.J.M. Klein Gebbink, *ChemSusChem*, 6 (2013) 1673-1680.
- [246] S. Raju, C.A.M.R. van Slagmaat, J. Li, M. Lutz, J.T.B.H. Jastrzebski, M.-E. Moret, R.J.M. Klein Gebbink, *Organometallics*, 35 (2016) 2178-2187.
- [247] R.G. Harms, I.I.E. Markovits, M. Drees, h.c.m.W.A. Herrmann, M. Cokoja, F.E. Kühn, *ChemSusChem*, 7 (2014) 429-434.
- [248] S. Raju, M.-E. Moret, R.J.M. Klein Gebbink, *ACS Catal.*, 5 (2015) 281-300.
- [249] J. Mukiza, T.I.A. Gerber, E. Hosten, A.S. Ogunlaja, F. Taherkhani, M. Amini, M. Nahali, *Inorg. Chem. Commun.*, 51 (2015) 83-86.
- [250] P.G. Edwards, G. Wilkinson, M.B. Hursthouse, K.M.A. Malik, *J. Chem. Soc., Dalton Trans.*, (1980) 2467-2475.
- [251] K. Mertis, D.H. Williamson, G. Wilkinson, *J. Chem. Soc., Dalton Trans.*, (1975) 607-611.
- [252] J.F. Gibson, K. Mertis, G. Wilkinson, *J. Chem. Soc., Dalton Trans.*, (1975) 1093-1096.
- [253] K. Mertis, J.F. Gibson, G. Wilkinson, *J. Chem. Soc., Chem. Commun.*, (1974) 93a-93a.
- [254] W.A. Herrmann, P. Watzlowik, P. Kiprof, *Chem. Ber.*, 124 (1991) 1101-1106.
- [255] K. Mertis, G. Wilkinson, *J. Chem. Soc., Dalton Trans.*, (1976) 1488-1492.
- [256] F.A. Cotton, L.D. Gage, K. Mertis, L.W. Shive, G. Wilkinson, *J. Am. Chem. Soc.*, 98 (1976) 6922-6926.

- [257] K. Mertis, L. Galyer, G. Wilkinson, *J. Organomet. Chem.*, 97 (1975) C65.
- [258] J. Abbenseth, M. Diefenbach, A. Hinz, L. Alig, C. Würtele, J.M. Goicoechea, M.C. Holthausen, S. Schneider, *Angew. Chem. Int. Ed.*, 58 (2019) 10966-10970.
- [259] T.D. Lohrey, G. Rao, R.D. Britt, R.G. Bergman, J. Arnold, *Inorg. Chem.*, 58 (2019) 13492-13501.
- [260] R.S. van Alten, F. Wätjen, S. Demeshko, A.J.M. Miller, C. Würtele, I. Siewert, S. Schneider, *Eur. J. Inorg. Chem.*, 2020 (2020) 1402-1410.
- [261] Q.J. Bruch, G.P. Connor, C.-H. Chen, P.L. Holland, J.M. Mayer, F. Hasanayn, A.J.M. Miller, *J. Am. Chem. Soc.*, 141 (2019) 20198-20208.
- [262] R. Bolliger, G. Meola, H. Braband, O. Blacque, L. Siebenmann, Q. Nadeem, R. Alberto, *Inorg. Chem.*, (2020).
- [263] M. Schmidt, H. Schmidbaur, *Chem. Ber.*, 92 (1959) 2667-2670.
- [264] S.C. Abrahams, A.P. Ginsberg, K. Knox, *Inorg. Chem.*, 3 (1964) 558-567.
- [265] R. Dagani, *Chem. Eng. News Archive*, 62 (1984) 26-28.
- [266] I.R. Beattie, P.J. Jones, *Inorg. Chem.*, 18 (1979) 2318-2319.
- [267] W.A. Herrmann, J.G. Kuchler, J.K. Felixberger, E. Herdtweck, W. Wagner, *Angew. Chem. Int. Ed.*, 27 (1988) 394-396.
- [268] X. Xiaoding, J.C. Mol, *J. Chem. Soc., Chem. Commun.*, (1985) 631-633.
- [269] J. Okuda, E. Herdtweck, W.A. Herrmann, *Inorg. Chem.*, 27 (1988) 1254-1257.
- [270] M. Flöel, E. Herdtweck, W. Wagner, J. Kulpe, P. Härter, W.A. Herrmann, *Angew. Chem.*, 99 (1987) 787-788.
- [271] K.P. Gable, T.N. Phan, *J. Organomet. Chem.*, 466 (1994) C5-C6.
- [272] W.A. Herrmann, P. Kiprof, K. Rypdal, J. Tremmel, R. Blom, R. Alberto, J. Behm, R.W. Albach, H. Bock, *J. Am. Chem. Soc.*, 113 (1991) 6527-6537.
- [273] W.A. Herrmann, F.E. Kühn, *Acc. Chem. Res.*, 30 (1997) 169-180.
- [274] P. Shcheglov, G.A. Seisenbaeva, D.V. Drobot, V.G. Kessler, *Inorg. Chem. Commun.*, 4 (2001) 227-229.
- [275] F. Dyckhoff, S. Li, R.M. Reich, B.J. Hofmann, E. Herdtweck, F.E. Kühn, *Dalton Trans.*, 47 (2018) 9755-9764.
- [276] B.J. Hofmann, S. Huber, R.M. Reich, M. Drees, F.E. Kühn, *J. Organomet. Chem.*, 885 (2019) 32-38.
- [277] H.B. Stoner, J.M. Barnes, J.I. Duff, *Br. J. Pharmacol. Chemo.*, 10 (1955) 16-25.
- [278] M. Hatano, S. Suzuki, K. Ishihara, *J. Am. Chem. Soc.*, 128 (2006) 9998-9999.
- [279] C. De Meric de Bellefon, W.A. Herrmann, P. Kiprof, C.R. Whitaker, *Organometallics*, 11 (1992) 1072-1081.
- [280] W.A. Herrmann, M. Taillefer, C. De Meric de Bellefon, J. Behm, *Inorg. Chem.*, 30 (1991) 3247-3248.
- [281] W.A. Herrmann, F.E. Kühn, C.C. Romão, M. Kleine, J. Mink, *Chem. Ber.*, 127 (1994) 47-54.
- [282] W.A. Herrmann, F.E. Kühn, R.W. Fischer, W.R. Thiel, C.C. Romao, *Inorg. Chem.*, 31 (1992) 4431-4432.
- [283] W.A. Herrmann, A.M.J. Rost, J.K.M. Mitterpleininger, N. Szesni, S. Sturm, R.W. Fischer, F.E. Kühn, *Angew. Chem. Int. Ed.*, 46 (2007) 7301-7303.
- [284] W.A. Herrmann, F.E. Kühn, C.C. Romão, H.T. Huy, M. Wang, R.W. Fischer, P. Kiprof, W. Scherer, *Chem. Ber.*, 126 (1993) 45-50.
- [285] W.A. Herrmann, C.C. Romao, R.W. Fischer, P. Kiprof, C. de Méric de Bellefon, *Angew. Chem. Int. Ed.*, 30 (1991) 185-187.
- [286] W.A. Herrmann, M. Ladwig, P. Kiprof, J. Riede, *J. Organomet. Chem.*, 371 (1989) C13-C17.
- [287] W.A. Herrmann, F.E. Kühn, C.C. Romão, H. Tran Huy, *J. Organomet. Chem.*, 481 (1994) 227-234.
- [288] W.A. Herrmann, F.E. Kühn, C.C. Romão, *J. Organomet. Chem.*, 495 (1995) 209-213.
- [289] W.A. Herrmann, F.E. Kühn, C.C. Romão, *J. Organomet. Chem.*, 489 (1995) C56-C59.
- [290] U. Abram, 5.3 - Rhenium, in: J.A. McCleverty, T.J. Meyer (Eds.) *Comprehensive Coordination Chemistry II*, Pergamon, Oxford, 2003, pp. 271-402.
- [291] S. Huber, A. Pöthig, W.A. Herrmann, F.E. Kühn, *J. Organomet. Chem.*, 760 (2014) 156-160.

- [292] P.J. Costa, M.J. Calhorda, J. Bossert, C. Daniel, C.C. Romão, *Organometallics*, 25 (2006) 5235-5241.
- [293] A.J. Downs, M.R. Geisberger, J.C. Green, T.M. Greene, A. Haaland, W.A. Herrmann, L.J. Morris, S. Parsons, W. Scherer, H.V. Volden, *J. Chem. Soc., Dalton Trans.*, (2002) 3342-3348.
- [294] C.J.L. Lock, G. Turner, *Acta Crystallographica Section B*, 31 (1975) 1764-1765.
- [295] W.A. Herrmann, W. Scherer, R.W. Fischer, J. Bluemel, M. Kleine, W. Mertin, R. Gruehn, J. Mink, H. Boysen, *J. Am. Chem. Soc.*, 117 (1995) 3231-3243.
- [296] F.E. Kühn, W.A. Herrmann, R. Hahn, M. Elison, J. Bluemel, E. Herdtweck, *Organometallics*, 13 (1994) 1601-1606.
- [297] G.M. Sheldrick, W.S. Sheldrick, *J. Chem. Soc. A*, (1969) 2160-2163.
- [298] F. Castiglione, A. Mele, G. Raos, Chapter Four - 170 NMR: A "Rare and Sensitive" Probe of Molecular Interactions and Dynamics, in: G.A. Webb (Ed.) *Annual Reports on NMR Spectroscopy*, Academic Press, 2015, pp. 143-193.
- [299] W.A. Herrmann, F.E. Kühn, P.W. Roesky, *J. Organomet. Chem.*, 485 (1995) 243-251.
- [300] G. Wu, *Prog. Nucl. Magn. Reson. Spectrosc.*, 52 (2008) 118-169.
- [301] W.A. Herrmann, F.E. Kuehn, M.U. Rauch, J.D.G. Correia, G. Artus, *Inorg. Chem.*, 34 (1995) 2914-2920.
- [302] S. Huber, M. Cokoja, M. Drees, J. Mink, F.E. Kühn, *Catal. Sci. Technol.*, 3 (2013) 388-393.
- [303] W.A. Herrmann, K. Öfele, M. Elison, F.E. Kühn, P.W. Roesky, *J. Organomet. Chem.*, 480 (1994) c7-c9.
- [304] H.B. Stuart, Introduction, in: *Infrared Spectroscopy: Fundamentals and Applications*, 2005, pp. 1-13.
- [305] W.A. Herrmann, W.R. Thiel, F.E. Kuehn, R.W. Fischer, M. Kleine, E. Herdtweck, W. Scherer, J. Mink, *Inorg. Chem.*, 32 (1993) 5188-5194.
- [306] W.A. Herrmann, *Angew. Chem. Int. Ed.*, 27 (1988) 1297-1313.
- [307] K.A. Joergensen, *Chem. Rev.*, 89 (1989) 431-458.
- [308] J. Sundermeyer, *Angew. Chem. Int. Ed.*, 32 (1993) 1144-1146.
- [309] W.A. Herrmann, W. Wagner, U.N. Flessner, U. Volkhardt, H. Komber, *Angew. Chem. Int. Ed.*, 30 (1991) 1636-1638.
- [310] W.A. Herrmann, R.W. Fischer, D.W. Marz, *Angew. Chem. Int. Ed.*, 30 (1991) 1638-1641.
- [311] W.A. Herrmann, M. Wang, *Angew. Chem. Int. Ed.*, 30 (1991) 1641-1643.
- [312] Z. Zhu, J.H. Espenson, *J. Org. Chem.*, 61 (1996) 324-328.
- [313] J.E. Ziegler, M.J. Zdilla, A.J. Evans, M.M. Abu-Omar, *Inorg. Chem.*, 48 (2009) 9998-10000.
- [314] J.R. Dethlefsen, P. Fristrup, *ChemSusChem*, 8 (2015) 767-775.
- [315] K.A. Vassell, J.H. Espenson, *Inorg. Chem.*, 33 (1994) 5491-5498.
- [316] W. Adam, C.M. Mitchell, C.R. Saha-Möller, *Tetrahedron*, 50 (1994) 13121-13124.
- [317] M.M. Abu-Omar, J.H. Espenson, *J. Am. Chem. Soc.*, 117 (1995) 272-280.
- [318] Z. Zhu, J.H. Espenson, *J. Org. Chem.*, 60 (1995) 1326-1332.
- [319] R.W. Murray, K. Iyanar, J. Chen, J.T. Wearing, *Tetrahedron Lett.*, 37 (1996) 805-808.
- [320] J.H. Espenson, O. Pestovsky, P. Huston, S. Staudt, *J. Am. Chem. Soc.*, 116 (1994) 2869-2877.
- [321] W.A. Herrmann, R.W. Fischer, J.D.G. Correia, *J. Mol. Catal.*, 94 (1994) 213-223.
- [322] Z. Zhu, J.H. Espenson, *J. Org. Chem.*, 60 (1995) 7728-7732.
- [323] R.W. Murray, K. Iyanar, J. Chen, J.T. Wearing, *Tetrahedron Lett.*, 36 (1995) 6415-6418.
- [324] W. Adam, J. Lin, C.R. Saha-Möller, W.A. Herrmann, R.W. Fischer, J.D.G. Correia, *Angew. Chem. Int. Ed.*, 33 (1995) 2475-2477.
- [325] K. Möller, G. Wienhöfer, F. Westerhaus, K. Junge, M. Beller, *Catal. Today*, 173 (2011) 68-75.
- [326] A. Bohle, A. Schubert, Y. Sun, W.R. Thiel, *Adv. Synth. Catal.*, 348 (2006) 1011-1015.
- [327] J.W. Kück, R.M. Reich, F.E. Kühn, *Chem. Rec.*, 16 (2016) 349-364.
- [328] S. Chikkali, S. Mecking, *Angew. Chem. Int. Ed.*, 51 (2012) 5802-5808.
- [329] P. Sözen-Aktaş, E. Manoury, F. Demirhan, R. Poli, *Eur. J. Inorg. Chem.*, 2013 (2013) 2728-2735.

- [330] N.N.E. Greenwood, A., 25 - Iron, Ruthenium and Osmium, in: N.N. Greenwood, A. Earnshaw (Eds.) *Chemistry of the Elements (Second Edition)*, Butterworth-Heinemann, Oxford, 1997, pp. 1070-1112.
- [331] L.R. Subbaraman, J. Subbaraman, E.J. Behrman, *Inorg. Chem.*, **11** (1972) 2621-2627.
- [332] W.A. Herrmann, R.W. Fischer, M.U. Rauch, W. Scherer, *J. Mol. Catal.*, **86** (1994) 243-266.
- [333] S. Yamazaki, J.H. Espenson, P. Huston, *Inorg. Chem.*, **32** (1993) 4683-4687.
- [334] O. Pestovsky, R. van Eldik, P. Huston, J.H. Espenson, *J. Chem. Soc., Dalton Trans.*, (1995) 133-137.
- [335] P. Huston, J.H. Espenson, A. Bakac, *Inorg. Chem.*, **32** (1993) 4517-4523.
- [336] B.R. Goldsmith, T. Hwang, S. Seritan, B. Peters, S.L. Scott, *J. Am. Chem. Soc.*, **137** (2015) 9604-9616.
- [337] W.A. Herrmann, J.D.G. Correia, G.R.J. Artus, R.W. Fischer, C.C. Romão, *J. Organomet. Chem.*, **520** (1996) 139-142.
- [338] C. Ehinger, C.P. Gordon, C. Copéret, *Chem. Sci.*, **10** (2019) 1786-1795.
- [339] A.M. Al-Ajlouni, J.H. Espenson, *J. Org. Chem.*, **61** (1996) 3969-3976.
- [340] J. Rudolph, K.L. Reddy, J.P. Chiang, K.B. Sharpless, *J. Am. Chem. Soc.*, **119** (1997) 6189-6190.
- [341] W.-D. Wang, J.H. Espenson, *Inorg. Chem.*, **36** (1997) 5069-5075.
- [342] M. C. A. van Vliet, I. W. C. E. Arends, R. A. Sheldon, *Chem. Commun.*, (1999) 821-822.
- [343] P. Altmann, M. Cokoja, F.E. Kühn, *Eur. J. Inorg. Chem.*, **2012** (2012) 3235-3239.
- [344] W. Adam, C.M. Mitchell, *Angew. Chem. Int. Ed.*, **35** (1996) 533-535.
- [345] M. Cokoja, R.M. Reich, M.E. Wilhelm, M. Kaposi, J. Schäffer, D.S. Morris, C.J. Münchmeyer, M.H. Anthofer, I.I.E. Markovits, F.E. Kühn, W.A. Herrmann, A. Jess, J.B. Love, *ChemSusChem*, **9** (2016) 1773-1776.
- [346] J. Schäffer, B. Zehner, W. Korth, M. Cokoja, A. Jess, *Chem. Eng. Technol.*, **42** (2019) 232-240.
- [347] J. Schäffer, M. Alber, W. Korth, M. Cokoja, A. Jess, *ChemistrySelect*, **2** (2017) 11891-11898.
- [348] R.M. Reich, M. Cokoja, I.I.E. Markovits, C.J. Münchmeyer, M. Kaposi, A. Pöthig, W.A. Herrmann, F.E. Kühn, *Dalton Trans.*, **44** (2015) 8669-8677.
- [349] R. Jira, *Oxidations*, in: *Applied Homogeneous Catalysis with Organometallic Compounds*, 2002, pp. 386-467.
- [350] M. Abrantes, A.M. Santos, J. Mink, F.E. Kühn, C.C. Romão, *Organometallics*, **22** (2003) 2112-2118.
- [351] S.A. Hauser, M. Cokoja, M. Drees, F.E. Kühn, *J. Mol. Catal. A: Chem.*, **363-364** (2012) 237-244.
- [352] A. Schmidt, N. Grover, T.K. Zimmermann, L. Graser, M. Cokoja, A. Pöthig, F.E. Kühn, *J. Catal.*, **319** (2014) 119-126.
- [353] N. Zwettler, J.A. Schachner, F. Belaj, N.C. Mösch-Zanetti, *Mol. Catal.*, **443** (2017) 209-219.
- [354] D. Betz, A. Raith, M. Cokoja, F.E. Kühn, *ChemSusChem*, **3** (2010) 559-562.
- [355] R. Mas-Ballesté, L. Que, *J. Am. Chem. Soc.*, **129** (2007) 15964-15972.
- [356] J.W. Kück, M.R. Anneser, B. Hofmann, A. Pöthig, M. Cokoja, F.E. Kühn, *ChemSusChem*, **8** (2015) 4056-4063.
- [357] F. Dyckhoff, J.F. Schlagintweit, R.M. Reich, F.E. Kühn, *Catal. Sci. Technol.*, **10** (2020) 3532-3536.
- [358] M.A. Bernd, F. Dyckhoff, B.J. Hofmann, A.D. Böth, J.F. Schlagintweit, J. Oberkofler, R.M. Reich, F.E. Kühn, *J. Catal.*, **391** (2020) 548-561.
- [359] I. Bauer, H.-J. Knölker, *Chem. Rev.*, **115** (2015) 3170-3387.
- [360] L. Que, W.B. Tolman, *Nature*, **455** (2008) 333-340.
- [361] K.P. Bryliakov, E.P. Talsi, *Coord. Chem. Rev.*, **276** (2014) 73-96.
- [362] I. Prat, J.S. Mathieson, M. Güell, X. Ribas, J.M. Luis, L. Cronin, M. Costas, *Nat. Chem.*, **3** (2011) 788-793.
- [363] W.N. Oloo, A.J. Fielding, L. Que, *J. Am. Chem. Soc.*, **135** (2013) 6438-6441.
- [364] I.Y. Skobelev, E.V. Kudrik, O.V. Zalomaeva, F. Albrieux, P. Afanasiev, O.A. Kholdeeva, A.B. Sorokin, *Chem. Commun.*, **49** (2013) 5577-5579.
- [365] M.R. Bukowski, P. Comba, A. Lienke, C. Limberg, C. Lopez de Laorden, R. Mas-Ballesté, M. Merz, L. Que Jr, *Angew. Chem. Int. Ed.*, **45** (2006) 3446-3449.

- [366] J.W. Kück, A. Raba, I.I.E. Markovits, M. Cokoja, F.E. Kühn, *ChemCatChem*, 6 (2014) 1882-1886.
- [367] D.T. Weiss, M.R. Anneser, S. Haslinger, A. Pöthig, M. Cokoja, J.-M. Basset, F.E. Kühn, *Organometallics*, 34 (2015) 5155-5166.
- [368] D.T. Weiss, P.J. Altmann, S. Haslinger, C. Jandl, A. Pöthig, M. Cokoja, F.E. Kühn, *Dalton Trans.*, 44 (2015) 18329-18339.
- [369] S. Meyer, I. Klawitter, S. Demeshko, E. Bill, F. Meyer, *Angew. Chem. Int. Ed.*, 52 (2013) 901-905.
- [370] J.M. Fraile, J.I. García, Z. Hormigón, J.A. Mayoral, C.J. Saavedra, L. Salvatella, *ACS Sustain. Chem. Eng.*, 6 (2018) 1837-1847.
- [371] W.R. Moser, R.W. Thompson, C.-C. Chiang, H. Tong, *J. Catal.*, 117 (1989) 19-32.
- [372] G. Larsen, E. Lotero, L.a.M. Petkovic, D.S. Shobe, *J. Catal.*, 169 (1997) 67-75.
- [373] H. Pines, J. Manassen, *The Mechanism of Dehydration of Alcohols over Alumina Catalysts*, in: D.D. Eley, H. Pines, P.B. Weisz (Eds.) *Advances in Catalysis*, Academic Press, 1966, pp. 49-93.
- [374] H. Wang, H. Wang, E. Kuhn, M.P. Tucker, B. Yang, *ChemSusChem*, 11 (2018) 285-291.
- [375] J. Zakzeski, P.C.A. Bruijninx, A.L. Jongerius, B.M. Weckhuysen, *Chem. Rev.*, 110 (2010) 3552-3599.
- [376] J. Keskiaväli, A. Parviainen, K. Lagerblom, T. Repo, *RSC Adv.*, 8 (2018) 15111-15118.
- [377] T. Yokoyama, *J. Wood Chem. Technol.*, 35 (2015) 27-42.
- [378] T. Imai, T. Yokoyama, Y. Matsumoto, *J. Wood Sci.*, 57 (2011) 219-225.
- [379] M.R. Sturgeon, S. Kim, K. Lawrence, R.S. Paton, S.C. Chmely, M. Nimlos, T.D. Foust, G.T. Beckham, *ACS Sustain. Chem. Eng.*, 2 (2014) 472-485.
- [380] P.J. Deuss, M. Scott, F. Tran, N.J. Westwood, J.G. de Vries, K. Barta, *J. Am. Chem. Soc.*, 137 (2015) 7456-7467.
- [381] Q. Cao, T. Ye, W. Li, J. Chen, Y. Lu, H. Gan, H. Wu, F. Cao, P. Wei, P. Ouyang, *Cellulose*, (2020).
- [382] N.N. Tshibalonza, J.-C.M. Monbaliu, *Green Chem.*, 22 (2020) 4801-4848.
- [383] C. Li, X. Zhao, A. Wang, G.W. Huber, T. Zhang, *Chem. Rev.*, 115 (2015) 11559-11624.
- [384] S. Akhtari, T. Sowlati, K. Day, *Renew. Sust. Energ. Rev.*, 33 (2014) 117-127.
- [385] A.J. Ragauskas, C.K. Williams, B.H. Davison, G. Britovsek, J. Cairney, C.A. Eckert, W.J. Frederick, J.P. Hallett, D.J. Leak, C.L. Liotta, J.R. Mielenz, R. Murphy, R. Templer, T. Tschaplinski, *Science*, 311 (2006) 484-489.
- [386] A.J. Ragauskas, G.T. Beckham, M.J. Bidy, R. Chandra, F. Chen, M.F. Davis, B.H. Davison, R.A. Dixon, P. Gilna, M. Keller, P. Langan, A.K. Naskar, J.N. Saddler, T.J. Tschaplinski, G.A. Tuskan, C.E. Wyman, *Science*, 344 (2014) 1246843.
- [387] J. Janlamool, B. Jongsomjit, *J. Oleo Sci.*, 66 (2017) 1029-1039.
- [388] J. Bi, X. Guo, M. Liu, X. Wang, *Catal. Today*, 149 (2010) 143-147.
- [389] J. Farrukh, A. Muhammad, H.A.-M. Ala'a, B. Awais, R. Sikander, K. Zakir, I. Abrar, A. Ashfaq, H. Shakhawat, K. Muhammad Shahzad, S.A.B. Muhammad, *Rev. Chem. Eng.*, 0 (2020).
- [390] Y. Zhang, P. Bi, J. Wang, P. Jiang, X. Wu, H. Xue, J. Liu, X. Zhou, Q. Li, *Appl. Energy*, 150 (2015) 128-137.
- [391] Y. Wang, W. Deng, L. Yan, B. Wang, Q. Zhang, H. Song, S. Wang, Q. Zhang, *Angew. Chem. Int. Ed.*, n/a (2020).
- [392] B. Wozniak, Y. Li, S. Tin, J.G. de Vries, *Green Chem.*, 20 (2018) 4433-4437.
- [393] Y. Kim, A. Mittal, D.J. Robichaud, H.M. Pilath, B.D. Etz, P.C. St. John, D.K. Johnson, S. Kim, *ACS Catal.*, (2020) 14707-14721.
- [394] J.H. Jang, I. Ro, P. Christopher, M.M. Abu-Omar, *ACS Catal.*, (2020) 95-109.
- [395] A. Corma, S. Iborra, A. Velty, *Chem. Rev.*, 107 (2007) 2411-2502.
- [396] Z. Sun, B. Fridrich, A. de Santi, S. Elangovan, K. Barta, *Chem. Rev.*, 118 (2018) 614-678.
- [397] T.J. Korstanje, J.T.B.H. Jastrzebski, R.J.M. Klein Gebbink, *ChemSusChem*, 3 (2010) 695-697.
- [398] T.J. Korstanje, E.F. de Waard, J.T.B.H. Jastrzebski, R.J.M. Klein Gebbink, *ACS Catal.*, 2 (2012) 2173-2181.
- [399] T.J. Korstanje, J.T.B.H. Jastrzebski, R.J.M. Klein Gebbink, *Chem. Eur. J.*, 19 (2013) 13224-13234.
- [400] R.L. Banks, G.C. Bailey, *I&EC Product Research and Development*, 3 (1964) 170-173.
- [401] D. Astruc, *New J. Chem.*, 29 (2005) 42-56.

- [402] P. Jean-Louis Hérisson, Y. Chauvin, *Macromol. Chem.*, 141 (1971) 161-176.
- [403] A. Mortreux, F. Petit, *Olefin Metathesis and Related Reactions*, in: A. Mortreux, F. Petit (Eds.) *Industrial Applications of Homogeneous Catalysis*, Springer Netherlands, Dordrecht, 1988, pp. 229-256.
- [404] W. Keim, *Angew. Chem. Int. Ed.*, 52 (2013) 12492-12496.
- [405] K.V. Williams, L. Turner, (1967), US 3485889 A. US
- [406] M. Valla, M.P. Conley, C. Copéret, *Catal. Sci. Technol.*, 5 (2015) 1438-1442.
- [407] L.J. Morris, A.J. Downs, T.M. Greene, G.S. McGrady, W.A. Herrmann, P. Sirsch, O. Gropen, W. Scherer, *Chem. Commun.*, (2000) 67-68.
- [408] L.J. Morris, A.J. Downs, T.M. Greene, G.S. McGrady, W.A. Herrmann, P. Sirsch, W. Scherer, O. Gropen, *Organometallics*, 20 (2001) 2344-2352.
- [409] S. Cai, D.M. Hoffman, D.A. Wierda, *J. Chem. Soc., Chem. Commun.*, (1988) 1489-1490.
- [410] R. Toreki, R.R. Schrock, *J. Am. Chem. Soc.*, 112 (1990) 2448-2449.
- [411] Y.-Y. Lai, M. Bornand, P. Chen, *Organometallics*, 31 (2012) 7558-7565.
- [412] M.A. Pietsch, T.V. Russo, R.B. Murphy, R.L. Martin, A.K. Rappé, *Organometallics*, 17 (1998) 2716-2719.
- [413] X. Chen, X. Zhang, P. Chen, *Angew. Chem. Int. Ed.*, 42 (2003) 3798-3801.
- [414] X. Zhang, X. Chen, P. Chen, *Organometallics*, 23 (2004) 3437-3447.
- [415] S. Narancic, P. Chen, *Organometallics*, 24 (2005) 10-12.
- [416] X. Zhang, S. Narancic, P. Chen, *Organometallics*, 24 (2005) 3040-3042.
- [417] A.H. Hoveyda, Z. Liu, C. Qin, T. Koenigter, Y. Mu, *Angew. Chem. Int. Ed.*, 59 (2020) 22324-22348.
- [418] J. Heppekausen, A. Fürstner, *Angew. Chem. Int. Ed.*, 50 (2011) 7829-7832.
- [419] M.J. Benedikter, J.V. Musso, W. Frey, R. Schowner, M.R. Buchmeiser, *Angew. Chem. Int. Ed.*, n/a (2020).
- [420] M. Benedikter, J. Musso, M.K. Kesharwani, K.L. Sterz, I. Elser, F. Ziegler, F. Fischer, B. Plietker, W. Frey, J. Kästner, M. Winkler, J. van Slageren, M. Nowakowski, M. Bauer, M.R. Buchmeiser, *ACS Catal.*, (2020) 14810-14823.
- [421] P.C.A. Bruijninx, B.M. Weckhuysen, *Nat. Chem.*, 6 (2014) 1035-1036.
- [422] S.V. Patil, D.S. Argyropoulos, *ChemSusChem*, 10 (2017) 3284-3303.
- [423] A. Rahimi, A. Ulbrich, J.J. Coon, S.S. Stahl, *Nature*, 515 (2014) 249-252.
- [424] S.C.A. Sousa, J.R. Bernardo, P.R. Florindo, A.C. Fernandes, *Catal. Commun.*, 40 (2013) 134-138.
- [425] T. Nakagiri, M. Murai, K. Takai, *Org. Lett.*, 17 (2015) 3346-3349.
- [426] A. Jefferson, R.S. Srivastava, *Polyhedron*, 160 (2019) 268-271.
- [427] Q. Qin, Y. Xie, P.E. Floreancig, *Chem. Sci.*, 9 (2018) 8528-8534.
- [428] R. Nallagonda, M. Rehan, P. Ghorai, *J. Org. Chem.*, 79 (2014) 2934-2943.
- [429] B.G. Das, R. Nallagonda, P. Ghorai, *J. Org. Chem.*, 77 (2012) 5577-5583.
- [430] W. Sittiwong, M.W. Richardson, C.E. Schiaffo, T.J. Fisher, P.H. Dussault, *Beilstein J. Org. Chem.*, 9 (2013) 1526-1532.
- [431] C. Afeke, Y. Xie, P.E. Floreancig, *Org. Lett.*, 21 (2019) 5064-5067.
- [432] M. Murai, T. Ogita, K. Takai, *Chem. Commun.*, 55 (2019) 2332-2335.
- [433] X. Wan, J. Hu, D. Xu, Y. Shang, Y. Zhen, C. Hu, F. Xiao, Y.-P. He, Y. Lai, W. Xie, *Tetrahedron Lett.*, 58 (2017) 1090-1093.
- [434] F. Yan, Y. Sang, Y. Bai, K. Wu, K. Cui, Z. Wen, F. Mai, Z. Ma, L. Yu, H. Chen, Y. Li, *Catal. Today*, 355 (2020) 231-237.
- [435] A. Jain, S.P. Ong, G. Hautier, W. Chen, W.D. Richards, S. Dacek, S. Cholia, D. Gunter, D. Skinner, G. Ceder, K.A. Persson, *APL Materials*, 1 (2013) 011002.

APPENDIX I

STRUCTURE OF GASEOUS Re_2O_7 DERIVED FROM DFT CALCULATIONS

Appendix I: Structure of gaseous Re₂O₇ derived from DFT Calculations

The structure of gaseous Re₂O₇ has recently been a point of debate. Experimental studies obtained by GED determine a Re-O-Re angle of 143.6(9)° at 230 °C.[1] In contrast, a recent DFT study suggests an almost linear Re-O-Re angle with 179.3°.[2] The authors argue that the calculated value and the experimental one are in agreement as the measured molecules are in an excited state due to the applied high temperature. In order to examine which of the given data is more precise, a series of different DFT functionals, basis sets and treatments for the relativistic effects are tested and the results summarized in Table A1.

Table A1-1: Calculated Re-O-Re angles using various different functionals, basis sets and relativistic treatments. If only one basis set is given, the same is applied for both atom types.

No.	Functional	Basis sets (O/Re) ¹	Relativistic treatment	Re-O-Re angle [°]
T1-1	B97D3	def2-TZVP/SDD	SDD-ECP	151.0
T1-2	B97D3	def2-TZVP	def2-ECP	174.5
T1-3	B97D3	def2-TZVP/SARC-ZORA-TZVP	ZORA	157.7
T1-4	PBE-D3	def2-TZVP/SDD	SDD-ECP	159.4
T1-5	PBE-D3	def2-TZVP	def2-ECP	180.0
T1-6	PBE	def2-TZVP/SARC-ZORA-TZVP	ZORA	179.9
T1-7	B3LYP	def2-TZVP/SDD	SDD-ECP	178.3
T1-8	B3LYP	def2-TZVP	def2-ECP	180.0
T1-9	B3LYP D3BJ	def2-TZVP/SARC-ZORA-TZVP	ZORA	178.4
T1-10	M06	def2-TZVP/SDD	SDD-ECP	170.9
T1-11	M06	def2-TZVP	def2-ECP	180.0
T1-12	M06	def2-TZVP/SARC-ZORA-TZVP	ZORA	180.0
T1-13	ωb97X-D	def2-TZVP/SDD	SDD-ECP	165.5
T1-14	ωb97X-D	def2-TZVP	def2-ECP	optimization fails
T1-15	ωb97X-D	def2-TZVP/SARC-ZORA-TZVP	ZORA	179.8
T1-16	B2PLYP-D3	def2-TZVP/SDD	SDD-ECP	158.3
T1-17	B2PLYP-D3	def2-TZVP	def2-ECP	179.1
T1-18	B2PLYP-D3	def2-TZVP/SARC-ZORA-TZVP	ZORA	173.8

The applied methods are generalized gradient approximation-type (GGA) density functionals like B97D3[3, 4] and PBE[5, 6], the popular hybrid GGA B3LYP[7], the highly parametrized hybrid meta-GGA M06[8], the range separated hybrid GGA ωb97X-D[9] and the double hybrid B2-PLYP-D3.[4, 10] The latter method mixes the GGA for exchange by Becke and correlation by Lee, Yang and Parr (LYP) and a perturbative second-order correlation part (Møller Plesset perturbation theory, MP2) based on the DFT derived orbitals.[11] Double hybrid DFT calculations are generally seen as superior when

compared to classical DFT calculations.[12-14] Although, in some rare cases (especially for transition metals) this class of functionals yields comparable or inferior results.[15, 16]

Three different sets of basis sets are used dependent on the respective treatment of the relativistic effect. The oxygen atoms are treated in Set 1 and 2 by the def2-TZVP basis set by Weigend.[17, 18] In set 1, a Stuttgart-Dresden effective core potential (ECP) and its corresponding basis set is applied to rhenium[19]. In set 2, def2 ECP, rhenium is treated with the more flexible triple zeta basis set (def2-TZVP) and the respective adapted Stuttgart-Dresden ECP (SDD).[17, 19, 20] The latter is obtained from Basis Set Exchange.[21] Finally, all-electron relativistic calculations are conducted using the zeroth order regular approximation (ZORA). For the treatment of both types of atoms, the corresponding recontracted ZORA-def2-TZVP basis sets are used.[22] Calculations with the basis set combinations 1 and 2 are conducted using Gaussian 16.B.01.[23] For calculations applying ZORA for the treatment of the relativistic effects, ORCA 4.2.1 is used instead.[24] The program uses the XCFun DFT library developed by Ekstrum and coworkers.[25]

After optimizing the structure of Re_2O_7 , several different conformers are obtained as “ground states”. Pure functionals (GGAs) are more prone to predict a bent structure in comparison to hybrid (m)GGAs. The exceptions are the range-separated $\omega\text{B97X-D}$ and double hybrid B2-PLYP functionals which result in an angle of 165.5° and 158.3° , respectively, when combined with the SDD ECP. A more pronounced trend is observed by comparison of the treatment of the relativistic effect. For the SDD ECP, most structures are bent with varying angle between $151.0^\circ - 165.5^\circ$ (**T1.1** and **T1.13**). Only when combined with B3LYP and M06, a linear structure is suggested. For the bigger def2 ECP, most structures are linear. Only the GGA B97D3 results in a slightly bent structure with 174.5° (**T1.2**). The results for all-electron calculations using ZORA are in between. Most structures are linear, except for the GGA B97D3 (**T1.3**) and P2-PLYP (**T1.18**). Therefore, following trends are derived for the tendency to obtain a bent structure ($\omega\text{B97X-D}$ is omitted as the optimization using the def2 ECP failed):

B97D3 > B2PLYP-D3 > PBE > M06 \approx B3LYP

SDD ECP > ZORA > def2 ECP

Concerning the different functionals, highest precision is expected for the double hybrid, the (range separated) hybrid (m)GGAs and finally the pure GGAs.[26] However, in this trend the methods with medium precision disagree to both the highly precise B2PLYP and the GGA B97D3. Neese and coworkers compared the performance of various different functionals in the optimization of 5d-transition metal complexes. Overall best results are obtained using pure GGAs: e.g. PBE is superior to B3LYP.[27] The observed low performance of the latter functional in the optimization of structures of organometallic Re(VII) compounds is in line with these findings.[28] Unfortunately, both benchmark sets are very small and most of the here presented modern functionals have not been tested. A recent and more extensive publication points out that hybrid functionals like B3LYP are indeed capable of giving very good results in the determination of bond dissociation energies (BDE) of transition metal oxides.[26] The structures were optimized using the GGA BP86 and single point calculations were performed in order to determine the energies. Combining the outcome of all three benchmark publications, hybrid functionals are highly likely inferior to pure GGAs in the optimization of structures even though they perform overall very well in the calculation of energies.

Concerning the treatment of the relativistic effects, Neese and coworkers’ publication is more descriptive as all three here presented methods were thoroughly tested.[27] Best results are obtained using ZORA, followed by def2 ECP combinations and SDD performs worst. However, the good performance of the def2 ECP is limited to the very high basis set def2-QZVP and the hybrid GGA PBE0.

As the best performing method (ZORA) also gives inconclusive results concerning the structure of Re_2O_7 it is still unclear whether the bent or linear structure is more reasonable. A more detailed comparison with literature data fails as most of the calculations were performed on a B3LYP/Lan2dz level of theory.[29] This might be surprising as it has been shown that this combination yields very poor results for 5d-transition metals.[27, 28] However, its broad application can be rationalized by the authors desire to compare their results to older literature.

Table A1-2: Comparison of the electronic energy and Gibbs free energy of fully optimized structures of Re_2O_7 and structures with the Re-O-Re angle constrained to the experimentally derived value of 143.6° . Energies are given in atomic units. The delta $E(\text{full})-E(\text{constrained})$ is given in kcal/mol.

No.	Method/Opt	Re-O-Re angle [°]	Imaginary frequencies	Electronic energy	Gibbs free energy
T2-1	T1-4/full	159.4	0	-683.2611	-683.2847
	T1-4/constrained	143.6	0	-683.2607	-683.2808
	delta [kcal/mol]			-0.24	-2.49
T2-2	T1-5/full	180.0	1 (-4.0 cm^{-1})	-683.3336	-683.3518
	T1-5/constrained	143.6	0	-683.3326	-683.3522
	delta [kcal/mol]			-0.64	0.28
T2-3	T1-6/full	179.9	1 (-12.0 cm^{-1})	-35282.7838	-35282.7988
	T1-6/constrained	143.6	0	-35282.7830	-35282.7995
	delta [kcal/mol]			-0.52	0.47
T2-4	T1-7/full	178.3	0	-683.6429	-683.6667
	T1-7/constrained	143.6	0	-683.6419	-683.6604
	delta [kcal/mol]			-0.65	-3.96
T2-5	T1-8/full	180.0	0	-683.7222	-683.7441
	T1-8/constrained	143.6	0	-683.7204	-683.7384
	delta [kcal/mol]			-1.14	-3.57
T2-6	T1-9/full	178.4	0	-35283.3462	-35283.3617
	T1-9/constrained	143.6	0	-35283.3455	-35283.3608
	delta [kcal/mol]			-0.42	-0.59
T2-7	T1-10/full	170.9	1 (-6.9 cm^{-1})	-683.2838	-683.3013
	T1-10/constrained	143.6	0	-683.2835	-683.3021
	delta [kcal/mol]			-0.22	0.55
T2-8	T1-11/full	180.0	1 (-9.0 cm^{-1})	-683.3675	-683.3829
	T1-11/constrained	143.6	0	-683.3661	-683.3836
	delta [kcal/mol]			-0.87	0.41
T2-9	T1-12/full	180.0	1 (-2.09 cm^{-1})	-35283.8971	-35283.9104
	T1-12/constrained	143.6	0	-35283.8960	-35283.9116
	delta [kcal/mol]			-0.69	0.79

As presented in Table 1, several optimizations yield Re-O-Re angles close to 180° . However, the calculations are not straightforward. For most converged structures with an almost linear Re-O-Re bond negative frequencies are obtained. Negative eigenvalues point to a non-converged structure or a transition state but may also occur due to numerical errors in the integration step. In contrast, when using a constrained Re-O-Re angle of 143.6° (experimentally derived value), the partial optimizations converge quickly without occurrence of any negative eigenvalues. The obtained electronic energies are slightly higher for the constraint geometry by 0.22 – 1.14 kcal/mol, depending on the level of theory (Table 2). By comparison of the Gibbs free energies, one might assume that in some cases the constrained structure is more stable than the fully optimized one at room temperature. However,

these values have to be handled with care. On the one hand, one low lying vibrational degree of freedom is neglected as the fully optimized structures contain negative eigenvalues. It constitutes usually for about 0.6 kcal/mol. On the other hand, the thermodynamic data is based on the calculation of the vibrational frequencies. Reasonable results are only obtained if the 1st derivative of the hessian matrix is close to zero (force on atoms). However, as the structures are overall very similar and only a marginal force is detected, this error is regarded as negligible. Therefore, the question whether the bent or the linear structure is more reasonable cannot be answered by the calculations presented in Table 2. It is evident that the electronic energy of the linear structure is lower, however, as the naturally occurring ground state structure depends on the Gibbs free enthalpy, more detailed calculations are needed.

Table A1-3: Comparison of the electronic energy, Gibbs free energy and rotational entropy at 298.15 K for the fully optimized structure of Re₂O₇ and its partially optimized structure with a constraint Re-O-Re angle of 143.6°. Calculations are performed using the benchmark functional PBE0 in combination with the most promising treatments of relativistic effects. Energies are given atomic units and the rotational entropy in kcal/mol.

No.	Method	Optimization	Symmetry	Electronic energy	Rotational entropy at 298.15 K	Gibbs free energy
T3-1	PBE0-D3/def2	full	D _{3h}	-683.2611	8.53	-683.2847
		constraint	C ₁	-683.2607	9.54	-683.2808
	delta [kcal/mol]			0.88	-1.01	1.72
T3-2	PBE0-D3/ZORA	full	D _{3h}	-35282.6042	8.51	-35282.6182
		constraint	C ₁	-35282.6034	9.52	-35282.6190
	delta [kcal/mol]			0.53	-1.01	-0.47

In order to discriminate between both structures, new calculations are performed using the functional PBE0 in combination with the def2 ECP or ZORA. Benchmarks clearly indicated best results for these levels of theory for both structural optimizations and energy calculations.[26, 27] Highest accuracy is achieved using significantly increased integration grids (for more details see next chapter) and (very)tight optimization criteria. All structures are true ground states as no negative eigenvalues are obtained. The benchmark calculations agree with the results of the previous screening of functionals that a linear structure of Re₂O₇ is more stable from the electronic perspective. However, for the Gibbs free energy one significant difference is observed between the bent and the linear structure. The strongest contribution to this difference is assigned to the rotational entropy S_{rot} . It is calculated according to Equation 1 with the universal gas constant R , the partial function of the entropy q_{rot} and the symmetry number sn :

$$S_{rot} = R * (\ln\left(\frac{q_{rot}}{sn}\right) + 1.5) \quad (A1-1)$$

For all four calculations, very similar values for the partial functions of the entropy are obtained, however, the symmetry number is increased from 1 for C₁ (bent) to 6 for D_{3h} (linear). Consequently, the rotational entropy is increased for the bent molecule. As the other contributions to the entropy are very similar, the difference in the Gibbs free energy is dominated by this term. As soon as the temperature is sufficient, the bent structure becomes more reasonable than the linear one. For the less precise calculation using the def2 ECP, a temperature of at least 770 K is necessary so that the bent structure is energetically more feasible, in contrast to the experimentally determined values. However, when using the more precise PBE0/ZORA method, the bent structure is prevalent already at

room temperature. Therefore, these results are in line with the experimentally derived structure, the vibrational spectra[30] but also the theoretical calculations by Forster and coworkers.[2] In line with their explanation, the linear structure is indeed more stable in terms of electronic energy. However, due to significant contributions of the entropy term, a bent structure is observed in the electron diffraction experiments.[1]

Calculation Details

Gaussian:

Optimizations are conducted with various functionals and the described ECPs with either no constraints or a constrained Re-O-Re angle. For standard calculations, maxstep is set to values between 8 – 10 in order to achieve tight convergence criteria. For the benchmark calculations using PBE0-D3 combined with the def2 ECP, verytight convergence criteria for the optimization and a very fine spherical product grid with 196 608 points per atom (int = -96032) are applied. Frequency calculations are performed on the calculated converged structures.

Orca:

For the screening of functionals, a fine grid 7 is applied and the final grid is suppressed. For rhenium, the integral accuracy is increased to 10. The relativistic effects are treated using the onecenter approximation for both the optimization and the frequency calculations. The SCF convergence criteria are set to tight. For the benchmark calculation using PBE0-D3/ZORA level of theory, the integration accuracy is further increased to 10 for oxygen and 20 for rhenium. Very tight convergence criteria for the SCF and tight convergence criteria for the optimization are applied. Frequency calculations are performed on the calculated converged structures.

Appendix I: Citations

- [1] W.A. Herrmann, W. Scherer, M. Kleine, M. Elison, P. Kiprof, K. Rypdal, H.V. Volden, S. Gundersen, A. Haaland, F.E. Kuehn, *Bull. Soc. Chim. Fr.*, 129 (1992) 655-662.
- [2] K.V. Lawler, B.C. Childs, D.S. Mast, K.R. Czerwinski, A.P. Sattelberger, F. Poineau, P.M. Forster, *Inorg. Chem.*, 56 (2017) 2448-2458.
- [3] S. Grimme, *J. Comput. Chem.*, 27 (2006) 1787-1799.
- [4] S. Grimme, S. Ehrlich, L. Goerigk, *J. Comput. Chem.*, 32 (2011) 1456-1465.
- [5] J.P. Perdew, K. Burke, M. Ernzerhof, *Phys. Rev. Lett.*, 77 (1996) 3865-3868.
- [6] J.P. Perdew, K. Burke, M. Ernzerhof, *Phys. Rev. Lett.*, 78 (1997) 1396-1396.
- [7] A.D. Becke, *J. Chem. Phys.*, 98 (1993) 5648-5652.
- [8] Y. Zhao, D.G. Truhlar, *Theor. Chem. Acc.*, 120 (2008) 215-241.
- [9] J.-D. Chai, M. Head-Gordon, *Phys. Chem. Chem. Phys.*, 10 (2008) 6615-6620.
- [10] S. Grimme, J. Antony, S. Ehrlich, H. Krieg, *J. Chem. Phys.*, 132 (2010) 154104.
- [11] S. Grimme, *J. Chem. Phys.*, 124 (2006) 034108.
- [12] T.H. Choi, Y.-K. Han, *Bull. Korean Chem. Soc.*, 32 (2011) 4195-4198.
- [13] D. Bousquet, E. Brémond, J.C. Sancho-García, I. Ciofini, C. Adamo, *J. Chem. Theory Comput.*, 9 (2013) 3444-3452.
- [14] L. Goerigk, S. Grimme, *Phys. Chem. Chem. Phys.*, 13 (2011) 6670-6688.
- [15] M. Steinmetz, S. Grimme, *ChemistryOpen*, 2 (2013) 115-124.
- [16] W. Jiang, M.L. Laury, M. Powell, A.K. Wilson, *J. Chem. Theory Comput.*, 8 (2012) 4102-4111.
- [17] F. Weigend, R. Ahlrichs, *Phys. Chem. Chem. Phys.*, 7 (2005) 3297-3305.
- [18] F. Weigend, *Phys. Chem. Chem. Phys.*, 8 (2006) 1057-1065.
- [19] D. Andrae, U. Häußermann, M. Dolg, H. Stoll, H. Preuß, *Theor. Chem. Acta*, 77 (1990) 123-141.
- [20] K. Eichkorn, F. Weigend, O. Treutler, R. Ahlrichs, *Theor. Chem. Acc.*, 97 (1997) 119-124.
- [21] B.P. Pritchard, D. Altarawy, B. Didier, T.D. Gibson, T.L. Windus, *J. Chem. Inf. Model.*, 59 (2019) 4814-4820.
- [22] D.A. Pantazis, X.-Y. Chen, C.R. Landis, F. Neese, *J. Chem. Theory Comput.*, 4 (2008) 908-919.
- [23] M.J. Frisch, G.W. Trucks, H.B. Schlegel, G.E. Scuseria, M.A. Robb, J.R. Cheeseman, G. Scalmani, V. Barone, G.A. Petersson, H. Nakatsuji, X. Li, M. Caricato, A.V. Marenich, J. Bloino, B.G. Janesko, R. Gomperts, B. Mennucci, H.P. Hratchian, J.V. Ortiz, A.F. Izmaylov, J.L. Sonnenberg, Williams, F. Ding, F. Lipparini, F. Egidi, J. Goings, B. Peng, A. Petrone, T. Henderson, D. Ranasinghe, V.G. Zakrzewski, J. Gao, N. Rega, G. Zheng, W. Liang, M. Hada, M. Ehara, K. Toyota, R. Fukuda, J. Hasegawa, M. Ishida, T. Nakajima, Y. Honda, O. Kitao, H. Nakai, T. Vreven, K. Throssell, J.A. Montgomery Jr., J.E. Peralta, F. Ogliaro, M.J. Bearpark, J.J. Heyd, E.N. Brothers, K.N. Kudin, V.N. Staroverov, T.A. Keith, R. Kobayashi, J. Normand, K. Raghavachari, A.P. Rendell, J.C. Burant, S.S. Iyengar, J. Tomasi, M. Cossi, J.M. Millam, M. Klene, C. Adamo, R. Cammi, J.W. Ochterski, R.L. Martin, K. Morokuma, O. Farkas, J.B. Foresman, D.J. Fox, *Gaussian 16 Rev. B.01*, in Wallingford, CT, 2016
- [24] F. Neese, *WIREs Computational Molecular Science*, 2 (2012) 73-78.
- [25] U. Ekström, L. Visscher, R. Bast, A.J. Thorvaldsen, K. Ruud, *J. Chem. Theory Comput.*, 6 (2010) 1971-1980.
- [26] K.A. Moltved, K.P. Kepp, *ChemPhysChem*, 20 (2019) 3210-3220.
- [27] M. Bühl, C. Reimann, D.A. Pantazis, T. Bredow, F. Neese, *J. Chem. Theory Comput.*, 4 (2008) 1449-1459.
- [28] S. Huber, A. Pöthig, W.A. Herrmann, F.E. Kühn, *J. Organomet. Chem.*, 760 (2014) 156-160.
- [29] D. Hernández-Valdés, R. Alberto, U. Jáuregui-Haza, *RSC Adv.*, 6 (2016) 107127-107140.
- [30] I.R. Beattie, G.A. Ozin, *J. Chem. Soc. A*, (1969) 2615-2619.

APPENDIX II

SCIENTIFIC IMPACT AND ORGANIZATIONAL MATTERS

SCIENTIFIC IMPACT

PUBLICATIONS PUBLISHED DURING THE DOCTORAL STUDIES

“Synthesis, characterization and application of organorhenium(VII) trioxides in metathesis reactions and epoxidation catalysis”

Florian Dyckhoff, Su Li, Robert M. Reich, Benjamin J. Hofmann, Eberhardt Herdtweck and Fritz E. Kühn.

Dalton Trans., **2018**, 47, 9755.

“A bench stable formal Cu(III) *N*-heterocyclic carbene accessible from simple copper(II) acetate”

Zoreh S. Ghavami, Markus R. Anneser, Felix Kaiser, Philipp J. Altmann, Benjamin J. Hofmann, Jonas F. Schlagintweit, Gholamhossein Grivani and Fritz E. Kühn.

Chem. Sci., **2018**, 9, 8307.

“Reactivity of Re₂O₇ in Aromatic Solvents – Cleavage of a β-O-4 Model Substrate by Lewis-acidic Rhenium Oxide Nanoparticles”

Benjamin J. Hofmann, Reentje G. Harms, Sebastian P. Schwaminger, Robert M. Reich and Fritz E. Kühn

J. Catal., **2019**, 373, 190.

“Network topology and cavity confinement-controlled diastereoselectivity in cyclopropanation reactions catalyzed by porphyrin-based MOFs”

Konstantin Epp, Bart Bueken, Benjamin J. Hofmann, Mirza Cokoja, Karina Hemmer, Dirk De Vos and Roland A. Fischer.

Cat. Sci. Tech., **2019**, 22, 6452.

“Highly Efficient Abnormal NHC Ruthenium Catalyst for Oppenauer-Type Oxidation and Transfer Hydrogenation Reactions”

Lorenz Pardatscher, Benjamin J. Hofmann, Pauline J. Fischer, Sebastian M. Hölzl, Robert M. Reich, Fritz E. Kühn and Walter Baratta.

ACS Catal., **2019**, 9, 11302.

“Ethyltrioxorhenium – Catalytic application and decomposition pathways”

Benjamin J. Hofmann, Stefan Huber, Robert M. Reich, Markus Drees and Fritz E. Kühn.

J. Organomet. Chem., **2019**, *885*, 32.

“Tuning the electronic properties of tetradentate iron-NHC complexes: Towards stable and selective epoxidation catalysts”

Marco A. Bernd, Florian Dyckhoff, Benjamin J. Hofmann, Alexander D. Böth, Jonas F. Schlagintweit, Jens Oberkofler, Robert M. Reich and Fritz E. Kühn.

J. Catal., **2020**, *391*, 548.

“Activation of Molecular Oxygen by a Cobalt(II) tetra-NHC Complex”

Jonas F. Schlagintweit, Philipp J. Altmann, Alexander D. Böth, Benjamin J. Hofmann, Christian Jandl, Clemens Kaußler, Linda Nguyen, Robert M. Reich, Alexander Pöthig and Fritz E. Kühn.

Chem. Eur. J., **2020**, *in press*. DOI: 10.1002/chem.202004758

“Degradation Pathways of a highly active iron(III) tetra-NHC Epoxidation Catalyst”

Florian Dyckhoff, Jonas Felix Schlagintweit, Marco Alexander Bernd, Christian H. G. Jakob, Tim Pascal Schlachta, Benjamin Hofmann, Robert M. Reich and Fritz Elmar Kühn.

Cat. Sci. Tech., **2021**, *in press*. DOI: 10.1039/D0CY02433C

OTHER PUBLICATIONS

“Toward Tunable Immobilized Molecular Catalysts: Functionalizing the Methylene Bridge of Bis(*N*-heterocyclic carbene) Ligands”

Rui Zhong, Alexander Pöthig, Stefan Haslinger, Benjamin Hofmann, Gabriele Raudaschl-Sieber, Eberhardt Herdtweck, Wolfgang A. Herrmann and Fritz E. Kühn.

ChemPlusChem, **2014**, *79(9)*, 1294.

“Dinuclear palladium complexes of pyrazolato-bridged imidazolium- and NHC-ligands: Synthesis and characterization”

Stefan A. Reindl, Alexander Pöthig, Benjamin Hofmann, Wolfgang A. Herrmann and Fritz E. Kühn.

J. Organomet. Chem., **2015**, 775, 130.

“Fighting Fenton Chemistry: A Highly Active Iron(III) Tetracarbene Complex in Epoxidation Catalysis”

Jens W. Kück, Markus R. Anneser, Benjamin Hofmann, Alexander Pöthig, Mirza Cokoja and Fritz E. Kühn.

ChemSusChem, **2015**, 8(23), 4056.

CONFERENCES

(1) 50. Jahrestreffen deutscher Katalytiker

Weimar, Deutschland, 15 – 17.03.2017

Poster presentation

(2) AC Get Together

Raitenhaslach, Deutschland, 09. – 12.04.2017

Poster presentation

(3) 9th European Silicon Days

Saarbrücken, Deutschland, 09. – 12.09.2018

REPRINT PERMISSIONS

- Figure 1: Mendeleev, Dmitry Ivanovich. "Periodic Table of the Elements." In *Osnovy Khimii (Principles of Chemistry), Volume II*. Saint Petersburg, Russia (Federation): Tip. t-va "Obshchestvennāiā pol'za, 1871.
From <https://digital.sciencehistory.org/works/9c67wp122> "Science History Institute"; The dark frame has been removed. Public Domain Mark 1.0 license.
- Figure 5: Structure of solid Re_2O_7 : From <https://materialsproject.org/materials/mp-1016092/> "The Materials Project" [435]; The black box indicating the rectangular substructure of four polyhedrons is added; CC BY 4.0 license.
- Figure 6: Structure of solid ReO_3 . Unchanged from <https://materialsproject.org/materials/mp-190/#> "The Materials Project" [435]; CC BY 4.0 license.
- Figure 7: Structure of solid ReO_2 .
Orthorhombic: Unchanged from <https://materialsproject.org/materials/mp-7228/>
Monocline: Unchanged from <https://materialsproject.org/materials/mp-1095546/> "The Materials Project" [435]; CC BY 4.0 license.
- Figure 10: Reprint permission gratefully obtained from Elsevier *via* Rightslink®.
License number 4958750930731

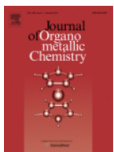
Main Publication 1:

F. Dyckhoff, S. Li, R.M. Reich, B.J. Hofmann, E. Herdtweck, F.E. Kühn, Dalton Trans., 47 (2018) 9755-9764.

Reproduced by permission of The Royal Society of Chemistry.

Main Publication 2:

B.J. Hofmann, S. Huber, R.M. Reich, M. Drees, F.E. Kühn, J. Organomet. Chem., 885 (2019) 32-38.



Ethyltrioxorhenium – Catalytic application and decomposition pathways
Author: Benjamin J. Hofmann, Stefan Huber, Robert M. Reich, Markus Drees, Fritz E. Kühn
Publication: Journal of Organometallic Chemistry
Publisher: Elsevier
Date: 1 April 2019
© 2019 Elsevier B.V. All rights reserved.

Please note that, as the author of this Elsevier article, you retain the right to include it in a thesis or dissertation, provided it is not published commercially. Permission is not required, but please ensure that you reference the journal as the original source. For more information on this and on your other retained rights, please visit: <https://www.elsevier.com/about/our-business/policies/copyright#Author-rights>

[BACK](#) [CLOSE WINDOW](#)

Main Publication 3:

B.J. Hofmann, R.G. Harms, S.P. Schwaminger, R.M. Reich, F.E. Kühn, J. Catal., 373 (2019) 190-200.



Reactivity of Re₂O₇ in aromatic solvents – Cleavage of a β -O-4 lignin model substrate by Lewis-acidic rhenium oxide nanoparticles

Author: Benjamin J. Hofmann, Reentje G. Harms, Sebastian P. Schwaminger, Robert M. Reich, Fritz E. Kühn

Publication: Journal of Catalysis

Publisher: Elsevier

Date: May 2019

© 2019 Elsevier Inc. All rights reserved.

Please note that, as the author of this Elsevier article, you retain the right to include it in a thesis or dissertation, provided it is not published commercially. Permission is not required, but please ensure that you reference the journal as the original source. For more information on this and on your other retained rights, please visit: <https://www.elsevier.com/about/our-business/policies/copyright#Author-rights>

BACK

CLOSE WINDOW

EIDESSTÄTTLICHE ERKLÄRUNG

Ich erkläre an Eides statt, dass ich die bei der promotionsführenden Einrichtung Fakultät Chemie der TUM zur Promotionsprüfung vorgelegte Arbeit mit dem Titel:

“High Valent Rhenium Compounds in Catalysis: Synthesis, Reactivity and Decomposition Pathways”

an der Fakultät für Chemie, Professur für Molekulare Katalyse unter der Anleitung und Betreuung durch Prof. Fritz E. Kühn ohne sonstige Hilfe erstellt und bei der Abfassung nur die gemäß § 6 Abs. 6 und 7 Satz 2 angegebenen Hilfsmittel benutzt habe.

Ich habe keine Organisation eingeschaltet, die gegen Entgelt Betreuerinnen und Betreuer für die Anfertigung von Dissertationen sucht, oder die mir obliegenden Pflichten hinsichtlich der Prüfungsleistungen für mich ganz oder teilweise erledigt.

Ich habe die Dissertation in dieser oder ähnlicher Form in keinem anderen Prüfungsverfahren als Prüfungsleistung vorgelegt.

Ich habe den angestrebten Doktorgrad noch nicht erworben und bin nicht in einem früheren Promotionsverfahren für den angestrebten Doktorgrad endgültig gescheitert.

Die öffentlich zugängliche Promotionsordnung der TUM ist mir bekannt, insbesondere habe ich die Bedeutung von § 28 (Nichtigkeit der Promotion) und § 29 (Entzug des Doktorgrades) zur Kenntnis genommen. Ich bin mir der Konsequenzen einer falschen Eidesstattlichen Erklärung bewusst.

Mit der Aufnahme meiner personenbezogenen Daten in die Alumni-Datei bei der TUM bin ich einverstanden.

Garching, 18.01.2021